UNIVERSITY OF CALIFORNIA, MERCED

Groundwater Surface Water Interactions in a Gold-Mined Dredged Floodplain of the Merced River

A Thesis submitted in partial satisfaction of the requirements for the degree
Master of Science

in

Environmental Systems

by

Lynn Sager Sullivan

Committee in charge:

Professor Martha H. Conklin, Chair
Professor Teamrat A. Ghezzehei
Professor Joseph E. Merz

2013

The Thesis of Lynn Sager Sullivan is approved, and it is acceptable in quality and form for publication on microfilm and electronically:

_____
Teamrat A. Ghezzehei, Ph.D.

_____
Joseph E. Merz, Ph.D.

_____
Martha H. Conklin, Ph. D.
Committee Chair

University of California, Merced

2013

Table of Contents

List of Figures

List of Tables

ABSTRACT OF THE THESIS

Groundwater Surface Water Interactions in a
Gold-mined Floodplain of the Merced River
by
Lynn Sager Sullivan
Master of Science in Environmental Systems
University of California, Merced, 2013

The Merced River, originating in the Sierra Nevada in California, drains a watershed with an area of approximately 3,305 km^2. The stream has been highly altered due to diversions, gold-dredged mining, damming, and subsequent modification to the hydrograph. Over the course of a year, groundwater-surface water interactions were studied to elucidate the hydrological connection between the Main Canal, an unlined engineered channel containing Merced River water and flowing parallel to the river (average elevation 89 m) and also a highly conductive previously-dredged floodplain, and the Merced River average (elevation 84 m). Upstream of the study reach, located in an undredged portion of the floodplain, are a state run salmon hatchery and a privately run trout farm that have been operating for approximately 40 years. Exchanges between the hyporheic and surrounding surface, groundwater, riparian, and alluvial floodplain habitats occur over a wide range of spatial and temporal scales. For this study, pressure transducers were installed in seven wells and four ponds located in the dredged floodplain. All wells were drilled to the Mehrten Formation, a confining layer, and screened for the last 3 m. These groundwater well water levels as well as the surface water elevations of the Main Canal and the Merced River were used to determine the direction of sublateral surface flows using Groundwater Vistas as a user interface for MODFLOW. The wells, the canal, the river, and seepage from the river banks were sampled for major anion and cation, dissolved organic carbon, total nitrogen, total iron, and total dissolved iron concentrations to determine water sources and the possibility of suboxic water. Field analysis indicated that water in all wells and ponds exhibits low dissolved oxygen, high conductivity, and oxidation/reduction potentials that switched from oxidizing to reductive during the course of the monitoring period. Chemical analysis indicates that there are three sources of water for this floodplain: the Merced River and Main Canal (which are chemically very similar), the waters from the trout farm, and precipitation. The well closest to the trout farm had a C:N

of 1, typical of a highly carbon-limited system. MODFLOW particle tracer experiments designed with homogeneous soils were performed and did not capture the near-surface preferential flow paths. These results indicate that travel time between the Main Canal and Merced River is approximately 10-15 years, while chemistry results indicate seasonal fluctuations. Based on the well levels and chemistry, this water system responds on a much faster scale than indicated by the particle tracer experiments. Reconciling these results, there must be significant preferential flow paths. Candidate flow paths are abandoned channels from the dredging era. The hydraulic gradient set up by the groundwater connection between Main Canal and the Merced River ensures that any effluent released by the trout farm will be transported to the Merced River. Conclusions of the year-long study are that the waters that seep from the Main Canal to the Merced River in this area can be suboxic, which is not conducive to spawning and incubation for native Chinook salmon (*Oncorhynchus tshawytscha*) an indicator species for the overall ecosystem's health. This study reach has been historically important for salmon spawning and rearing, as the area examined is where more than 50% of the Chinook salmon of the Merced River spawn. Currently, salmon restoration efforts are focusing on gravel augmentation and adding a side channel, but ignoring groundwater influences. Due to the causal connections between the hydrological system of the Merced River floodplain and the riverine system, habitat rehabilitation should target not only the surface water but also important subsurface hydrological components.

Chapter 1 Introduction, Background, and History

1.1 Introduction

John Muir, known as “The Father of Our National Parks” because he inspired countless people to cherish the United States’ natural heritage, remarked that the Merced River Valley was probably the loveliest in California (Sierra Club, 2012). Over the years, surface water from the Merced River has been rerouted with levees, crib dams, diversion dams, and canals to provide water to irrigate cropland, aquaculture, and the budding population of the city of Merced. Larger and more permanent dams were built between 1901 and 1967 to provide flood protection (McSwain, 1977). This manipulation of unimpaired stream flow altered the hydrology of the Merced River floodplain. When the Great Depression hit, the Snelling Gold Dredging Company and others acquired mining rights to the Merced River, turning the floodplain upside down. The mechanical dredging process that was done during the 1930s more than likely further disrupted the natural ground- and surface-water interactions and flow patterns of the Merced River’s riparian habitat. Artificial dikes were built to flood specific areas and reroute water to others, thereby changing groundwater flow paths.

Exchanges between the hyporheic and surrounding surface, groundwater, riparian, and alluvial floodplain habitats occur over a wide range of spatial and temporal scales (Boulton et al., 1998). The hydrology of the dredged floodplain is further complicated by the presence of an unlined canal (Main Canal) with hydrological connectivity to the stream (Stillwater, 2007). The Main Canal to the south of the Merced River is at a higher elevation compared to the Merced River. In this section of the Dredger Tailings Reach of the Merced River, surface water from the Main Canal may be stored sublaterally in the complex channel systems of the dredged floodplain and then released to the stream during lower stages. Slight changes in water quality over time beneath the site suggest that the primary source of groundwater under Merced River Ranch (MRR) is seepage from the Main Canal and that this groundwater ultimately discharges to the stream (Stillwater Science, 2007). Furthermore, an evaluation of the hydrochemistry of the groundwater systems of the gold-dredged fields in the riparian zone of the Merced River determined seasonal fluctuations and possible subsurface connections (Stillwater 2001).

It is necessary to consider the connectivity of the channel bed forms, elevation, up-stream influences from artificial fish habitats, and stream processes to apprehend the variability of groundwater-surface water interactions (Pringle and Triska, 2000). Two fish farms are located upstream of the study reach where the Merced River water is diverted into the Main Canal. Immediately downstream from Crocker Huffman Dam is a salmon hatchery, and proximally downstream and adjacent to the study reach is the trout farm with unlined raceways. Nutrient-enrichment and flow paths, such as those

provided by groundwater flow through the river rock tailings, are likely to have effects on the hydrochemistry of the subsurface and groundwater.

Studies at other dredged California river beds have discovered that as a result of the high permeability of the rocky tailings, water levels in swale ponds and canals rise and fall in sync with the stages of the river (California Department of Water Resources, 1999). In addition, the precipitation that falls during the winter months appears to permeate quickly down through the rocky tailings.

An artificial source of nutrients from a trout farm in an area upstream has been previously dredged for gold. As a result, this floodplain no longer offers a natural filtration process and the effluent from the trout farm could pose threats to aquatic life of the hyporheic zone. It is during the marginal stream flows with critical river temperatures that the chemically-reduced surface water runoff could have the most serious impact on the survival and growth of salmon embryos, which incubate in the hyporheic zone (Malcolm, 2003; 2005).

The goal of this study is to provide information regarding the chemical composition and quality of the subsurface water in the vicinity of the Dredger Tailings Reach of the Merced River. Temperatures and low oxygen content in discharging groundwater water could have significant effects on spawning salmon and success of developing embryos. Our hypothesis is that suboxic waters exist in the river bottom during spawning season and incubation season, when critical low flows are present. An analysis of the chemistry in the groundwater and stream was performed over the course of one year in order to establish the importance of these seeps to salmon spawning and their incubation habitat. This was done by installing a series groundwater monitoring wells and constructing a numeric groundwater model for the MRR located between the Main Canal and the Merced River.

During the process of evaluating the hydrochemical and groundwater modeling results, the following six questions were addressed: (1) Is there a hydrological connection between the Merced River, the Main Canal, and the surrounding dredged floodplain? (2) Are there seasonal sublateral surface flows that occur in the area of the MRR and its upstream influences? (3) Does the hydrochemistry and water quality of the ground- and surface-water exhibit seasonal variations? (4) What are the sources of water in this dredged floodplain?

In addition, (5) are there additional upstream influences that have not yet been addressed that could potentially influence the hydrochemistry and water quality of the Merced River? Finally, (6) could the seepage waters potentially impact salmon spawning and incubating habitats? While this question will not be directly answered, the potential for this to occur will be discussed.

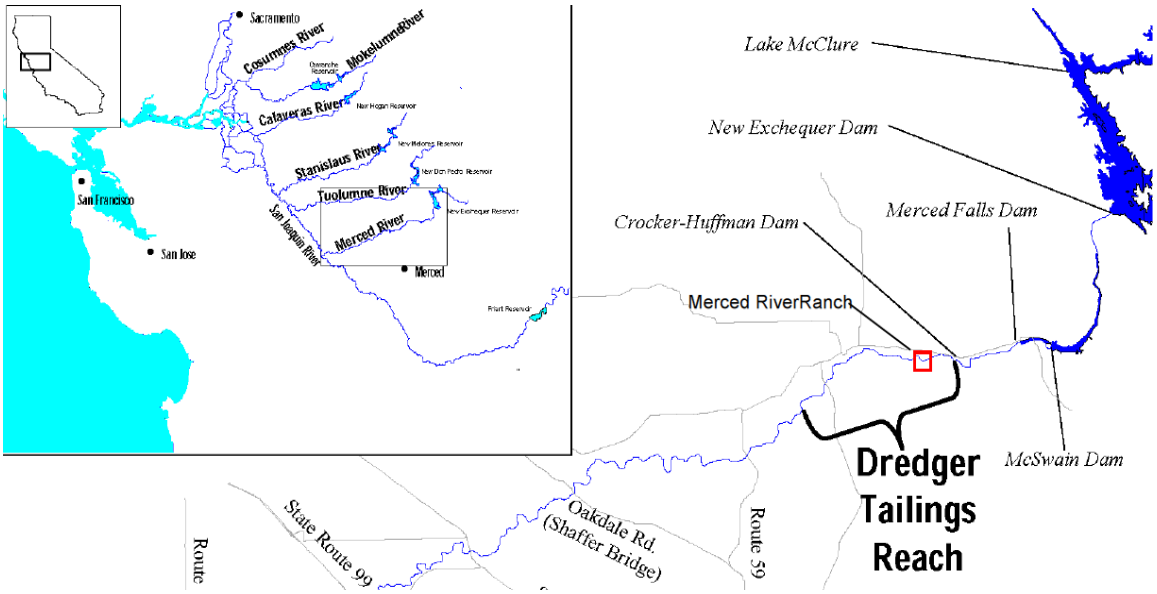

Figure 1 Location of the Merced River Ranch study site in the Dredger Tailings Reach of the Merced River. Map courtesy of Stillwater Sciences.

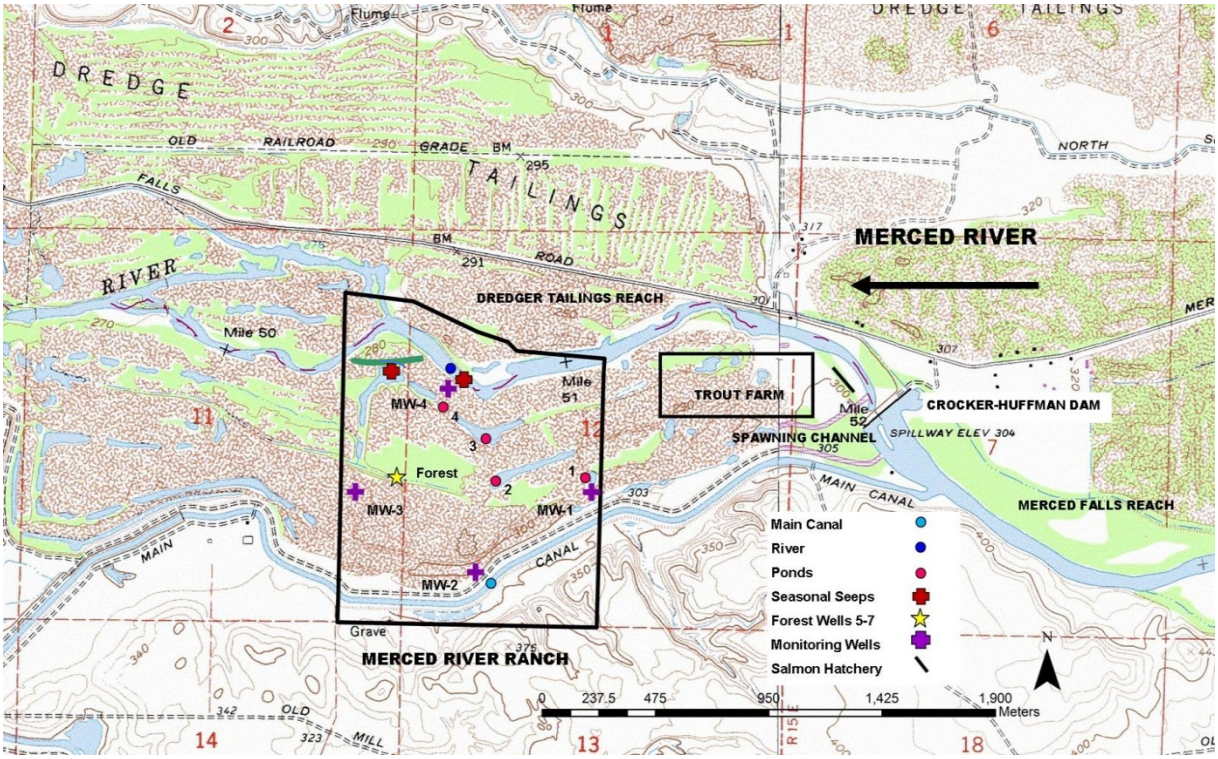

Figure 2 Local site map near Snelling, CA. The study site, Merced River Ranch (MRR) is located between the Main Canal and the Merced River downstream from Crocker Huffman Dam. Calaveras Trout Farm (trout farm) and Merced River Fish Hatchery (salmon hatchery) (not drawn to scale) are located to the east of MRR. Locations of the monitoring wells, ponds, and seeps within MRR are depicted. In 2011, a side channel was constructed and its approximate location is depicted as a blue green line ( ). This is a modified version of United States Geological Service and California Department of Fish and Game Merced Riffle Atlas of 2006.

Figure 3 Arial view of the Merced River Ranch. There is a stark contrast between the vibrant blue of the Merced River, the reflective white dredged tailings, and the red azola, green duckweed-covered swale ponds of the Merced River Ranch. Image courtesy of Cramer Fish Sciences.

1.2 Background

1.2.1 Merced River Site Description

The Merced River, a tributary of the San Joaquin River, originates in the Sierra Nevada mountain range and then flows through the middle of California's Central Valley. Its headwaters lie in Yosemite National Park at an altitude above 4,000 m, after which it flows west to an elevation of 15 m at its confluence with San Joaquin River. The San Joaquin River then continues north to join the Sacramento River and ultimately empties into the San Francisco Bay and the Pacific Ocean (Figure 1).

The Merced River drains a watershed with an area of approximately 330,500 hectares (3,305 km^2). Most of the stream's basin has a Mediterranean climate characterized by mild, wet winters and hot, dry summers. The majority of precipitation occurs between the months of November and March (Gronberg and Kratzer, 2006), and at higher elevations, this precipitation forms the basis of the winter snowpack that provides flow to the stream via snowmelt in late spring and early summer. Fall and winter rainstorms create peak surface runoff, though by late summer the stream exudes low base flows. Snowmelt constitutes a majority of the stream's springtime and early summer flow.

The Upper Merced River Basin has been classified as a watershed above Exchequer Dam. The Lower Merced River Basin covers 831 km^2 and is underlain by a primary unconfined aquifer composed of alluvial deposits from the Sierra Nevada to the east and the Costal Ranges to the west (Gronberg and Kratzer, 2006). After leaving Exchequer Dam, the Merced River then flows through a narrow V-shaped corridor and passes through Lake McSwain and Merced Falls Dam prior to reaching Crocker Huffman Dam, a diversion dam owned and operated by Merced Irrigation District. It is

here that water as impoundment is used to create the head for the Main Canal diversion and is allocated for agricultural use in the Central Valley (Figure 2). The discharge rates measured at the Merced Falls Dam, the discharge rates measured just downstream from the Crocker Huffman Dam, and the subsequent flows of the Main Canal are depicted (Figure 4). Merced Irrigation District operates the irrigation infrastructure in the area after it purchased water rights from the Farmers Canal Company prior to 1914 to divert flows for irrigation (McSwain, 1977).

In the lower one-sixth portion of the Crocker Huffman Dam impoundment, which is a narrow and shallow 4.8km-long reservoir, the substrate is dominated by silt; this is not surprising due to the “back-water influence” of the dam (Vogel, 2007). Furthermore, near the dam site, there is an abundance of aquatic weeds (personal observation). The residence time has been measured to be hours or days depending on the discharge rate of the Merced River (Vogel, 2007). The salmon hatchery receives water from a pipe installed in 1991 from the bottom of Crocker Huffman Dam impoundment (Vogel, 2007). Water is diverted from the Crocker Huffman Dam impoundment to the trout farm via a combination of canals and pipes (Vogel, 2007).

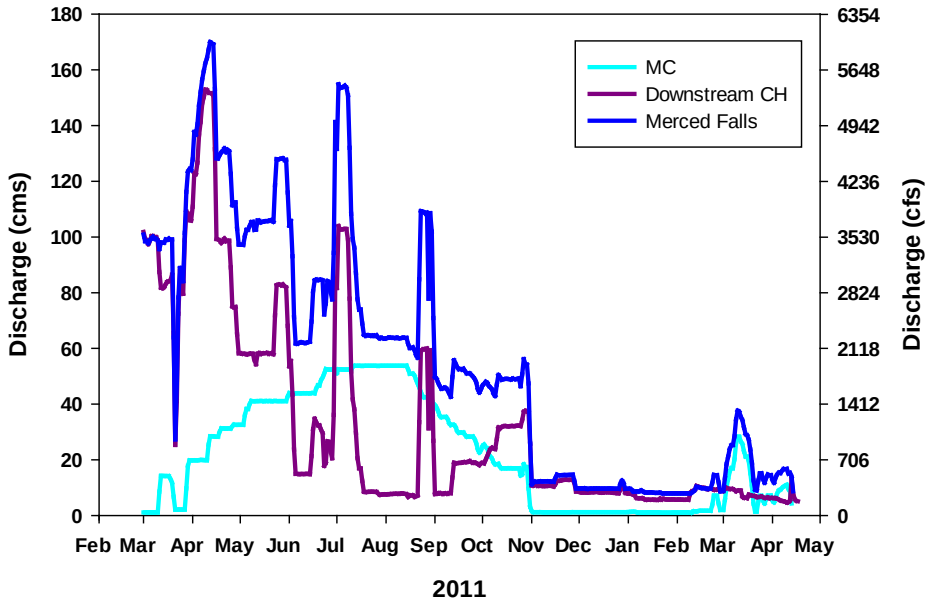

Figure 4 Merced River Hydrograph of the Merced Falls Reach, downstream from Crocker Huffman Dam and the Main Canal. Information obtained from CDEC, and Merced Irrigation District. Merced Irrigation District controls the discharge rates and frequency of water flows at Exchequer Dam. The Merced Falls Reach waters, which are part of the Merced River riverine system, are diverted at Crocker Huffman Dam; this diversion forms the flow of the Main Canal and discharges into the Dredger Tailings Reach.

1.2.2 Hydrogeologic Setting of the Dredger Tailings Reach

The physiography of the Dredger Tailings Reach consists of stream channel, floodplain, and dissected uplands (Page and Balding, 1973). The floodplain and channel deposits are made up of alluvium, which consists primarily of sands, gravels, and cobbles derived from the granites of the nearby Sierra Nevada (Page and Balding, 1973). The thickness of the channel and flood plain deposits typically range from 6 m to 15 m (Page and Balding, 1973).

The primary hydrogeologic units in the Modesto Subbasin here include both consolidated and unconsolidated sedimentary deposits (Figure 6). The consolidated deposits include the Ione Formation from the Miocene Age, the Valley Springs Formation from the Eocene Age, and the Mehrten Formation (MF), a layer of volcanically-derived sediments mixed with volcanic mudflows, which was deposited between the Miocene and Pliocene Epochs (California Department of Water Resources, 1980). The MF is considered to be one of the oldest water-bearing aquifers on Earth; in this region, it can range between 90 and 400 m deep (Figure 7 and 8). Reports indicate that the specific yield—the amount of water released from the aquifer per unit land surface area per unit drop in water table—can be between 7.3% and 8.8% (Page and Balding, 1973; California Department of Water Resources, 1980).

Figure 5 Mehrten Formation found on the south bank of the Merced River in the Merced Falls Reach.

The MF bluffs with alluring hues of red, pink, yellow, and grey are evident on both sides of the Merced River floodplain (Figure 5). The MF that underlays the channel and floodplain deposits is composed of up to 250 m of sandstone, breccia, tuff, siltstone, and claystone (Figures 6-8)(Page and Balding, 1973). Cobbles consist of purple slate, greenstone, meta-rhyolite, diorite, dacite tuff, and iron-stain quartz (American Geological Service Inc. and Wondijina Research Institute, 2007). The China Hat pediment, a triangular soil formation composed of iron-silicon described as a variant of the Redding soil series, cuts through pre-dredged cobbles that were once held together with sand, silt, and clay (California Department of Water Resources, 1980). The MF is impervious and its drainage retarded, thus creating semi-confined conditions on the floodplain (California Department of Water Resources, 1980). Groundwater surfaces and rainwater collect within the floodplain as swale ponds and at locations between the tailing rows. The turbidity in these ponds could be a result of iron oxyhydroxide flocs.

The iron-bearing groundwater surfaces as seeps when it comes into contact with the oxygen, quickly oxidizing to ferric hydroxide. Ferric compounds may be reduced when buried beneath the sediment, placed in anoxic conditions, and reoxidized upon surfacing. Residence times may control the concentration of dissolved iron (Bricker, USGS 03-346, 2003). Pockets of red soil within the mudflows of the MF (personal observation and documented, see Figures 5 and 7) are visible.

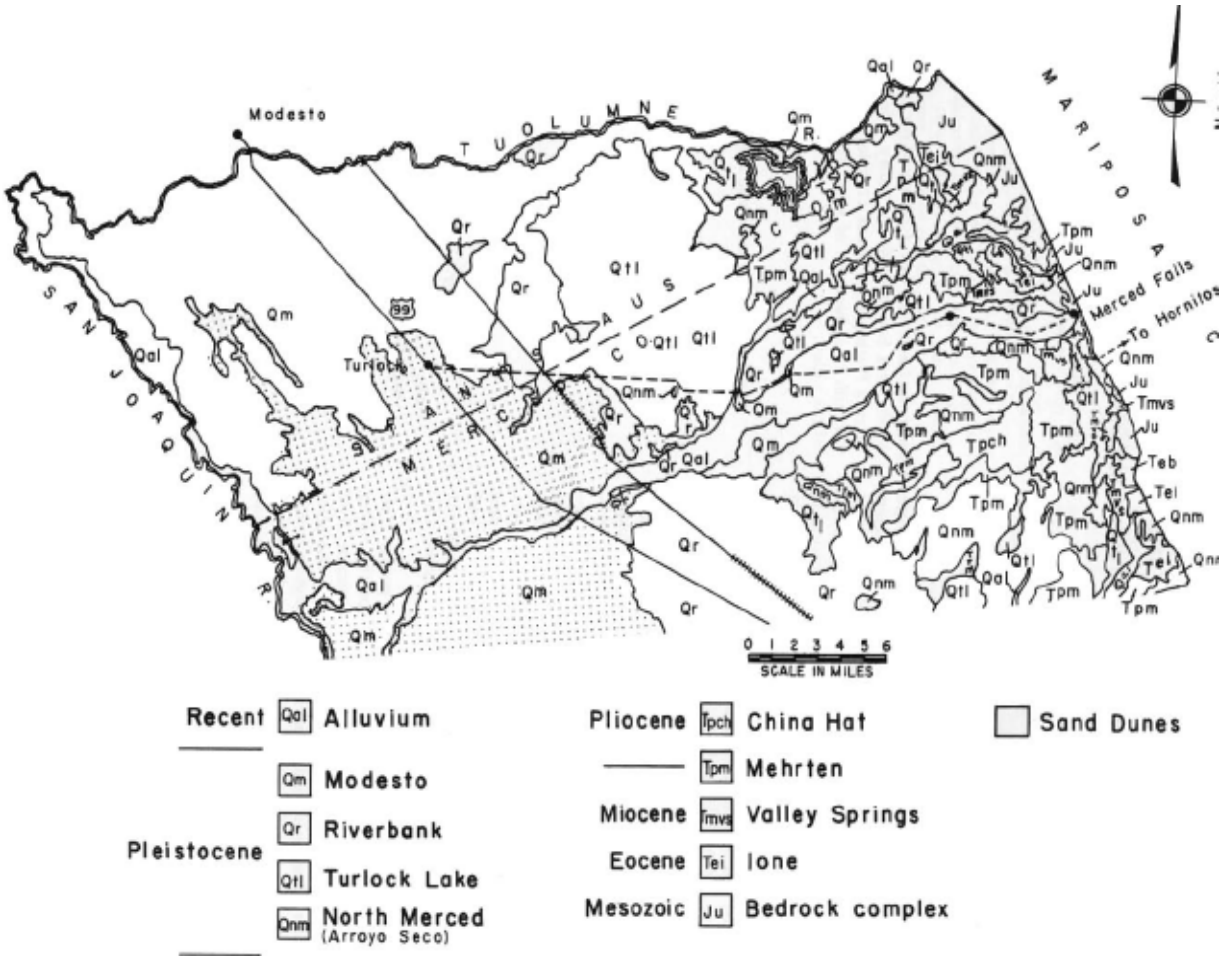

Figure 6 Historical soils map of an area from the Tuolumne River to a region south of the Merced River (Arkley, Bulletin 182, California Division of Mines).

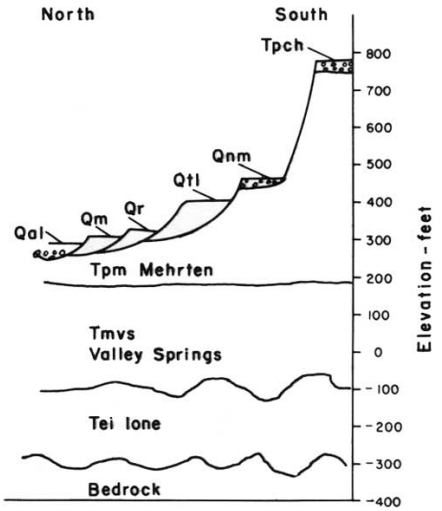

Figure 7 Schematic section (north to south) three miles west of Merced Falls in Merced County, California (Arkley, Bulletin 182, California Division of Mines).

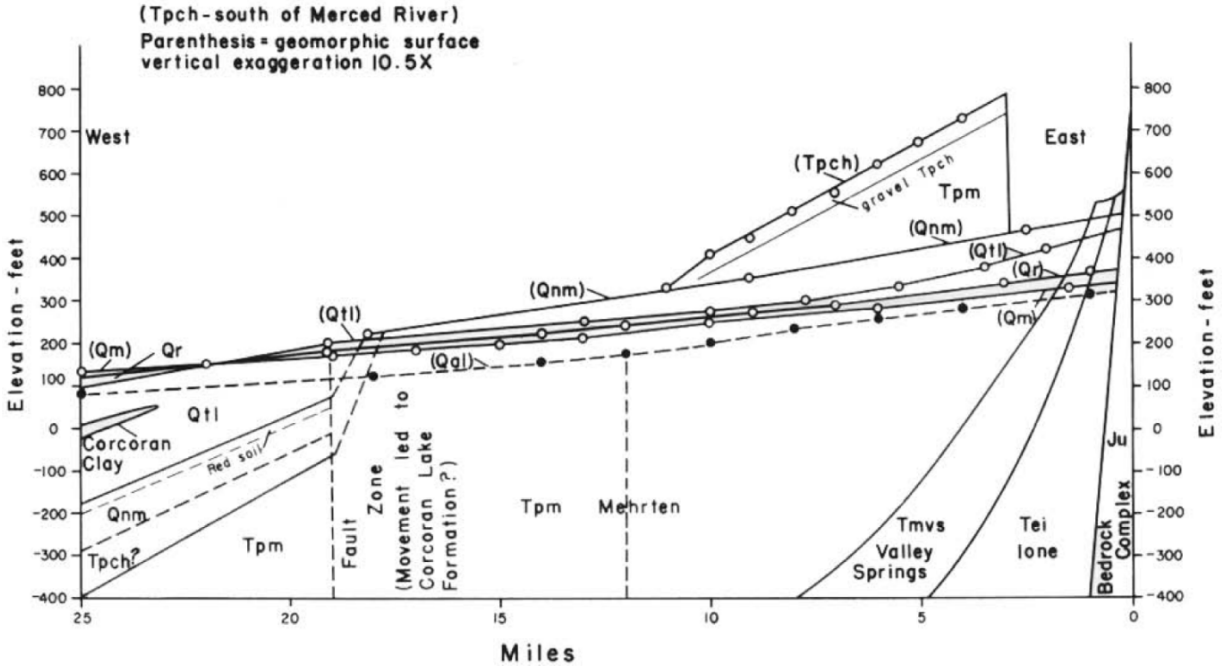

Figure 8 Schematic cross-section (east to west) north of the Merced River. Note the layer of red soil found above the Mehrten Formation, designated in the chart as Tpm (Arkley, Bulletin 182, California Division of Mines).

The Merced River has dissected the MF as much as 46 m in some locations and is visible in many locations in the stream from Merced Falls Road. In the Dredger Tailings Reach, the MF typically ranges from 6-61 m thick (Page and Balding, 1973).

1.2.3 Description of Dredger Tailings Reach

1.2.3.1 History

The Dredger Tailings Reach of the Merced River extends roughly 11.6 km from Crocker Huffman Dam at River Mile 52 (RM 52) to approximately 1.9 km downstream of the Snelling Road Bridge, located at RM 45.2 (Figure 2). Since 1926, sediment supply from the upper 81% of the watershed has been intercepted at the original Exchequer Dam and then at the New Exchequer Dam (Stillwater, 2007).

The hydrology of the lower Merced River has been profoundly altered by a combination of factors: the construction of dams and subsequent flow diversion for agricultural purposes, as well as wide-scale dredging activities for precious metals. Manmade alterations to the Merced River have blocked access for anadromous fish to the upper watershed, eliminated habitats, and impaired fluvial processes that naturally form and maintain riverine habitats and ecological processes (Vick, 1997).

The water supply requirements of agriculture and flood control operations together have reduced flood frequency, reduced peak flow magnitude, altered seasonal flow patterns, and reduced the temporal variability of flows. These changes in hydrologic conditions have changed the frequency, duration, and magnitude of floodplain inundation, and reduced the frequency of sediment transport and bed mobilization. The lack of sediment supply has caused bed scour and armoring in the remaining flood events (Stillwater Sciences, 2001).

Figure 9 Historical photo, designated ABF-12-45 by the United States Geological Survey, depicting parallel river flows and initial dredging efforts at the northeast corner of the MRR, dated 08/02/1937 (USGS, 1937).

Historically, this reach was part of a highly dynamic, multiple-channel system with the location of the main channel switching to occupy various secondary channels or sloughs over time. Prior to the construction of the dams, the river spread out across a broad alluvial valley floor that ranged up to 7.24 km in width (Stillwater Sciences, 2001). The flow of the river left a sequence of steeply sloping, westerly nested quaternary alluvial fans (Harden, 1987). These alluvial fans were sequentially deposited, such that younger fans overlie older fan deposits (Figure 9).

The rapid switching of channel courses during a flood event in combination with progressive channel migration likely maintained a diversity in channel, riparian, wetland, and floodplain habitats and channel avulsion. Floodplain inundation was episodic in the winter, following large precipitation events, and prolonged during the spring snowmelt period. The riparian corridor in this area was extensive, supporting large populations of migratory waterfowl and neotropical songbirds, resident bird species, mammals, and non-anadromous and anadromous fish (Grinnell, 1915-20; Camp, 1915; Yoshiyama, 1998; Stillwater Sciences, 2005).

The Merced River and its floodplain historically supported dense riparian woodland. While much of the Central Valley upland and foothills were generally covered

with thinly wooded grasslands, riparian zones supported thick, multistoried stands of broadleaf trees, including Valley Oak (*Quercus lobata*), Fremont cottonwood (*Populus fremontii*), Western sycamore (*Platanus racemosa*), willow (*Salix spp.*), Oregon ash (*Fraxinus latifolia*), box elder (*Acer negundo*), and other species (Thompson 1961, 1980, Holland and Keil 1995, Roberts et al. 1980, Conard et al. 1980). These riparian forests varied markedly in width, from a narrow strip in confined reaches to several miles wide on broad alluvial floodplains.

However, through the combined effects of dredging, flow regulation, and elimination of coarse sediment, this reach has been converted from a multiple-channel system to a single-channel system flanked by a thin ribbon of vegetation.

1.2.3.2 Current Description of the Dredger Tailings Reach and Floodplain

Piles of dredger tailings, which have replaced the natural floodplain soils and floodplain forest and have increased floodplain elevations along the stream, confine the Merced River channel in the Dredger Tailings Reach.

At the MRR in the Dredger Tailings Reach, a network of channels and swale ponds has been left behind by the gold-dredging process. Between the rows of cobbles are long narrow ponds. Occasionally large ponds are present where the dredgers turned around during the dredging process after excavating the porous media. These ponds are depressions in the cobbled landscape; remnants of previous soil may remain in the wetland swales and perhaps in pockets under the cobbles (Santé Fe Aggregates, 2009).

The various sloughs that once dominated the floodplain have been converted to irrigation and return-flow ditches. Numerous abandoned channels remain from the dredging era that may offer preferential flow paths for groundwater and near-surface water. The river channel in this reach is dominated by pool-riffle morphology, with a slope averaging 0.0023 and a riverbed composed of coarse gravel and cobble (Stillwater Sciences, 2001-2005).

Riparian vegetation is sparse, occurring primarily in narrow bands along the river channel and in fragmented patches in low-lying areas among the dredger tailings piles.

The dredger tailings on the floodplain confine the river channel width, resulting in high shear stress in the reach during even moderate-flow events. High shear stresses, combined with the lack of coarse sediment supply caused by upstream dams, have produced a channel that is typified by long, deep pools scoured to bedrock or to a coarse cobble armor layer (Stillwater Sciences, 2001, 2004, 2007).

Merced River Fish Hatchery, constructed and operated by the California Department of Fish and Game (now known as California Department of Fish and

Wildlife) to mitigate salmon production loss above Crocker Huffman Dam, is located immediately downstream from the dam. In 1970, to augment salmon runs, a spawning channel (Figure 2) was constructed around Crocker Huffman Dam. Water enters the channel from the Crocker Huffman impoundment at the rate of 2.83-4.25 m^3/s, flows west and down gradient, and turns north and then east to reenter the Merced River downstream from the dam (Vogle, 2007). At times of low flow, the only water that discharges to the Dredger Tailings Reach from the Merced Falls Reach of the Merced River flows through this spawning channel. Modifications to the facility were made during the 1980s and 1990s to modernize and increase fish production (Vogel, 2007). The current salmon hatchery (Figure 2) consists of two concrete raceways, a fish trapping and spawning building and a nursery building. Water is supplied by a gravity-flow pipeline from the Crocker Huffman impoundment and delivers 0.17 m^3/s during the spawning and rearing season of October-May. There is a settling pond down gradient from the concrete raceways. The Merced River Fish Hatchery is the only hatchery that utilizes San Joaquin basin Chinook salmon brood stock in California (CDFG, 1998) to supplement and boost in-river natural production of salmon (Vogel, 2007).

Figure 10 This photo depicts the harvesting fish at Calaveras Trout Farm for export to the sporting industry. Note unlined cobble raceways. Photo taken 4/2010

Calaveras Trout Farm (TF) (Figure 2) leases fifty acres of land from Merced Irrigation District adjacent to the Merced River Fish Hatchery. It was constructed in 1968 and designed to receive 1.4 m^3/s through a combination of canals and pipeline from Crocker Huffman Dam impoundment. While this hatchery specializes in rearing rainbow trout; it also rears white sturgeon *(Acipenser transmontanus)*, brown trout (*Salmo trutta*), and brook trout (*Salvelinus fontinalis*). It supplies over 227,000 kilograms annually to the sport fishing industry (Figure 10). The TF consists of ten unlined raceways and sixteen tanks that are 5.5 m in diameter. Each raceway has the capability to sustain 70,000 trout (Vogel, 2007). The hatchery building contains six concrete raceways. After the water travels through the raceways and tanks, the TF has the potential to increase the nutrient capacity of the water by adding phosphorous, nitrogen, and particulate matter in the form of high-protein fish food (Hardy, 2000). Wastewater, which includes undigested food, carcasses, and urea, flows from the raceway to seven settling ponds located down gradient from the TF.

The MRR, a 129-ha parcel of land, is located from River Mile 51 to River Mile 50 (Figures 1, 2, and 3). The California Department of Fish and Game (CDFG) purchased

Figure 11 Newly created side channel of the Merced River located in the northeast corner of the MRR. The aim of the side channel is to increase "in-channel habitat complexity" and to "reengineer low-flow and bank-full channel geometry" of the Merced River (Cramer Fish Sciences). River flow is from right to left. Photo taken mid-construction 10/24/11.

the property in 1998 as a site for river and floodplain restoration, with the intention of using the abundant coarse sediment for gravel augmentation within sediment-deficient regulated streams of the Central Valley. The total cost to excavate, process, and haul the rocks away was estimated to be $64,600,000 (Stillwater, 2004). During the 2000s, MRR was the site of numerous baseline investigations to guide the rehabilitation process of the Merced River floodplain and a remaining spawning reach for Chinook salmon (*Oncorhynchus tshawytscha*). During the course of our field studies conducted between 2011 and 2012, construction of a side channel to increase "in-channel habitat complexity" and to "reengineer low-flow and bank-full channel geometry" of the Merced River was initiated (Figures 2 and 11) (Cramer Fish Sciences).

1.2.4 Historic and Current Salmon Habitats in the Merced River

Dams on the Merced River currently block access to extensive amounts of historical spawning and rearing habitat for anadromous fish (Yoshiyama, 1998). At one time, salmon may have migrated to the vicinity of El Portal and ascended the South Fork of the Merced River at least as far as Peach Tree Bar, 11.3 km above the confluence with the main stem, where a waterfall presents the first significant obstruction (Yoshiyama, 1998).

Chinook tend to run up larger river systems and occur in the Central Valley, with the southernmost populations of the species in the world found in the Merced River (personal communication, Merz, 2012). Warmer water temperatures downstream of the dams have been cited as a factor contributing to the disappearance of spring-run Chinook salmon from the Merced River basin (Skinner 1962; Yoshiyama et al. 1998, 2001). The inability to access upper habitats is another cause for their extirpation (Yoshiyama et al. 1998, 2001). The Dredger Tailing Reach of the Merced River remains an important spawning reach for fall-run Chinook salmon, as it is where greater than 50% of the Chinook in the Merced River spawned from 2002 to 2006 (personal communication, Blakeman, 2010).

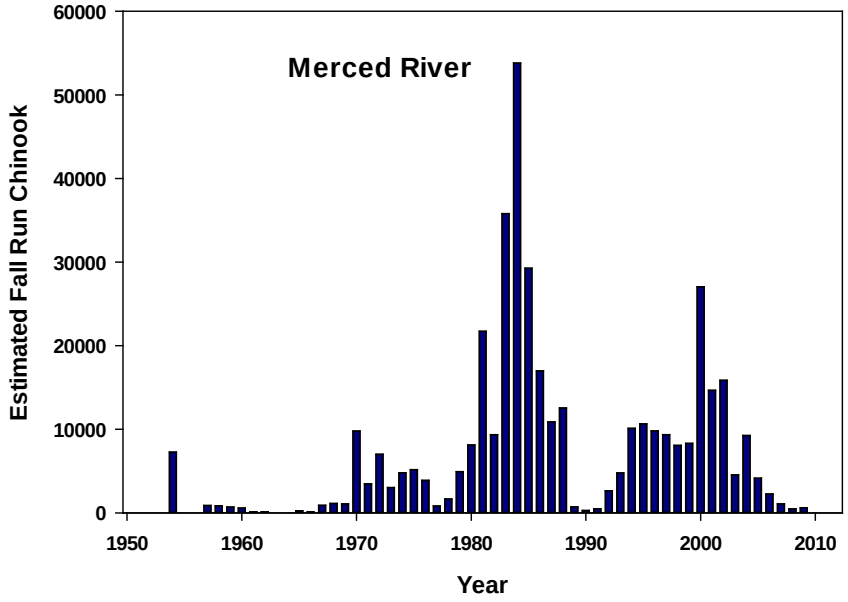

Figure 12 Estimated natural production of Merced River adult fall-run Chinook salmon. CDFG presented 1952-1966 and 1992-2010 numbers from CDFG Grand Tab (February 2, 2011). Please note data were not available for periods of 1952-1953 and 1955-1956 (CDFG Grand Tab, 2011).

In May 1995, the Anadromous Fish Restoration Program Core Group recognized that the Fall-run Chinook salmon in the Merced River required attention to restore and to protect the in-stream and riparian habitat. The organization developed a plan designed to ensure the long-term sustainability of physical, chemical, and biological conditions needed to meet production goals for Chinook salmon through restoration and protection of the stream ecosystem (United States Fish and Wildlife Service, 1995). California Fish and Game estimates of the natural production of the Merced River adult fall-run Chinook salmon are shown in Figure 12. The Central Valley Improvement Act was enacted to improve the fish and wildlife habitats of the Central Valley and Trinity basins. The Act mandated that federal and state agencies utilize all reasonable efforts to improve and rehabilitate the natural production of anadromous fish in the Central Valley Rivers and streams, so that they are sustainable on a long-term basis at levels not less than twice the average levels attained during the period of 1967-1991 (Department of Water Resources, 1999). However, complex alterations to biological systems are often beyond the control of managers because they lie outside the perimeter of their jurisdiction (Pringle, 2001).

1.2.5 Factors That Influence Reproductive Success of Salmon

Fall Chinook salmon in the California Central Valley typically spawn from mid-October through December and are brood hiders (Nielsen et al., 1994). Females construct nests by constructing a shallow depression, or redd, in the gravel with their caudal fin. During redd construction, females lay their eggs where one or more males deposit their milt. The female then covers the egg pockets with loose gravel. Depths at which eggs are buried vary in accordance to female size and can range from 30 cm (e.g., Devries, 1997) to 45 cm (Geist, 2000). The female will repeat this action, depositing one to several pockets within the redd and moving upstream as she works (Peterson and Quinn, 1996). The excavation process removes most silt and debris, leaving a highly porous substrate and allowing for increased flow and oxygenated waters for the incubating eggs (embryos). The incubation period of the developing embryos is between 40-50 days (SJRRP 2010) and is highly dependent on thermal units that the embryos receive. Moreover, for salmon, a large but highly variable proportion of lifetime mortality takes place between the time fertilized eggs are deposited in the gravel and fry emergence several months later (Peterson, 1996). Limiting factors for embryo development and fry emergence include water temperature, DO, ammonia, ammonium, and suitable hyporheic flow and substrate permeability (Malcolm et al. 2006).

Water temperature. Water temperature directly influences metabolic rates, physiology, and life history traits of Pacific salmon (Brett, 1962). Chinook in California's American River have been observed to spawn when temperatures fall below 15° C (Williams, 2001a).

Water temperature ranges for emergence may vary significantly across species; however, in Chinook salmon, the temperature range is between 10°C and 14°C occurring over a period of 40 to 60 days (Piper et al. 1982). In most cases, after the alevin has converted the majority of the yolk reserve, exogenous feeding may begin and emergence may then occur. Temperatures above optimal levels can alter metabolic rates by decreasing the efficiency of yolk-to-tissue conversion (Heming 1982), and premature hatching may result. These premature juveniles may not be as successful in their ultimate survival. In a laboratory study, Brett (1952) showed that juvenile Chinook salmon acclimatized to a temperature of 20°C, but favored locations where the temperatures ranged between 12°C and 13°C. Fifty percent of the population died when temperatures exceeded 25°C, and in this laboratory setting, fatalities occurred when the temperature was between 24-24.5°C (Brett, 1952).

Dissolved oxygen (DO). DO is one of the most important indicators of water quality for aquatic life and is essential for both plants and animals. For salmon, the amount of DO required—not only to sustain life but also to support important physiological processes, such as tissue growth, organ development, and metabolic rates—changes as salmon pass through various life stages. For embryos and larvae incubating within the hyporheic environment, through-gravel flow is also important. The developing salmon ova require cool, clean, and highly oxygenated water (Peterson, 1996) for respiration and to flush away waste metabolites (Crisp, 1993). For instance, in a field study of Atlantic salmon (*Salmo salar*), when DO content fell below 7.6 mg O_2/L, survival rates were negligible (Malcom, 2003). For Chinook salmon, lethal DO levels may be lower, but this has not been fully evaluated (see below). Hypoxia, or lack of adequate oxygen supply, during incubation can impact future life stages (Mason, 1969). The sublethal consequences include altered rates of embryological development, increases in the length of time to emergence, and decreases in fry size (Spence et al., 1996).

Salmon need both an appropriate oxygen tension gradient to move oxygen into the blood as well as adequate oxygen to satisfy their metabolism needs. Saturation values of oxygen vary in accordance to temperatures (Davis, 1975). The fertilized egg obtains its oxygen via a passive-diffusion process from the environment of the hyporheic zone. After the salmon has emerged, the circulatory system of the fish is able to extract the oxygen from the water. Fertilized eggs may demand less than 2 mg O_2/L; in contrast, in the post-hatch phase, the alevin may require up to 10 mg O_2/L (Alderdice et al. 1958).

Silver et al. (1961) reported in a laboratory experiment with steelhead trout (*Oncorhynchus mykiss*) that no embryos survived to hatch successfully at 1.6 mg O_2/L DO, but had 100% survival at 2.5 mg O_2 /L. They found reduced growth and extended hatching period for concentrations lower than 11 mg O_2/L.

According to Geist et al. (2006), who conducted field studies of fall-run Chinook salmon, initial DO levels as low as 4 mg O_2/L over a range of temperatures from 15° C to 16.5 °C did not affect embryo survival to emergence. There were no significant differences in alevin and fry size at hatch and emergence across the range of initial temperature exposures. The number of days from fertilization to eyed egg, hatch, and emergence was highly related to temperature and DO; fish required from 6 to 10 days longer to reach hatch at 4 mg O_2/L than at saturation and up to 24 days longer to reach emergence. Bjornn and Reiser (1991) endorsed similar levels of DO compared to Malcom's (2003) for the growth of a vigorous embryo in an intra-gravel environment; the DO must average 8 mg O_2/L. Additionally, that DO should not drop lower than 5 mg O_2/L, and should be at or near saturation for successful incubation. Pacific Northwest

government agencies agree that a one-day minimum criteria concentration of DO within the intra-gravel zone should be in the range of 5-8 mg O_2 /L (Brown and Hollack, 2009), while the EPA (1986) set a mean value of 6.5 mg O_2/L and a one-day minimum of 5 mg O_2/L for success of the developing embryo.

Ammonia. Metabolic wastes, such as ammonia, may also have serious implications for early developmental stages of salmon, including retardation of early growth and mortality (Burkhalter and Kaya, 1977). In aquaculture systems, the concentration of ammonia is often a limiting water quality parameter and is the most important parameter after DO (Thomas and Piedrahita, 1998). The foremost waste product as a result of metabolizing protein in teleost fish is ammonia (Wood, 1993). The continuous excretion, predominately through the gills, is dependent on protein intake, metabolic efficiency, and accumulated ammonia concentrations in the aquatic environment (Dosdat et al., 2003).

Exposure to ammonia levels as low as 0.05 mg NH_3-N/L may yield detrimental effects to developing embryos of rainbow trout (*O. mykiss*). As damage to gills, skin, and internal organs ensues, the effects may prove fatal as the fry are unable to complete the hatching process and may perish when partial hatching occurs. Numerous fatalities were recorded as the sac fry perished with only the head protruding from the egg casing (Burkhalter and Kaya, 1977).

Hyporheic flow and substrate permeability. Embryos and alevins have a long contact time with the intra-gravel environment. Water quality parameters of this environment are important signals about well-being in early life stages of salmon populations. Development of the embryo can be stunted and future performance arrested by exposure to groundwater that has experienced long residence times (Malcom, 2003). Intra-gravel water quality is not entirely controlled by surface water quality, and various parameters may be altered significantly by the intrusion of groundwater (Soulsby et al., 2001). The temperature and DO content in the hyporheic spawning gravel are influenced by groundwater and surface water interactions. The intrusion of low DO groundwater to spawning gravels, which is a natural feature of the hyporheic zone, has the potential to substantially restrict juvenile salmon recruitment (Figure 13; Malcom, 2005).

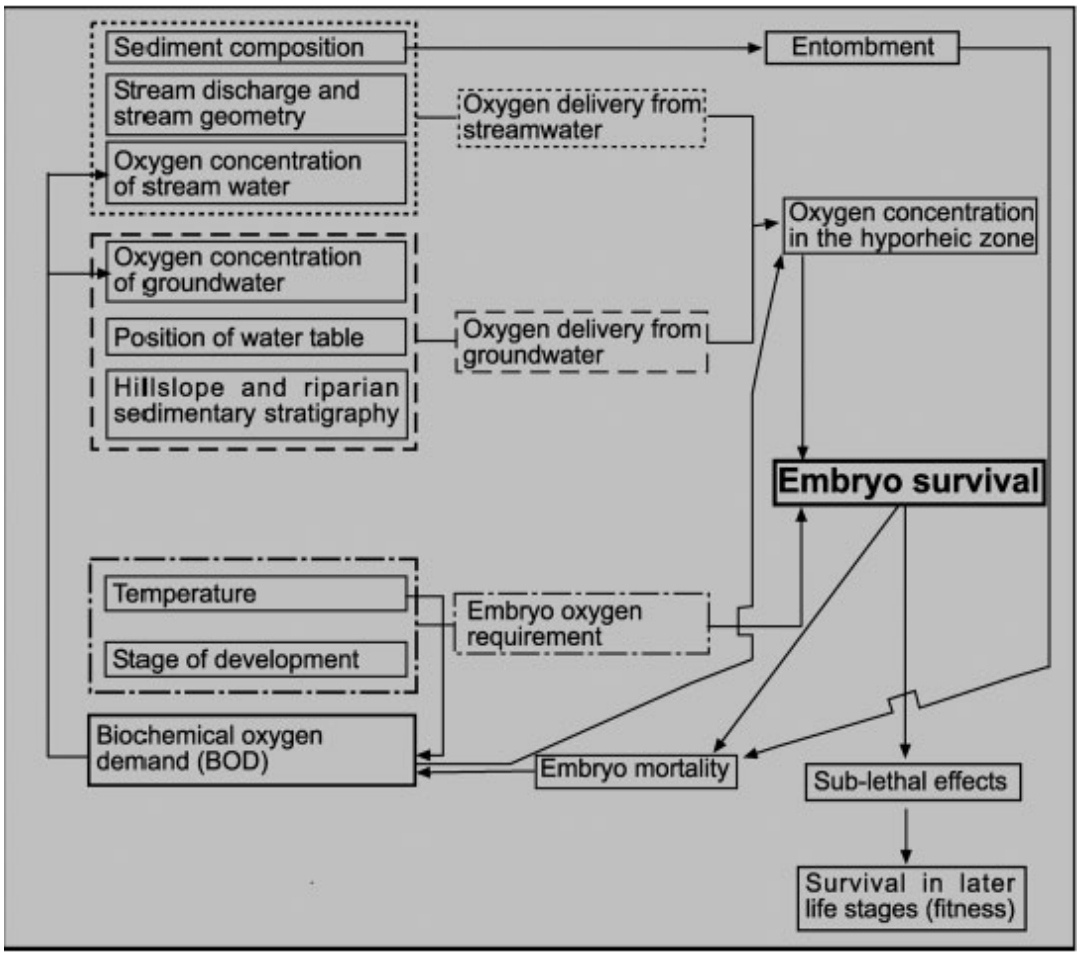

Figure 13 Conceptual diagram showing the complex interaction of processes that can influence salmon embryo survival. Hyporheic water quality is determined by the relative contributions of groundwater (as indicated by dashes: ---) and surface water (as indicated by dots: ……), which are in turn influenced by a variety of interacting physical and chemical processes. The oxygen requirement of embryos (as indicated by alternating dashes and dots: _._._.) interacts with oxygen availability in the hyporheic environment to determine survival. The oxygen demand of embryos depends on a combination of metabolic rate and respiring mass, which is influenced by embryonic stage and water temperature (Malcolm, 2005).

1.2.6 Hydrological Connectivity of the River Corridor

Hydrologic connectivity is a “water-mediated transfer of matter, energy, and organisms within or between elements of the hydrologic cycle” (Ward, 1989, 1997; Pringle, 2001). Ground- and surface water are interconnected as a single resource that maintains the balance of life (Winter, 1998). When this balance in hydrological connectivity between the ground- and surface water and their respective entities is disrupted, it can lead to the extinction of various species. In this study, the entities include riverine-riparian/floodplain and riverine-groundwater. Much of the earth’s surface has been manipulated, altering the drainage framework of rivers that once formed a

predictable structural system affecting watershed geochemistry, topography, climate, vegetation, and life in the riverine and terrestrial ecosystems. These hydrological alterations have disrupted reserves and exploited aquifers through extensive feedback loops (Pringle, 2001).

The hyporheic zone is an active transitional region between the surface stream and groundwater. It is influenced on a number of scales by water movement, permeability, substrate particle size, resident biota, and the hydrochemical composition of the stream and adjacent aquifers (Boulton, 1998). The connectivity between different habitats is dynamically linked to hydrological connectivity, both between the landscape and within the riverscape itself (Pringle, 2000).

The riparian zone is a vegetative corridor of land adjacent to the hyporheic zone of the river where there is significant interaction between groundwater and river water. It is a transitional area between aquatic and upland ecosystems. For small streams, it can be only a short distance (from meters to hundreds of meters) laterally from the channel margin. For larger rivers, however, it can extend for kilometers (Poole, 2001). Riparian zones, which usually have heterogeneous structures, connect streams to their watersheds, consequently allowing them to alter or integrate the concentrations of individual chemical species before entering a riverine system (Osborn, 2006). Surface and subsurface water runoff flowing through the riparian zone can acquire the chemical signature of the exchangeable cations present within the porous media. Restoration of riparian zones can improve surface water runoff that has reducing conditions and subsurface groundwater connections to the hyporheic zone. Analyses of the hydrochemistry of soil exchange would benefit efforts to accurately predict the chemical composition of stream water (Smart, 2001).

Topography, geology, and human interventions are limiting factors that disrupt the lateral connectivity of these various entities. The riparian zone, which floods periodically, facilitates the exchange of water, nutrients, and sediments, thereby increasing its connectivity and driving the biological processes that contribute to the ecological integrity of the streams and rivers (Ward, 1989). Floods encourage lateral connectivity of streams with floodplains and riparian systems. They offer an interconnection of the stream and the floodplain, a major driver of energy and nutrient transfer. One ecosystem function of the floodplain is to improve water quality by filtering pollutants and increasing biogeochemical cycling. Another is to offer refuge and a rearing habitat for developing young salmon (Sommer, 2001). The floodplain in this study has been replaced with dredger tailings. Natural riparian corridors often have greater diversity of wildlife and higher concentrations of plant and animal communities. Fluctuations in the water levels drive succession patterns of vegetation and offer highly oxygenated water at cooler temperatures. Floods are a natural part of the dynamic equilibrium in stream systems (Pringle, 2001).

In order to meet demands for supplies of water and flood control, numerous dams have been built around the world. Using state-of-the-art technology and cutting-

edge engineering techniques, the construction of these various dams was undertaken with little to no thought for aquatic or terrestrial life. The presence of a dam in a river system is one of the most significant disruptions that humans have introduced to various hydrological systems across the world.

The development of dams to manage water flow, flood control, and diversion for agriculture has impacted the timing of high river flows, river temperatures, and sediment supplies to lower rivers. One of the consequences of damming rivers in California is the severe reduction of the spawning habitats for Pacific salmon. For example, the Chinook salmon and Steelhead (*Oncorhynchus mykiss*) are classified as “threatened” under the Federal Endangered Species Act due to the drastic changes in their habitat conditions, such as location, water temperature, and suitability (Stillwater Sciences, 2001; Vogel, 2003).

In early attempts at habitat restoration, fish ladders were built around the dams to solve location problems within the habitat and to facilitate the salmon’s return to their spawning grounds. However, many such attempts had problems with design or functioned poorly. Most seemed to disorient the fish, elevate their stress levels, and increase their mortality rates. Even fish ladders that were built with the salmon’s swimming abilities in mind failed to consider the predatory aspect. Mortality rates of adult salmon at various fish ladders bypassing the dams along the Columbia River were between 5% and 25% per impoundment (National Research Council, 1996). Fish hatcheries were built around the world to supplement the salmon fry numbers; the implementation of such hatcheries has indeed forestalled the decline of the salmon. However, they are not the only solution. Only 13 salmon returned to California Department of Fish and Game Merced River Fish Hatchery in the winter of 2008. The 33,000 fry were trucked downstream rather than released along the Merced River. Fish hatcheries have failed to resurrect salmon runs in France, Scotland, England, Eastern Canada, Oregon, and Washington (Montgomery, 2003). We are approaching a time when serious restoration efforts need to be made. The salmon is teetering on the brink of extinction in the lower Tuolumne and Merced River system (Mesik, 2009, 2010).

Increased flows within a stream system decrease the effects of subsurface and groundwater flows of contaminants. The San Joaquin River Agreement has implemented additional releases of water to entice the return of salmon in November and to help the smolts in April reach the ocean (California Department of Water Resources, 2005). Until 2013, during critically dry years, the Merced Irrigation District was not required to release the additional water flows to the Merced River. The Bay Delta Conservation Plan may implement more natural flow patterns, which may improve current marginal conditions (Bay Delta Conservation Plan, 2013).

Many populations of wild salmon are in decline worldwide, most notably due to the loss of suitable spawning grounds and conditions (Stanford, 2005). Management of river temperature and water quality during spawning season is crucial to the survival of this sensitive anadromous fish. It is probable that faster-moving water leads to colder and cleaner water. “Among salmonid fishes, a large but highly variable fraction of the

life-time mortality takes place between the time fertilized eggs are deposited in the gravel and when they emerge as fry several months later" (Peterson and Quinn, 1996).

The most straightforward approach is to strategically release water at times that correlate to the needs of the ecosystem. Flows should be designed to consider the entire riverine ecosystem, including surface-groundwater systems (Naiman, 2002).

Chapter 2 Methods

2.1 Hydrology Methods and Analyses

2.1.1 Monitoring Wells, Ponds, and Pressure Transducers

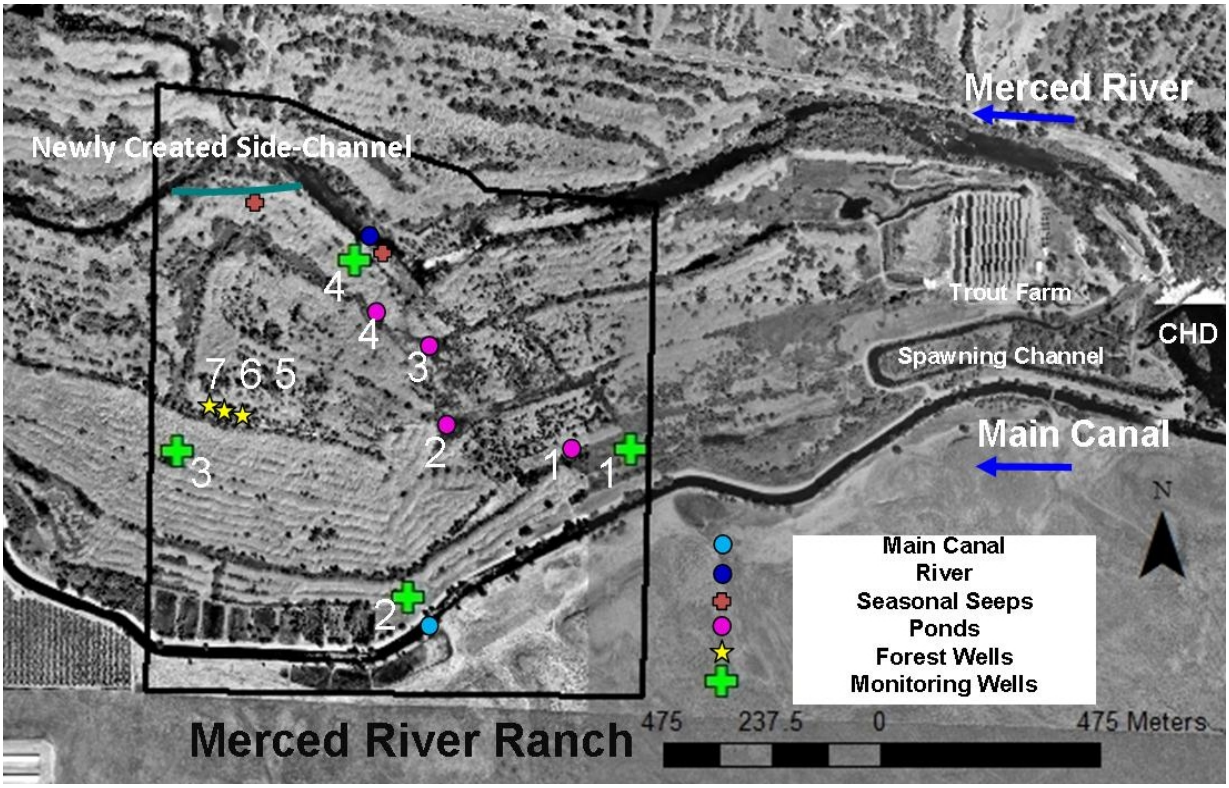

Figure 14 Locations of the pressure transducers and water quality sample sites. The pressure transducers were placed in swale ponds and monitoring wells at the Merced River Ranch. The newly created side channel is drawn in blue-green. The seasonal groundwater seepage sites are approximate. Note the upstream location of the trout farm and spawning channel. Basic GIS map courtesy of Stillwater Sciences.

At the MRR and in the Dredger Tailing Reach, the gold-dredging process left behind a network of channels and swale ponds. This network complicates the flow paths of subsurface waters that seep into the stream. Two transects of monitoring wells were installed, four wells in 2006 and three wells in 2011, to measure pressure gradients inundation and recession in the floodplain over the course of a year. In 2011, additional pressure transducers were placed in swale ponds in a transect between the Main Canal and the Merced River (Figure 14).

The four primary monitoring wells (MW-1, MW-2, MW-3, and MW-4) were all placed in the dredger tailings to maximize the observational area within the MRR property boundaries. They were installed with a sonic, rotary-vibrating drill that is capable of boring through the cobbles. The sonic drill rig was mounted on tracks, enabling it to negotiate the difficult terrain of the cobbles. All wells were drilled down to

the Mehrten Formation (personal communication, Bean, 2010). The well pipes were slotted three meters above the Mehrten Formation.

MW-1, located on the easternmost edge of the MRR, is surrounded by wetlands. The well was drilled initially through 0.025-0.052 m of gravel for the first 0.16 m, through silty sand for 1.52 m, reaching lean clay at 3.66 m below ground level, bgl. The water table was reached at 2.13 m bgl. The vegetation can be described as predominately willows, Himalayan blackberries, elderberry bushes (which may be a habitat for the endangered valley elderberry longhorn beetle), Valley oak, and Fremont cottonwood. Although this area has been disturbed in the past, the Valley oaks are approximately 80 years old.

There are more fines in the soil, and growth of invasive and native vegetation has occurred since the dredging for gold. The ponds that surround the well are thickly matted with pennywort, duckweed, and azola. Cattails exist around the perimeters of the year-round ponds.

Figure 15 Drilled down to the Mehrten Formation for the Forest Wells. Note the dry yellow, white, and red fine porous material.

MW-2 is located closest to the canal on a leveled field of cobbles. This well was drilled through highly porous materials. The well was initially drilled through cobbles 7.62 cm or greater for the first 0.3 m, then sand with gravel or gravel with sand until lean clay was reached at 11 m blg. Vegetation is sparse; there are only a few willows surrounding this well.

MW-3 is in the middle of a vast landmass that has been extensively dredged. The width of the gullies between the rows of tailings is negligent and virtually no vegetation exists. The sonic drilling rig bored through greater than 8 cm cobbles for 3.4 m before reaching poorly graded sand. The Mehrten was hit at 5.5 m bgl.

MW-4 is located closest to the stream. The well was drilled through gravel and 8 cm cobbles for the first 2.14 m, before reaching sand with silt and gravel. At 5.5 m bgl, clay was reached, yet drilling continued; at 9.14 m blg, a layer of dark grey poorly graded sand was found. Located 30 cm below at 9.45 m blg, the Mehrten's composition is "lean clay: pale yellow, dry, 100% fines, low plasticity and high toughness" (Geomatrix, 2007).

Figure 16 Forest MW-6 casing designed to protect the wells against vandals. The ponded water has receded since first viewed in April 2011. This photo was taken 9/13/11.

For this study three additional monitoring wells were drilled down to the Mehrten Formation in an area undisturbed by gold-mining and dredging activities (Figure 15). Several attempts to drill wells in closer proximity to the stream were made. However, two-meter blg 7-9 cm stones would unbalance the shaft of the auger and prevent further drilling. Instead, an area that was once ponded in April 2010 was selected. In June, at the start of drilling, the surface was dry. The area is surrounded by cottonwood trees and willows set below an elevated road.

The Forest Wells (FW) were first drilled with a hand auger, then with a 5.7 cm diamond core bit attached to a gasoline-powered mighty auger. Soil types were noted and well logs can be viewed in Table 3 of the Appendix. These well pipes were slotted for the final 3 meters in depth and placed in a triangular formation. Forest Monitoring Wells 5 and 7 (MW-5 and MW-7) were drilled on June 17, 2011. Forest Monitoring Well 6 (MW-6) was drilled on June 15, 2011 (Appendix, Table 3).

All of the wells were sealed with sand and were protected with a larger diameter iron pipe set in concrete ¼ m below ground level. A metal cap was designed to lock the well casing in an attempt to prevent vandalism and theft (Figure 16). Forest MW-5 was surveyed with a Leica SR 530 GPS system, utilizing the real-time kinematic procedure for location and elevation. Forest MW-6 and Forest MW-7 were surveyed for location only (Appendix, Table 4). Determining elevation for these wells involved the use of stakes, string, a level, and a ruler.

Water depth in the monitoring wells was measured periodically with a Solinst Mini Water Level Meter by deploying the tape into each well until the buzzer sounded, signifying the depth to groundwater. This is an unconfined aquifer; the depth to groundwater coincides with the water table.

In situ pressure heads were measured with a water level logger (Solinst Junior). These measurements were downloaded periodically and barometrically corrected utilizing information recorded with a Barologger Gold.

The pressure transducer or level logger within the monitoring well measures a combination of water pressure and air pressure (Figure 17). In order to obtain the actual water pressure, one must subtract the air pressure. The groundwater elevation is calculated by taking the known elevation, subtracting the line length, and adding actual water pressure.

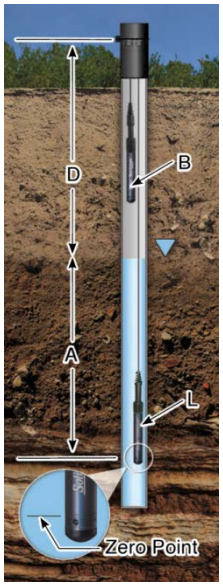

Figure 17 Actual water pressure (A) is equal to the levelogger pressure (L) – barometric pressure (B) (Solinist Levelogger Manual).

2.2 Groundwater Flow-Modeling Methods

2.2.1 2-D Model Conception & Description

Field conditions of complex hydrological systems are often too complicated to be precisely simulated by a numeric model, and assumptions and boundary conditions can be restrictive (Zhang, 2012). Initially, a two-dimensional groundwater model was created using the USGS computer simulation program MODFLOW. Our goal was initially to use MODFLOW to model the potential seepage from the main canal to the Merced River through two layers of distinct soil types: the upper layer consisting of coarse rocky cobbles, and the lower layer of sand and fine sediment that had been buried under a layer of cobbles for almost eighty years. These two layers are perched upon the underlying clay of the Mehrten Formation.

The bulk density was estimated by visual assessment in place to be 2203 kg/m^3 (Stillwater, 2004). Particle-sized distributions were examined from the 26 sample locations for the grain diameter at 50% finer D_{50} mm, converted to the radius of the grain R_{50} mm, R_{50} mm. Given that the bulk density (ρb) of coarse rock is 2203 kg/m³, we were able to calculate the hydraulic conductivity utilizing the following formulas:

$$\text{Volume} = 4/3\pi\,(R_{50})^3 \qquad (1);$$

where the volume of a sphere is equal to 4/3π times the radius of the grains cubed.

$$N = Vs/V \qquad (2);$$

where the number of grains (N) is equal to volume of the solid grains divided by the total volume.

$$s = 4\pi r^2 \quad (3);$$

where the surface area (s) is equal to 4π times the radius (r) squared.

$$S = N*s \quad (4);$$

where specific surface (S) is equal to the number of grains (N) times the surface area (Kozeny Carmen equation).

$$k = c\Phi^3/S^2 \quad (5);$$

where intrinsic permeability (k) is equal to the shape factor of a grain (c) times the porosity (Φ) cubed divided by the specific surface (S) squared.

$$\Phi = 1-\rho b \quad (6);$$

where the porosity (Φ) is equal to 1- the particle density (ρb).

$$K = k * g\ \rho/\mu \quad (7);$$

where hydraulic conductivity is equal to intrinsic permeability (k) times gravity and pressure (ρ) divided by the viscosity of the fluid (μ).

The average hydraulic conductivity of the 26 sample sites for the upper layer of coarse cobbles was 8.6×10^{-2} m/s. No data were available for the lower layer of sand and fine sediment. In an attempt to discover possible duplications of the environment, three different simulations were modeled with varying lower-layer hydraulic conductivities. We chose grain sizes with R_{50} of 0.25mm, 0.05mm, and 0.025 mm. Elevation, positional, and depth data from Stillwater's Volume and Texture Analysis allowed us to create the geometry of the model and to assign the elevations of the two layers (Stillwater, 2004).

Assumptions and boundary conditions of the data that were obtained from the Merced Irrigation District, California Irrigation Management Information System, and Stillwater Sciences are correct. Additionally, the assumption that seepage and infiltration are uniform and continuous throughout the year between the Main Canal to the south and the Merced River to the north is also correct.

We transformed and grouped the three-dimensional problem into a two-dimensional problem by neglecting the x-position of the wells. The complex topography was generalized using a first-degree, interpolating polynomial to create a simpler geometry. It was assumed that each layer of soil is homogeneous and has a hydraulic conductivity uniform throughout the entire study site. The two layers of soils perch upon the impervious underlying clay of the Mehrten Formation. We were able to use a no-flow boundary condition.

2.2.2 3-D Modeling Using Groundwater Vistas as User Interface with MODFLOW with the Assistance of David Bean, Amex

To gain insight into the upstream forces that might drive the flow of groundwater three-dimensionally across and through the Dredger Tailings Reach downstream from Crocker Huffman Dam between the Main Canal and the Merced River, a larger scale of the groundwater model was created. We mapped the project site in relationship to the upstream pressures, including possible upstream point sources of pollution. This broader floodplain section incorporated the MRR, the Crocker Huffman Dam and its impounding waters, the Merced River channel network, the Main Canal, the salmon spawning channel, TF, and CDFG Merced River Fish Hatchery.

Data collected for this model included: flow rates of the Main Canal from Merced Irrigation District; flow rates of the stream downstream from Crocker Huffman Dam (Figure 4) and from Merced Irrigation District; surface water elevation of the Merced River from Cramer Fish Sciences; and my own groundwater elevations, which were used as target information to validate the model. Evapotranspiration for Merced County (CIMIS) Station #148 was added as a zone property evenly to every cell in the top layer along the stream corridor to finetune the result.

An attempt was made to utilize a digital elevation map (DEM) generated by Stillwater Sciences in 2001, accurate to 6 $x10^{-2}$ m. Unfortunately the map did not cover upstream pressures of the Crocker Huffman impoundment, the salmon hatchery, the trout farm, the salmon spawning channel, and the diversion point of the Main Canal. Some cells also lacked data due to the reflective nature of the stream and ponds. A DEM was obtained from Global Mapper for the area accurate to 0.5 m, which encompassed an area of 2,000 m x 3,700 m, and a photo BIT map was attached. The topographical structure of ravines and stacks of cobbles are beyond the scope of this MODFLOW project.

The numeric model grid was set to 200 x 370 with three layers to specify the aquifer's properties, each cell representing 10 meters. In an attempt to duplicate realistic conditions, a transient model, simulating change in head with time, was calibrated by matching measured groundwater levels of MW 1-4 over 13 time steps, each consisting of 30 days. Twelve models were created and tested using inverse, or automatic-calibration, codes provided by Groundwater Vistas. Each simulation utilized a "preconditioned constant gradient package 2" simulating pumping and reiterations (Rumbaugh, 2011).

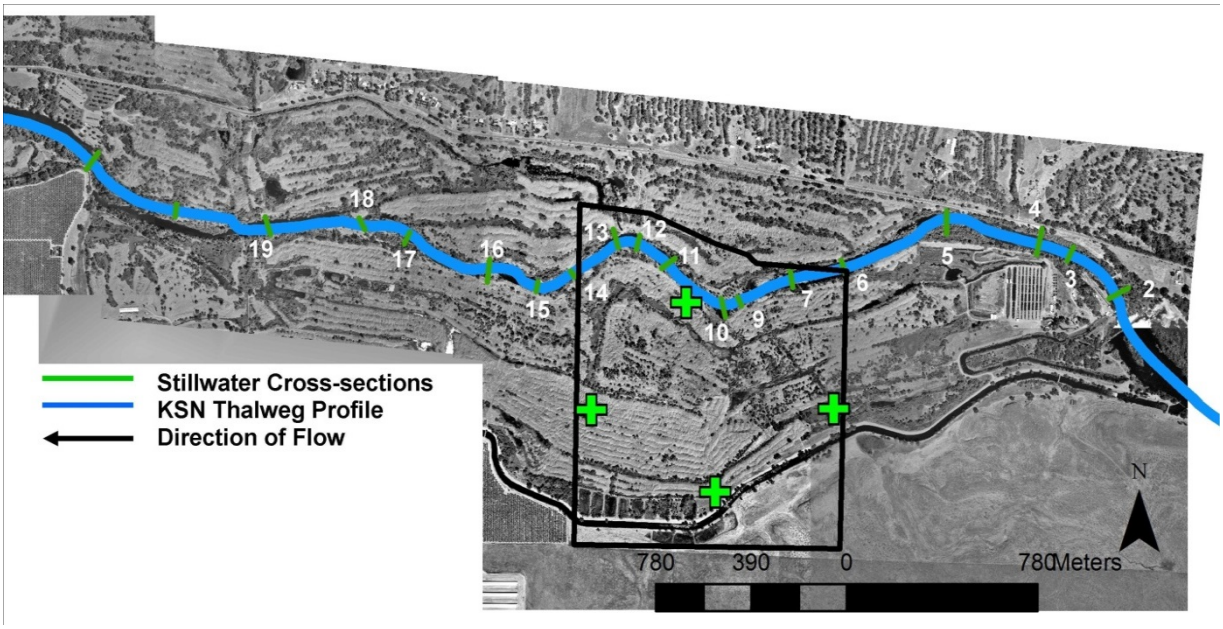

Figure 18 Thalweg profile and cross-sections within the Dredger Tailings Reach (Stillwater Sciences, 2004). Kjeldsen, Sinnock, and Neudeck Consulting Engineers and Land Surveyors (KSN).

A model developed by Stillwater Sciences for estimating local and reach-scale hydraulic conditions under various flow scenarios offered critical components for comprehending floodplain inundation throughout the system (Stillwater, 2004). Channel elevation data included fine-scale bed elevation at 40 cross-sections and channel thalweg elevations approximately every 30 m throughout the Dredger Tailings Reach (Figure 18). Endpoint locations were recorded using differential GPS. The hydraulic model included surveyed cross-sections, reach distance, water elevation, channel depth, top width, shear stress, and bed texture. This model offered data for top and bottom river elevations for 1.5-year and five-year discharges that were imported into the groundwater flow model as boundary conditions (Stillwater, 2004). Three MODFLOW river packages were smoothly distributed over the longitudinal profile of the river to represent the Merced River (Harbaugh and McDonald, 1996).

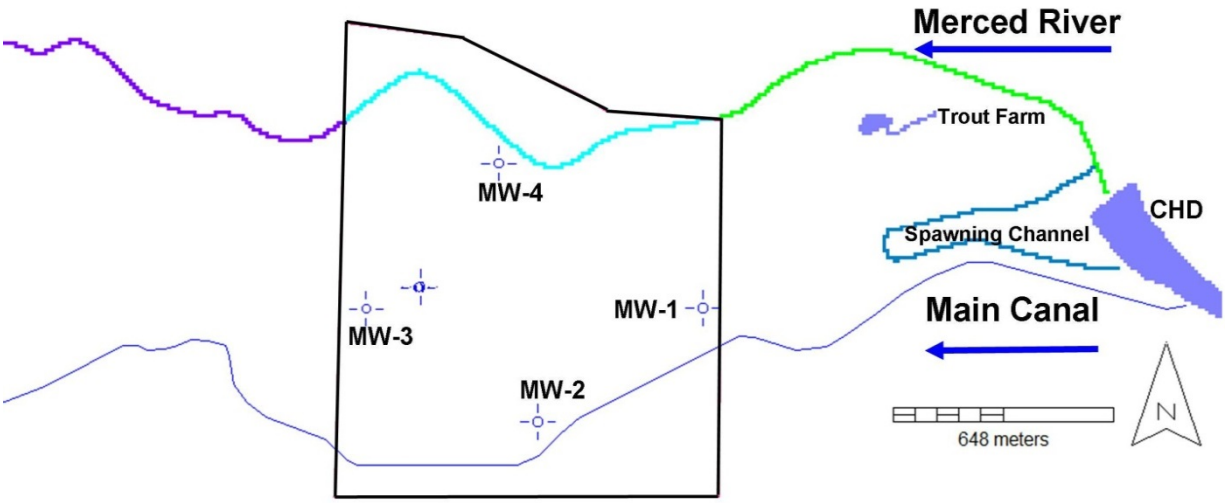

Figure 19 The framework of the MODFLOW numeric model of the Merced River Ranch and its upstream river influences. The Merced River contains three MODFLOW river packages, depicted here in green, light blue, and purple. The spawning channel is incorporated as a river package drawn in dark blue. The Trout Farm and Crocker Huffman Dam (CHD) were installed as a lake package. The Main Canal was analytically drawn into the figure. Groundwater levels of MW 1-4 were utilized as targets to validate the numeric model.

A Groundwater Vistas river package, a simulation where the segment never goes dry, was added to represent the artificial salmon spawning channel. The hydraulic head for this reach was determined by calculating the recharge/discharge rates represented by differences between the Merced Falls Reach and the combined flow rates of the Main Canal and Dredger Tailings Reach, as measured by Merced Irrigation District. This was in agreement with a report prepared for the U.S. Fish and Wildlife Service that stated that the salmon channel diverts from the Merced River 2.83-4.25 m^3/s, the TF diverts 1.4 m^3/s, and Merced River Hatchery diverts an additional 0.17 m^3/s (Vogel, 2007). A conservative figure of 2.83 m^3/s was imported as a constant head for the spawning channel as a river package, while the TF was inserted as a lake package (Figure 19). Crocker Huffman Dam was also incorporated as a lake package with the elevation of the impoundment fluctuating around three meters during the course of the study. The Merced River Hatchery, a salmon hatchery, was omitted from the model because the amount of water it diverts is seasonal. The hatchery raceways are lined with concrete, and the water returns quickly to the river downstream from Crocker Huffman Dam.

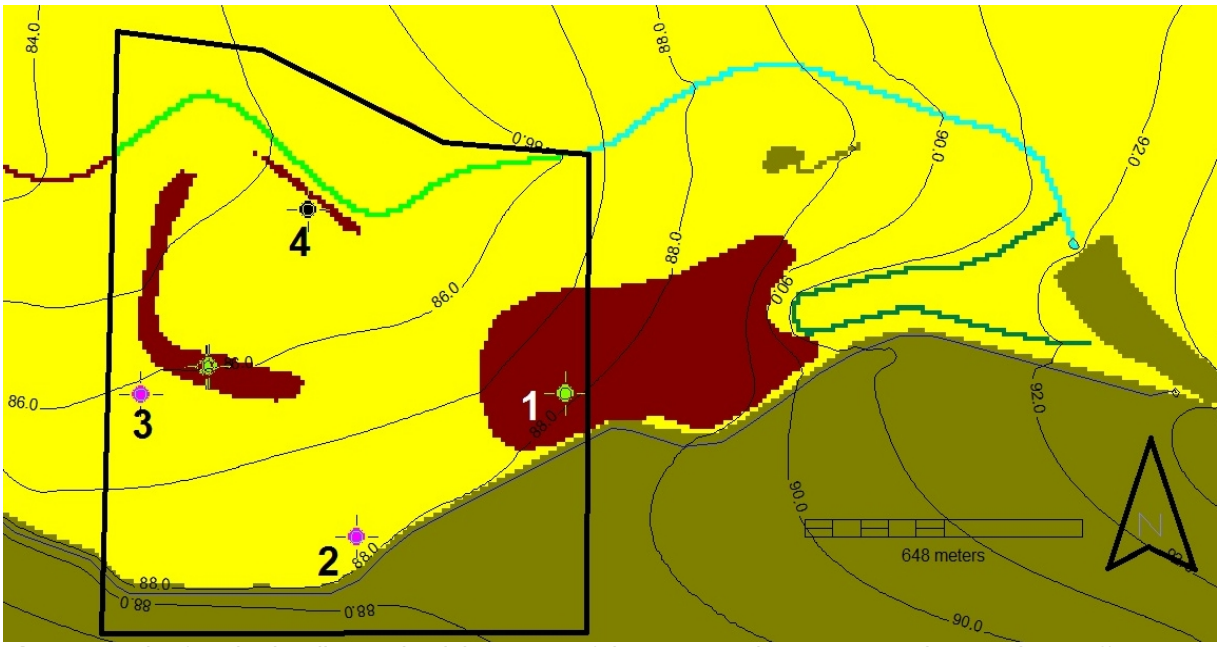

Figure 20 The four hydraulic conductivity zones of the MRR and upstream to the Crocker Huffman Dam. The MF is represented in olive green, clay lenses in russet brown, and the cobbles in yellow. The Merced River is conceptualized by three MODFLOW river packages, depicted here in green, light blue, and purple. The spawning channel is incorporated as a river package shown in dark blue. The Trout Farm and Crocker Huffman Dam (CHD) were installed as a lake package. The Main Canal was analytically drawn into the figure. Groundwater levels of MW 1-4 were utilized as targets to validate the numeric model. Direction of flow is from east to west.

Four homogenous hydraulic conductivity zones were established: the top layer of cobbles set to 20 m/day, the underlying layer of one meter of soil set to 20 m/day, the MF set to 1 m/day, and a clay lens area set to 5 m/day (Figure 20). Another model was designed with the top layer of cobbles set to 20 m/day, the one meter of soil to 5m/day, the MF to 1 m/day, and retaining the clay lens to 5 m/day.

General head boundaries were set to allow water to flow into and out of the model. Our MODFLOW model was manipulated so that flooding was minimal; however, invisible flooding in the cobbles in the near surface could produce faster groundwater/surface water flow through the study site. This may be occurring through the ravines, abandoned channels, and ponds. There may be continuous flow that we did not capture with this model. This flooding could become preferential flow paths.

Calibration of the model was done by performing numerous experiments on each occasion with slightly altered physical aspects, and ultimately breaking the river into three river packages. The calibration goal was to minimize the sum of squared errors between the simulated groundwater levels of MW 1-4 and the groundwater levels measured by the pressure transducers placed in MW 1-4 during the time period between March 2011 and March 2012.

In order to obtain temporal information, Groundwater Vistas tracked particles placed in the aquifer during specific timeframes. Particles were placed in cells along with the groundwater flow. This represents a cell-by-cell groundwater flow simulation.

After the MODFLOW model constructed the output files, the files were input into MODPATH, which utilizes transport mechanisms of the substrate by the fluids' bulk motion. The particles move with the groundwater. The only output is the flow path of the particles through the aquifer. These particles were tracked along with groundwater flow, representing a cell-by-cell groundwater flow. Particles were released in the middle of the top layer and traced the groundwater flow for 13 months, from March 2011 to March 2012. A second experiment was designed to trace the groundwater flow over a five-year period. This longer timeframe was developed utilizing information obtained during the one-year monitoring period and replicating it for five years. The near-surface groundwater flow patterns are beyond the scope of this model.

2.3 Water Quality Sampling and Hydrologic Measurements

To investigate temporal variations in groundwater quality, water was extracted from the monitoring wells by inserting a short length of plastic tubing and applying a vacuum with a portable pump. An equilibration period was needed before the recording of final field measurements. The time needed for equilibration depended on the design of the perforated interval and the hydraulic conductivity of the streambed material (Hvorslev, 1951; Bouwer and Rice, 1976; Freeze and Cherry, 1979).

The wells were evacuated for five to ten minutes (or at least three volumes of the well) to ensure that the water sampled was from the surrounding aquifer. The plastic collection bottles and caps were rinsed three times with the well water prior to obtaining the groundwater samples. Groundwater levels and water quality parameters were then measured and recorded a second time. Water samples were collected, and field measurements for water quality parameters were taken for the Main Canal and the Merced River during this same timeframe. The sample location for the Main Canal was approximately 2,000 meters downstream from the headwaters of the Main Canal, while the sample location of the Merced River was approximately 2,100 meters downstream from the Crocker Huffman Dam (Figure 14).

Figure 21 A panorama view of the newly created side channel of the Merced River. A Jack Russell terrier can be seen quite near the western seep site. Flow direction is from right to left. The design of the side channel is to increase "in-channel habitat complexity" and to "reengineer low-flow and bank-full channel geometry" of the Merced River (Cramer Fish Sciences). River flow is from right to left. Photo taken mid-construction on 10/24/11.

Groundwater seepage was sampled in seasonal locations (Figures 2 and 14). From May through September, the eastern seep was sampled from the bank of the Merced River. After the construction of the side channel, the eastern seep was no longer flowing. The western seep located in the newly created side channel (Figure 11) was sampled December through March from just below the water level (Figure 21). The flow emanating from this seep has been estimated to be 4×10^{-3} m^3/s (personal communication, Merz).

Initial water quality measurements of groundwater were made *in situ*. Water quality measurements, which included temperature (Celsius), DO (% saturation and mg O_2/L), conductivity (µS/cm), pH, pH (mV), and oxidation-reduction potential (ORP) (mV), were taken with an YSI Professional Plus multiparameter reader. The amount of DO in water is a commonly made environmental measurement. Aquatic life requires sufficient oxygen to survive, and measurement of DO is an indicator of overall water quality. The solubility of oxygen in water depends on pressure, temperature, and ionic strength (O'Day, 2009). When describing varying levels of dissolved oxygen in aquatic environments: oxic conditions occur when measurable values of oxygen are present (>0.06 mg/L to about 16 mg/L; >2 µM to 500 µM); low oxygen conditions are less than 4 mg/L; hypoxic conditions exist when the dissolved oxygen falls below 2 mg/L and are stressful for all aerobic organisms; and anoxic conditions occur when 0 mg O_2/L is present, or below detectable level and only anaerobic bacteria can survive (Reinfelder, 2013).

In addition, further exploration of the chemical properties of groundwater and stream water was done by measuring the ORP to determine the availability of electrons in this system. ORP probes are extremely useful tools for monitoring biological reactions within groundwater systems (Gerardi, 2007). While ORP measurements are a measurement of ORP, they reflect the relative concentration of a dominant redox complex, such as DO and bacteria in oxic waters. It is possible that reducing or oxidizing species dissolved in solution alter the accuracy of the measurement DO

concentration (Hauer and Lamberti, 2006). ORP levels reflect the DO content of the water. Moreover, oxidation-reduction conditions are essential in determining the likely oxidation state of nitrogen, iron, and sulfate in the system. Gradients of ORP may be indicative of water flow patterns.

The nature and degree of nitrification-denitrification in groundwater and subsurface sediments is unclear (Hill, 2000). In biological phosphorus removal, fermentative bacteria produce fatty acids in an anaerobic tank with an ORP range that is measured in millivolts (mV). Therefore, the presence of a reducing agent decreases the ORP in biological phosphorous removal from -100 to -225 mV. The ORP scale for nitrification, which is the oxidation of ionized ammonium (NH_4^+) to molecular nitrogen (N_2), is in the range of +100 to +350 mV. In other words, DO is consumed by ammonia and ammonium ions in the nitrification process. The ORP scale for denitrification, which is the reduction of nitrate (NO_3^-) to nitrogen (N_2), is in the range of +50 to -50 mV (YSI, 2008).

For the anion and cation analyses, samples were filtered with a 0.45-µm filter before they were stored at 4C. A Dionex ICS-2000 Ion Chromatograph system was used for measurement of major soluble ionic species, including chloride, nitrate, sulfate, sodium, total ammonium, potassium, magnesium, and calcium in the well samples. A small sample volume was introduced into the system through AS-40 autosampler, and the ions of interest were separated on an ion-exchange column and measured using a system comprised of a suppressor and conductivity detector. AS-18 and CS-12A guard and analytical columns were used to separate the anions and cations, respectively. Five calibration standards were prepared from series of dilutions of seven anion and six cation mixtures of stock standard solutions, and were used to calibrate the instrument response with respect to analyzed ion concentrations. Blanks and instrument check standards were run every 12 samples as a QA/QC procedure. The detection limit for most ions was 0.05 mg/L with a Residual Standard Deviation (RSD) better than 5%.

Samples were collected for total iron, i.e., particle-bound fraction and total dissolved iron, which included the aggregation of iron hydroxide and humic complex iron. For total iron—including the particle-bound fraction—a 10-ml portion of 0.2ml of 6M hydrochloric acid (HCl) was added immediately after collection and stored in the refrigerator overnight. The next day, the sample was filtered through the 0.45-µm filter and then stored in refrigeration until analysis. For total dissolved iron, including the aggregation of iron hydroxide and humic complex iron, after sample collection, it was immediately filtered with a 0.45-µm millipore filter, acidified using 0.2 ml of 6M HCl for a 10ml alloquate, and allowed to sit for 30 minutes prior to storage in the refrigerator. Both total and total dissolved irons were analyzed using the Perkins-Elmer Optima 5300dv, inductively coupled plasma optical emission spectroscopy (ICP-OES) with a detection limit of <1µg/L (personal communication, Zhao, 2012).

In addition to the small representative sample collection, dissolved organic carbon (DOC) and total nitrogen (TN) were measured using a Shimadzu TOC analyzer. This highly sensitive model utilizes a combustion catalytic oxidation/non-dispersive infrared (NDIR) detection method to measure dissolved carbon content and TN in water samples (personal communication, Zhao, 2012).

For the alkalinity titration process, 25 mL of each sample were pipetted into 25 mL beakers. This process was repeated three times for each sample in order to obtain comparable results, as well as an accurate average and standard deviation. Furthermore, in order to avoid contamination caused by different samples mixing, distilled water was pipetted two times, before and after the samples, in the 25mL beakers. The samples were then placed in a SAC80 Sample Changer. The process of titration for each sample was then done using a TIM870 Titration Manager. The TIM870 measures pH change as 0.01M of hydrochloric acid (HCl) is distributed in increments of 0.02mL. This titration process continued until either the sample solution reached a pH of 3.0 or 5mL of HCl was distributed. If the maximum buffer capacity was not reached, then the solution was diluted by 50% and retested (personal communication, Carrillo, 2012).

Chapter 3 Results

3.1 Surface Water and Groundwater Elevations

To understand groundwater flow directions, surface water elevations for the Merced River and the Main Canal were plotted along with groundwater elevations for MW 1-4 and precipitation events (Figure 22). Due to the fact that the level loggers were not recovered, there are only short records for MW-2 and MW-4. For the time period of mid-July to mid-September, the Main Canal's surface water elevation is always higher than that of Merced River, with the result that the Main Canal is the source and the Merced River is the sink, with the general direction of groundwater heading toward the Merced River.

Evaluating the temporal trends in surface water elevations, one recognizes that the stream system in this area is managed by an upstream force that is not natural. Releases of surface water from the Exchequer Dam to the Merced River are done in blocks of time; diversions of water at Crocker Huffman Dam to the Main Canal are also done in blocks of time. These events are obvious in the abrupt change in surface water elevation observed in November and in March. Large seasonal differences in surface water elevations of the Main Canal and Merced River appear to be mostly due to diversions for agricultural use. Surface elevations are also responsive to precipitation events and increase. Following precipitation events in late May and late September of 2006, as well as in early March, late March, early April and early May of 2007, diversions to the Main Canal from the Merced River actually decreased (Figure 22).

The pressure transducers that were placed in the wells allowed us some insight into the connections to the water sources. At first glance, the groundwater elevations all appeared rather stable and did not exhibit much fluctuation. During the monitoring period of July to September 2006, when the Main Canal was in operation for the irrigation season (Figure 22), MW-2 and MW-3 showed slight increases in their groundwater elevations. During this same time period, the groundwater elevation of MW-4 dropped. The MW-4 groundwater responded to the change in surface water elevation of the Merced River. After the irrigation season ended, the groundwater in MW-3 gradually subsided. No information is available after mid-September 2006 for MW-2 and MW-4, as the water level loggers were not present at the time of data retrieval.

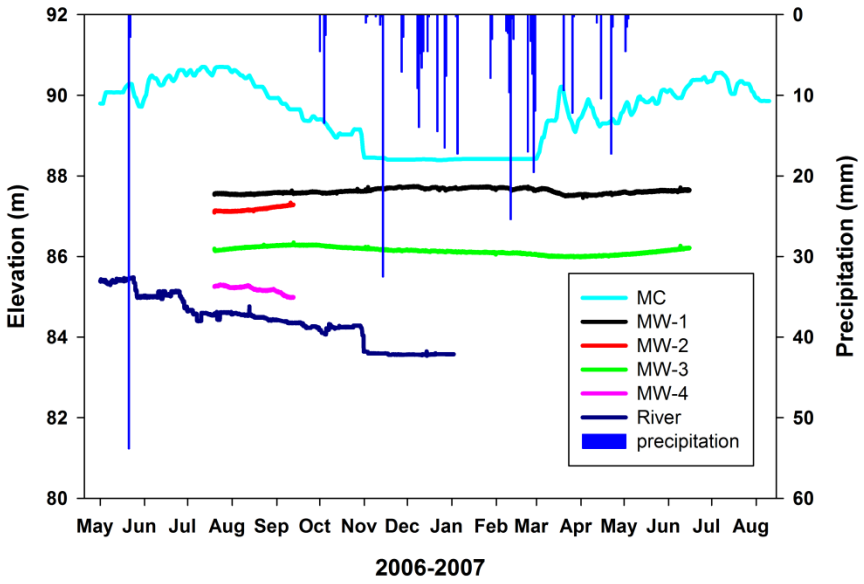

Figure 22 Surface water and groundwater elevations MW 1-4 and for the Main Canal (MC) and Merced River (River) for 2006-2007. Precipitation was measured at Exchequer Dam for the duration of this study (May 2006 to August 2007) is shown at the top of the graph. The retrieval of pressure transducers that were placed in the field in 2006 allowed us to augment the initial groundwater survey of the MRR from 2006. The Main Canal serves as a source and the Merced River as a sink (personal communication, Bean, 2010).

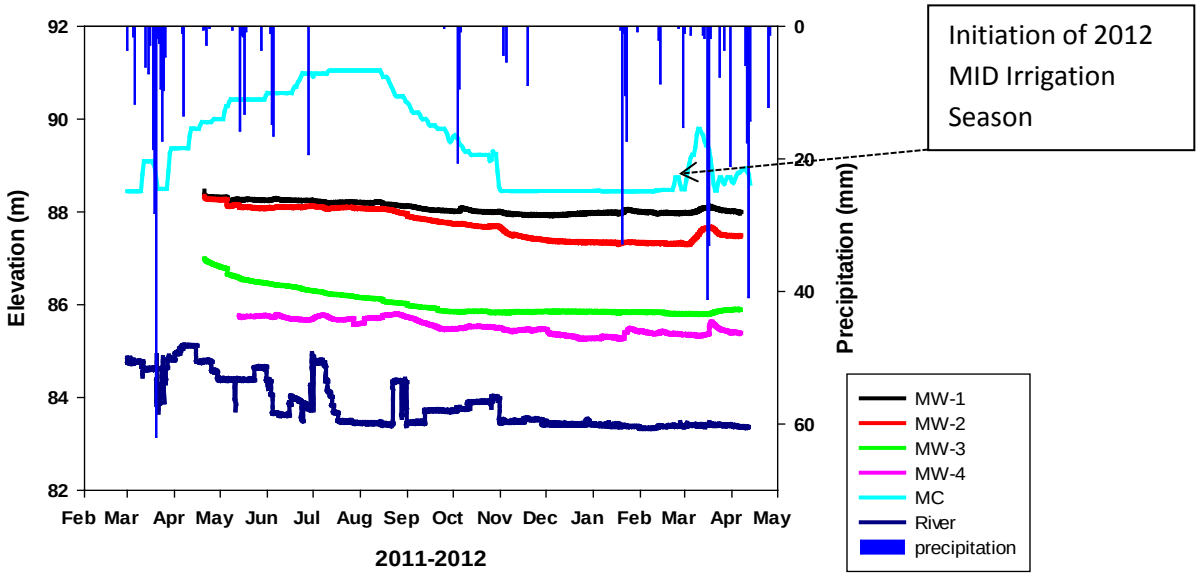

Figure 23 Surface water and groundwater elevations MW 1-4 and for the Main Canal (MC) and Merced River (River) in 2011 and 2012. This figure represents surface water elevation of the Main Canal and the Merced River, as well as the groundwater elevation of MW 1-4. Precipitation was measured at Exchequer Dam for the duration of this study (February 2011 to May 2012). Flow rates were obtained from Merced Irrigation District (MID), and Merced River surface elevations were obtained from Cramer Fish Sciences. The Groundwater Vistas MODFLOW model incorporates this observational data.

For this study, the original four pressure transducers were augmented, and in April 2011, replacement transducers were added to MW 1-4 (Figure 23). Level loggers recorded groundwater levels in various locations, as indicated in Figure 14, during the river flood stage, maximum diversion of water to the Main Canal, and the decline in MRR groundwater levels after the irrigation season had ended. Groundwater elevations in MW 1-3 rose upon the initialization of the irrigation season of March 2012 (Figure 23). The precipitation events that occurred during October and January contributed to an increase in groundwater levels in MW 1 and 4. Decreases in MW-2 mirror the reduction of water level in the Main Canal. Rain that occurred in late March is responsible for the increase in groundwater elevations in MW-4. MW-1, 2, and 3 levels had similar trends as MW-2 and MW-4, decreasing after November, but these did not appear responsive to rain events. Following precipitation events in mid-March, late June and early October of 2011, as well as early and mid-March and early April of 2012, diversions to the Main Canal from the Merced River actually decreased (Figure 23).

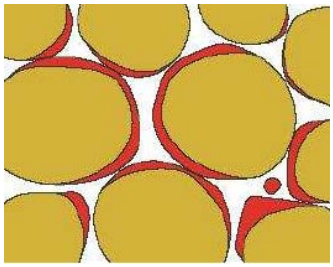

Figure 24 Conceptual diagram depicting an accumulation of fine particles within the pore spaces (Teunissen, 2007).

MW-1 is the most isolated and least similar to the other wells, showing more constant levels throughout the study period. The hydraulic conductivity of the soil and surrounding vegetation seemed to dampen the effects of the hydrological influences of the area. In the vicinity of MW-1, the gullies between the rows of tailings are virtually filled in with matted pennywort (*Hydrocotyle spp.*) and cattails (*Typha spp*.). Furthermore, water appeared to be draining from the settling ponds of the TF down through the ravines. The average pore size of the sand-soil matrix may have decreased with the accumulation of solids (Figure 24). As the ingress of fines into the interstices increased, pore clogging and the resistance of the soil bed both increased. Over time, the sand-soil matrix reached a maximum head loss, and the growth of biomass occurred on the sediment (Teunissen, 2007).

MW-2 is the closest well to the Main Canal and exhibited the greatest synchronization with the canal surface water elevation. In relation to the Main Canal, MW-2 decreased approximately 0.25 m at the cessation of Main Canal's diversion of water in late October of 2011 and increased approximately 0.5 m in mid-March of 2012. The groundwater of MW-2 responded within four days to the surface water in the Main Canal in mid-March. It should be noted that there was a gradual waning of MW-2's groundwater levels from mid-August of 2011 through early March of 2012 (Figure 23).

The level loggers placed in MW-3 recorded the greatest decrease in groundwater levels in the MRR. It gradually dropped 1.25 m over the monitoring period. The only significant subsequent rise of water was due to the precipitation event that occurred in late March of 2012. The increase in groundwater levels was gradual and did not return to the initial groundwater levels recorded at the start of the monitoring period.

The most frequent fluctuations occurred in the groundwater levels of MW-4. These fluctuations were most synchronized with the stream. Increases in groundwater levels occurred with increases in the surface water elevations from July 1 to July 10 of 2011 and then again from August 22 to August 31 of 2011. Precipitation events that occurred in mid-January of 2012 and mid-March of 2012 raised the groundwater levels of MW-4.

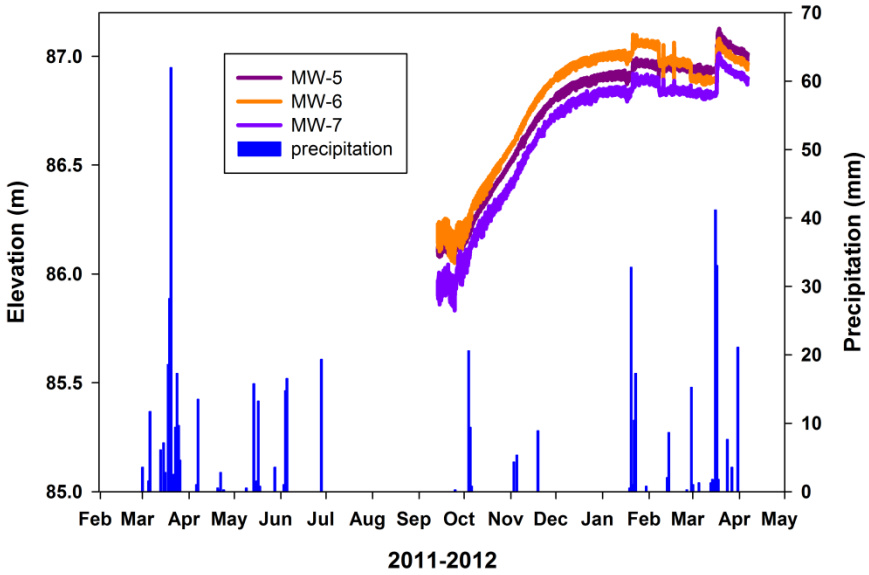

Figure 25 Groundwater levels in the Forest Monitoring Wells and precipitation for 2011-2012. Precipitation was measured at Exchequer Dam for the duration of this study (February 2011 to May 2012). The transducers placed in the Forest Monitoring Wells reflected a dramatic increase in groundwater levels during winter rain events. Declines in groundwater levels during this timeframe were due to pump tests.

The groundwater levels in the Forest Monitoring Wells (FW) did not correlate with the levels found in Monitoring Wells (MW) 1 through 4. The FWs' water levels indicated a gradual increase in groundwater levels during the months of October 2011 to January 2012, while MW 1-4 were decreasing during this same timeframe. FWs responded to precipitation events of February through May 2012. An attempt to duplicate the drilling and screening method of the MWs was made for the FWs. Though the wells extended downward through soil levels until they reached the Mehrten Formation (MF), they were drilled using different equipment than the MWs, and sand screens for the entire wells were not included. The MF and the lens of clay-sand soil above offered a stratigraphic, perched aquifer.

Due to the delay because protective well casings (Figure 16) had to be constructed, the pressure transducers were not placed in the Forest Monitoring Wells until September 2011. After a long, hot summer, the cottonwood trees drained the formerly ponded area of April 2011. The water level loggers were placed in time to record the cessation of evapotranspiration of the cottonwoods in late September 2012

(Figure 25). Decreases in the groundwater level profile were caused by pump tests and water samples that were taken in January, February, and March of 2012 (Figure 25). The loggers recorded a dramatic rise in groundwater levels with the rain event that occurred mid-March of 2012.

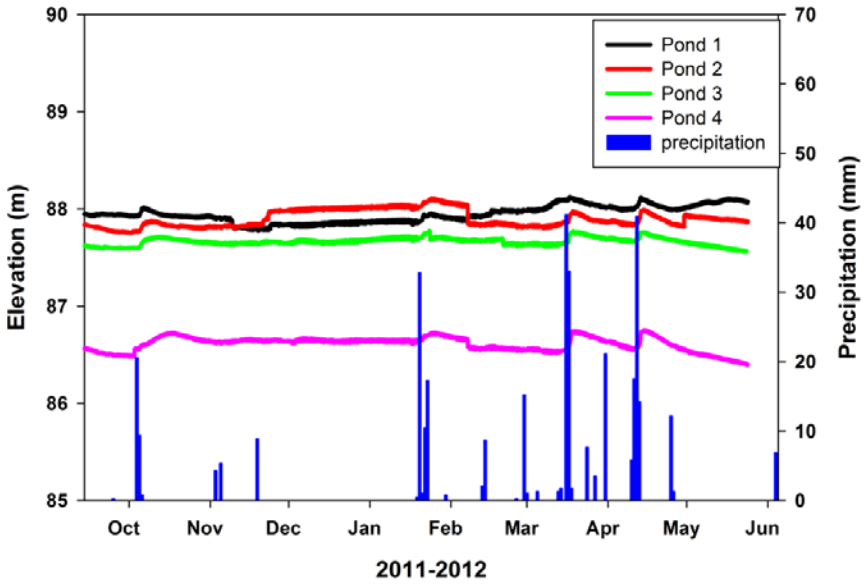

Figure 26 Surface water elevations in MRR ponds for 2011-2012. Precipitation measured by the California Data Exchange Center (CDEC) at Exchequer for the period of late September 2011 to June 2012. A transect of swale ponds from the Main Canal to the Merced River was selected within the MRR to represent surface water elevations. The decreases in elevations of Ponds 2 and 4 in early February were due to downloading data.

The pressure transducers that were placed in all four ponds recorded the surface water levels of the ponds (Figure 26 and Table 4, Appendix). The surface water in the ponds increased and decreased due to the effects of evapotranspiration of the weedy vegetation on the surface of the ponds, as well as the surrounding reeds, willows, and cottonwoods. Rain events in October 2011 and in January, mid-March, and mid-April of 2012 increased the surface water elevations of all the ponds. A pattern of gradually decreasing elevations followed for approximately 15 to 20 days.

Based on personal observation, the bottoms of the ponds are probably covered with fine silt that overlays the Mehrten Formation. These swale ponds are separated by ridges of coarse cobble with a ledge of fine, silty soil at a lower level than the ridges. During the summer months, as the pond dries somewhat during low stream flow and extreme evaporative conditions, the fine soil cracks, while only centimeters away, a mass of soil is wet and pliant. There is no evident layering within this soil profile. Four core samples were taken from the sides of the ponds by another student (Appendix Figure 51). Two core samples from the side of Pond 4 consisted of very fine silt (<2 mm). Core samples taken from Ponds 1 and 2 were a complete mat of rooting fiber.

3.2.1 2-D Groundwater Modeling

Merced Irrigation District calculated the canal system seepage to be 5.3 x10^{-6} m³/sec per meter of canal (CH2M Hill, 2001); however, the canal does not flow year-round. Evapotranspiration figures for Merced County are quite high, as reported by California Irrigation Management System (CIMIS) at Station #148, which is located near Bear Creek in Merced, California: approximately 134 cm/year (CIMIS). CIMIS Station #148 is located near Bear Creek at the intersection of the Kibby and Arboleda thoroughfares in Merced County. Average annual precipitation as reported by Exchequer CDEC station for this area is 38 cm/year, significantly lower than the evapotranspiration.

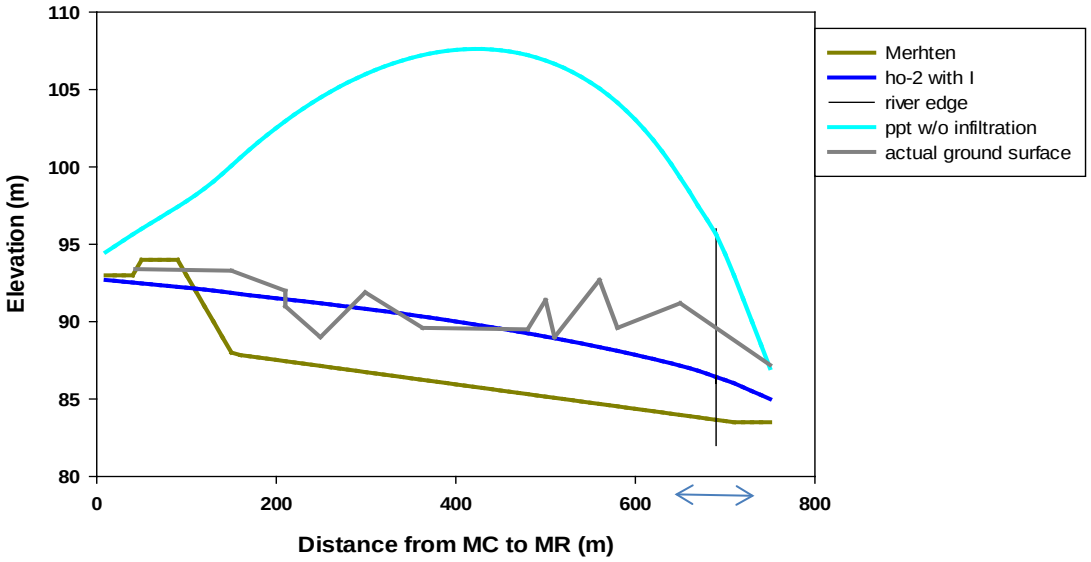

Figure 27 Results from two MODFLOW simulations. Simulated seepage (a) of 5.3 x10^{-6} m³/s of water from the canal bank of the Main Canal (MC) to the Merced River (MR) with a balloon of maximum precipitation without infiltration as depicted with the light blue line (ppt w/o infiltration), and (b) simulated seepage of 2.65 x10^{-6} m³/s of water from the canal bank of the Main Canal to the Merced River. This groundwater flows through cobbles with hydraulic conductivity of 8.6 x10^{-2} m/s over a layer of sand and silt with hydraulic conductivity of 2.5 x10^{-5} m/s and 30% infiltration represented by the dark blue line (ho-2 with I). The light blue arrows indicate the unknown variable of the physical location of the stream edge. The streams edge will vary with discharge rates of the stream.

Several simulations of MODFLOW were performed utilizing different infiltration seepage rates, elevation heads, and hydraulic conductivities for the lower layer of sand and fine sediment. The MODFLOW simulated seepage of 5.3 x10^{-6}m³/sec of water from the canal bank, which has an approximate elevation of 94 m, included 30% of the infiltration of precipitation through the two layers, with a bottom layer composed of fine sand K = 2.4x10^{-7}m/s (0.025 mm), ultimately yielding a ponded volume of 201 m³/year/unit depth water. After this simulation, we cut the seepage in half while

maintaining the 30% infiltration rate and lowering the elevation head 2 m below the top of the canal bank. We also modified the lower layer of sand and fine silt to K = $2.5x10^{-5}$ m/sec (0.25mm). This model produced a realistic result, as depicted by the dark blue line (ho-2 with infiltration) in the graph above (Figure 27).

This model, however, did not determine the exact seepage site in the river. Given that seepage and infiltration rates remain constant throughout the two homogeneous layers, MODFLOW demonstrates that water ponding can occur above the lower layer of sand and fine sediment. Consequently, by utilizing Darcy's Law that discharge is proportional to the medium's permeability and to the magnitude of pressure drop between two points, groundwater will ultimately seep from the Main Canal into the Merced River.

3.2.2 3-D Modeling with Groundwater Vistas

This numeric model reproduces spatial and temporal groundwater elevations throughout the MRR and its upstream influences. Incorporated within the model were Crocker Huffman Dam reservoir surface water elevations, which varied by 3 m during the course of this study. Groundwater elevations across the numeric model were calibrated to fit one year of field observations of MW 1-4 (Figure 28). The hydraulic model of the Dredger Tailings Reach generated 1.5-year and five-year estimated peak discharges and elevations for the top and the bottom of the river. These values were imported into the MODFLOW model; the five-year water elevations for the Merced River were a better fit to the field conditions exhibited in 2011-2012.

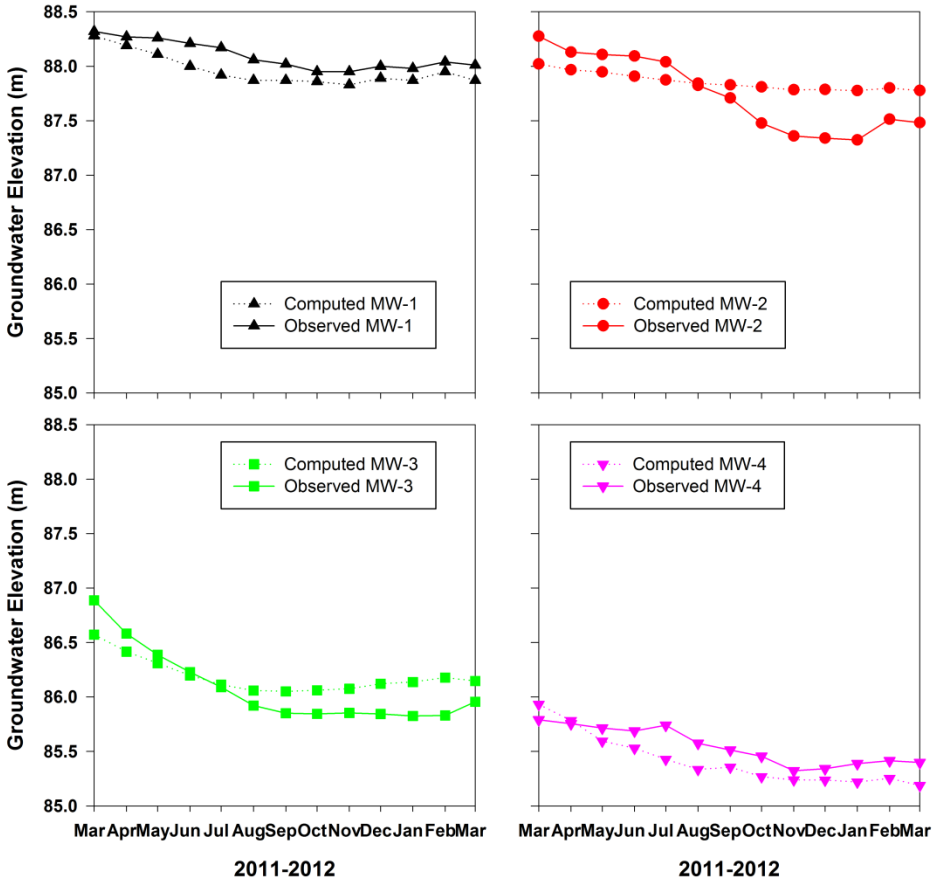

Figure 28 Calibration results for the MODFLOW model with Groundwater Vistas as a user interface. Calibration was performed by matching computed groundwater levels of MW 1-4 to observed groundwater levels. Each time step consisted of 30 days for the time period of March 2011 through March of 2012. The accuracy of the ultimate model design produced a sum of squared residuals of 1.7.

In order to compute calibration statistics, each target's error must be calculated and the entire population of targets must then be further statistically analyzed. The groundwater levels of MW 1-4 are the targets for this model. The accuracy of the ultimate model design produced a sum of squared residuals of 1.7. Initially trials were run with the numeric model depicting the Merced River as a single river package. Three MODFLOW river packages were smoothly distributed over the longitudinal profile of the river to represent the Merced River (McDonald and Harbough, 1996). The model is most accurate within the boundaries of the MRR.

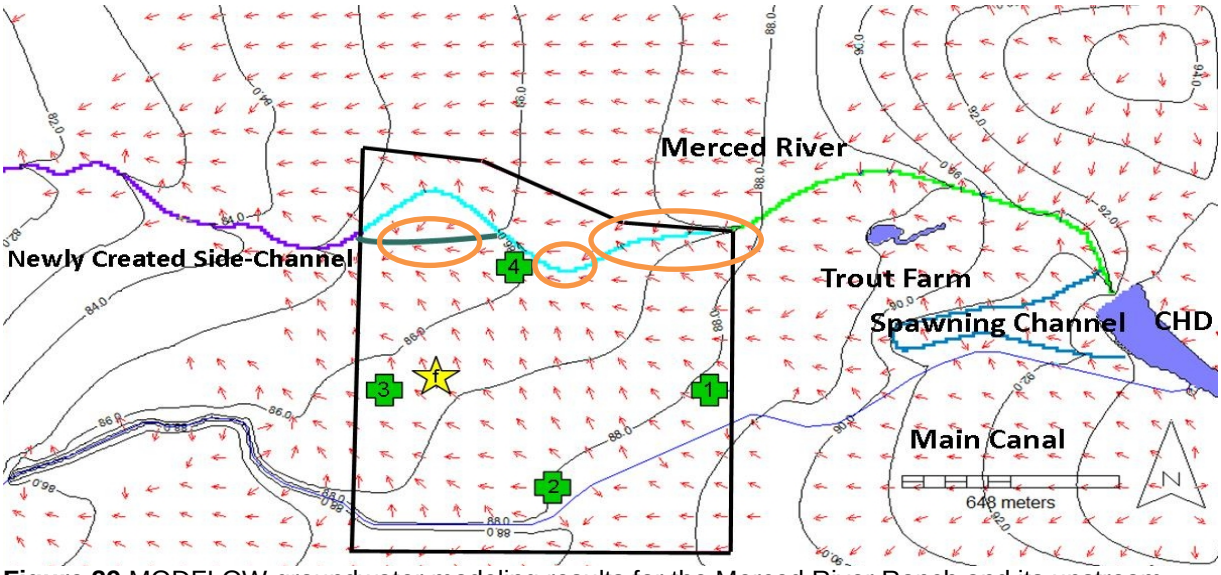

Figure 29 MODFLOW groundwater modeling results for the Merced River Ranch and its upstream influences. Each vector arrow depicts *any* directional flow of groundwater. Of considerable importance are the flow paths from the Trout Farm to the Merced River through MW-4. The presence of potential seepage sites can be noted at convergent vectors (depicted in the figure as orange circles) at the main channel of the Merced River, as well as its newly created side channel. The groundwater appears to flow across the Merced River Ranch beginning at the Main Canal, continuing through the swale ponds, and ultimately ending at the Merced River. Green crosses represent Monitoring Wells 1-4, and the yellow star (f) represents Forest Monitoring Wells 5-8. The Merced River contains three MODFLOW river packages, depicted here in green, light blue, and purple. The spawning channel is incorporated as a river package drawn in dark blue, while the Trout Farm and Crocker Huffman Dam (CHD) were installed as lake packages. The Main Canal was analytically drawn into the figure. Direction of stream flow is from east to west. Groundwater levels of MW 1-4 were utilized as targets to validate the numeric model.

The results from this model represent a complex system of subsurface water connections that may surface at the swale ponds and ultimately discharge to the stream either as seeps or under the stream in the hyporheic zone (Figure 29). This subsurface water most likely contains dissolved salts and nutrients. However, the velocity of groundwater flow is so low that, for the purposes of this diagram, the numeric value was removed, thereby making each vector arrow represent *any* groundwater flow. The model predicted two major surface-subsurface head gradients that drive groundwater flow. One flow path originates at the TF and flows across the MRR through the swale ponds to the Merced River. The other groundwater flow path appears to transect the MRR beginning at the Main Canal, continuing through the swale ponds and in due course ending at the Merced River. Potential seepage sites to the main channel of the Merced River, as well as the newly created side channel, can be noted as convergent vectors in Figure 29.

Due to all the dredging activity, the specific groundwater flow paths are probably quite complex. The highest conductivity is the cobble layer, so water can flow through surface water channels to swale ponds and then seep through cobble layers to the Merced River.

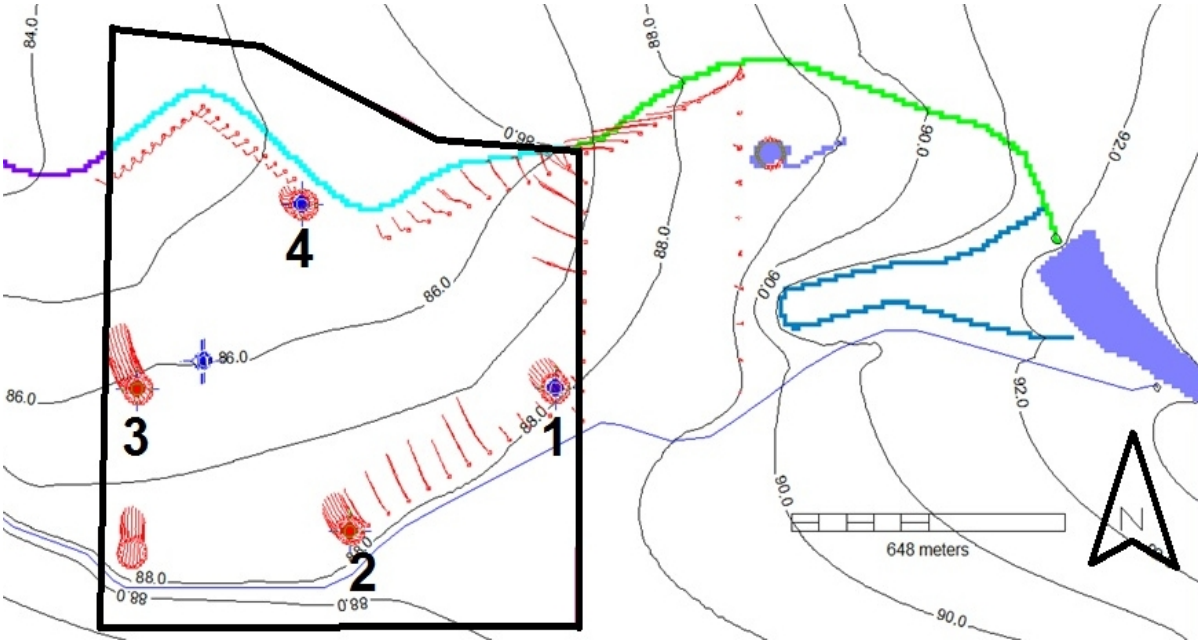

Figure 30 One-year particle-tracing results for modeling year March 2011-March 2012. One-year particle tracers were applied to the Groundwater Vistas program, thereby allowing seepage sites to be identified. The newly created side channel is located in the northwest corner of the study site. MW-3 seems to be located in an area with the greatest hydraulic conductivity. The Merced River contains three MODFLOW river packages, depicted here in green, light blue, and purple. The spawning channel is incorporated as a river package drawn in dark blue. The Trout Farm and Crocker Huffman Dam (CHD) were installed as a lake package. The Main Canal was analytically drawn into the figure. Groundwater levels of MW 1-4 were utilized as targets to validate the numeric model. The stream flows from east to west.

Groundwater Vistas can track particles placed in the aquifer during specific timeframes, thereby modeling temporal changes and flow paths. A cell-by-cell groundwater flow simulation is represented by particles that were placed in cells along with the groundwater flow in the middle of the top layer. This simulation traced the groundwater flow for 13 months, from March 2011 to March 2012. One-year tracer particle simulation results for the information provided to the model indicate that water moved the furthest from MW-3, followed closely by MW-2 (Figure 30). Particles placed in a circle around MW-1 and MW-4 did not drift as far. Particles that were placed along the stream's edge are predicted to seep into the Merced River at the northeast corner of the MRR. The only output is the flow path of the particles through the aquifer.

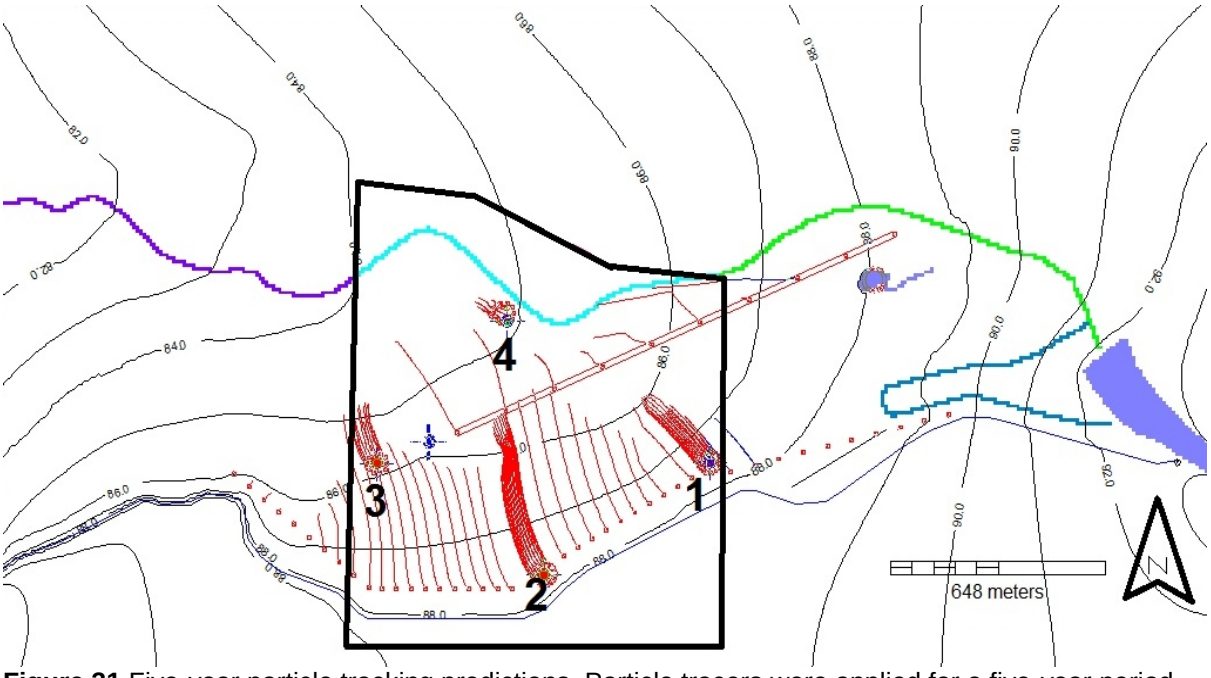

Figure 31 Five-year particle tracking predictions. Particle tracers were applied for a five-year period, unrealistically duplicating each year of the five years with data acquired during this one-year monitoring period (March 2011 through March 2012). Notice that MW-2 is located in an area with the greatest hydraulic conductivity. It also dominates the profile of the groundwater flow through the swale ponds of the MRR. Of particular importance is the fact that MW-1, despite its isolated appearance, is connected through groundwater flow paths to the ponds. The Merced River contains three MODFLOW river packages, depicted here in green, light blue, and purple. The spawning channel is incorporated as a river package drawn in dark blue. The Trout Farm and Crocker Huffman Dam (CHD) were installed as a lake package. The Main Canal was analytically drawn into the figure. Groundwater levels of MW 1-4 were utilized as targets to validate the numeric model. The stream flow is from east to west.

The five-year particle tracking results predict that the hydraulic conductivity around MW-2 is the highest, allowing for the fastest rate of travel through the porous media. These particles travel through the swale ponds of the MRR. The particles placed around MW-2 traveled the furthest across the MRR through its center (Figure 31). The particles placed in the vicinity of MW-1 also traveled to the ponds. Based on this theoretical model, it takes ten to 15 years for the groundwater to flow from the Main Canal to the Merced River. In addition, it would take ten to 15 years for the water to seep from the Trout Farm through the MRR to the Merced River. The particles near the stream's edge once again had a tendency to collect in a few seepage locations.

Due to the limitations of the model, swifter flow paths—such as preferential flows through the top cobble with possible lenses of multiple soil types—were not considered. This model is only accurate for the information that it was designed to interpret. The direction of groundwater flow with homogeneous porous media is mapped and described above. The complexity of the ravines and ponds is beyond the scope of this model. There may be preferential flow paths in the near-surface cobble layer that allow for faster groundwater surface water flow through the study site.

3.3 Water Quality Sampling and Chemistry Results

During the monitoring period, the conductivity of MW-1 was consistently higher than that of MW 2-4, the Main Canal, and the Merced River, at times being 70 times greater than that of the Merced River (Figure 32). Furthermore, the conductivity of the Forest Monitoring Wells exceeded that of MW-1. MW-1 and MW-2 groundwater conductivity increased during the winter months, while the conductivity of MW-3 decreased (Appendix Table 5). The Main Canal and the Merced River's conductivity are virtually the same, with MW-2 being somewhat similar, indicating that perhaps they share the same water source. During high flows of the Merced River, the conductivity decreased in the groundwater of MW-4.

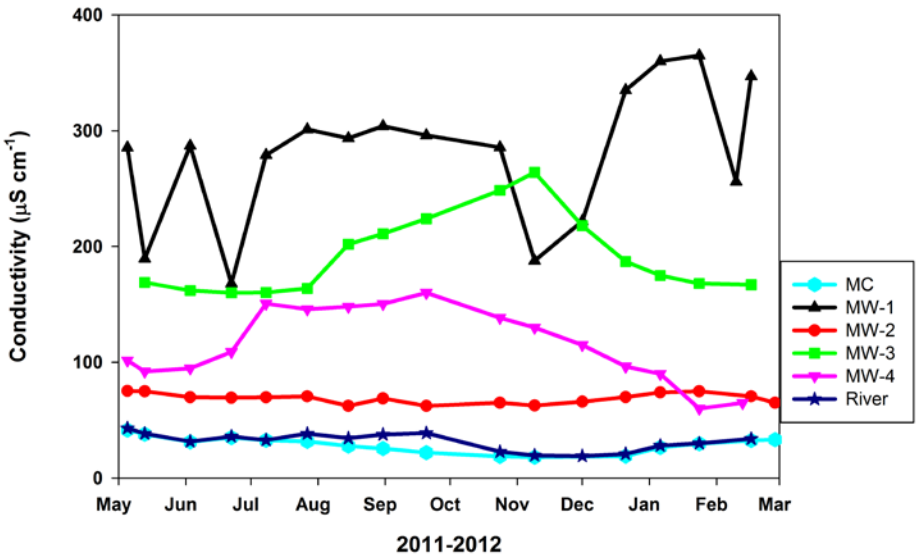

Figure 32 Measured conductivity for the period of May 2011-March 2012. The Merced River (River) and Main Canal share the same profile of conductivity levels. MW-2 is slightly higher. MW-1, 3, and 4 have distinct conductivity profiles as they are considerably higher than the Merced River, Main Canal, and MW-2.

All Monitoring Wells exhibited very low DO in the range of 0.3 mg O_2/L - 3.9 mg O_2/L, especially during the winter months of December through February (Figure 33). The groundwater within MW-1 had the lowest DO content of all the wells, ranging from 0.3 mg O_2/L - 1.75 mg O_2/L. Although the DO levels of the surface water in the Merced River and Main Canal varied, they were consistently at least ten times higher than the levels found in the wells. MW-2 had the highest DO content of all the wells because it is closest to the Main Canal. At times, MW-4 had the second-highest DO levels of all the wells due to its proximity to the Merced River.

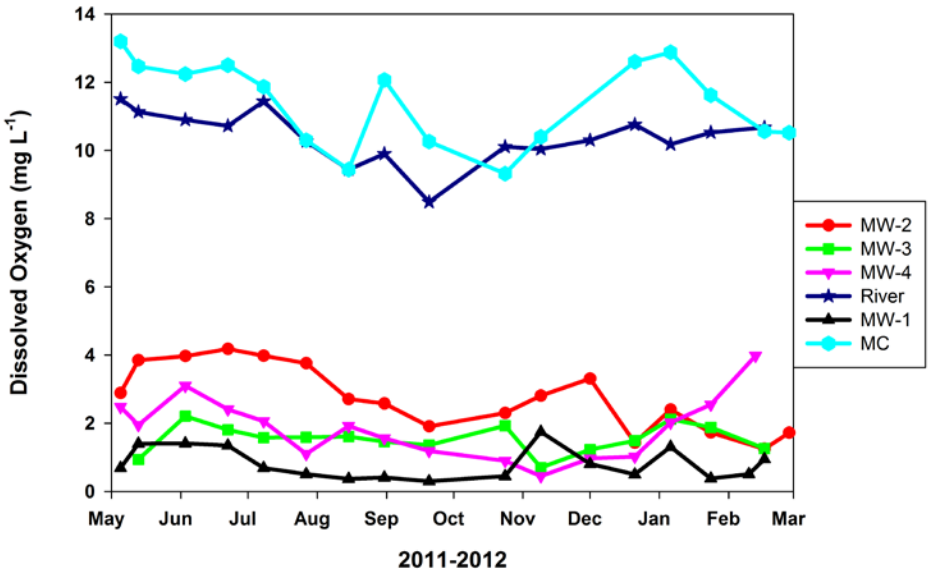

Figure 33 Dissolved oxygen (DO) levels in MW 1-4, Main Canal (MC), and Merced River (River) for May 2011-March 2012. All Monitoring Wells exhibited low DO levels. When comparing Monitoring Wells, MW-2 exhibited the highest levels of DO. The greatest fluctuation in DO levels occurred during the winter months, salmon spawning season, and the timeframe of rearing juveniles.

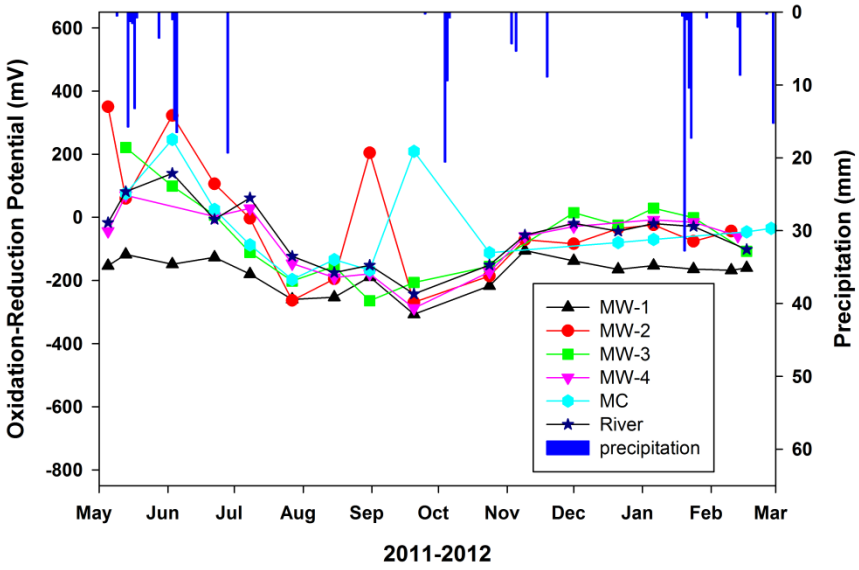

Figure 34 Field measurements of the oxidation-reduction potential in MW 1-4, Main Canal (MC), and Merced River (River) for May 2011-2012. These measurements offer us a snapshot of possible nitrification-denitrification processes and biological phosphorus removal. Note the seasonal oscillations between the winter and summer months. Lines are utilized for a visual reference.

In our case, the Merced River was in a flood stage between April and July of 2011. It is possible that the Merced River and the Main Canal could have contributed

highly oxygenated waters to the riparian system. Apparently there was enough oxygen in the system to present oxidizing conditions during this timeframe for all wells except MW-1. Furthermore, MW-1 consistently presented conditions conducive to the reduction process. The ORPs observed in MW-1 are typical of denitrification and methanogenis (YSI, 2008) (Figure 34).

MW-1 exhibited some fluctuations yet maintained reducing conditions throughout the year. For MW-2, MW-3, the Main Canal, and Merced River during May, June, and July of 2011, high flows allowed for oxidizing conditions. Water in streams and rivers is constantly replenished with oxygen. Oddly, during the period of late October of 2011 through March of 2012, the Merced River and the Main Canal had ORP values that were near zero, which are not consistent with a highly-oxygenated system (Figure 34). Coincidentally, it is during this period of time that the Merced River and the Main Canal were at their lowest flow. The May 5, 2011 field measurement of conductivity, DO, and ORP for MW-3 was discarded due to possible sampling error.

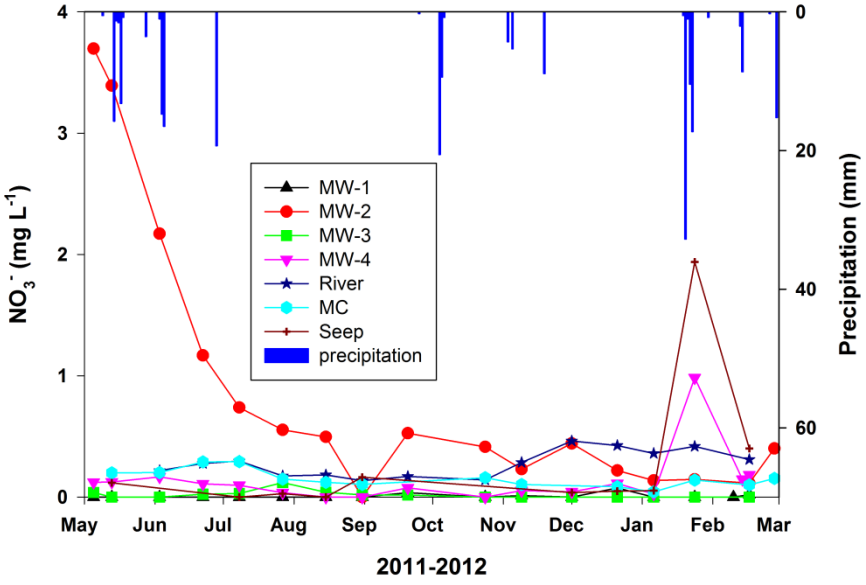

Figure 35 Trends in nitrate concentrations and precipitation for May 2011 to March 2012. Note the declining nitrate (NO_3^-) in MW-2. The high nitrate level that could be caused by the oxidation of ammonium (NH_4^+) to nitrate (NO_3^-) occurred in MW-2 during May to July 2011. Precipitation was measured at Exchequer Dam for the duration of this study (May 2011 to March 2012) and is shown at the top of the graph. Lines are utilized for a visual reference.

Of note are the elevated nitrate levels in MW-2 May through July 2011 (Figure 35), which coincided with oxic conditions (Figure 34). Peak concentrations were measured in May 2011, followed by a gradual decrease until July. Concentrations of

nitrate within MW-2 were lower in the months of September, November, and late December through late February. The concentrations may have risen again in March 2012. The rest of the monitoring wells did not show similar trends. However, there was an increase in nitrate levels in the Merced River starting in December 2011. MW-4 and the seep show elevated nitrate levels after a precipitation event (February 2012). These levels could be the result of ammonium oxidation.

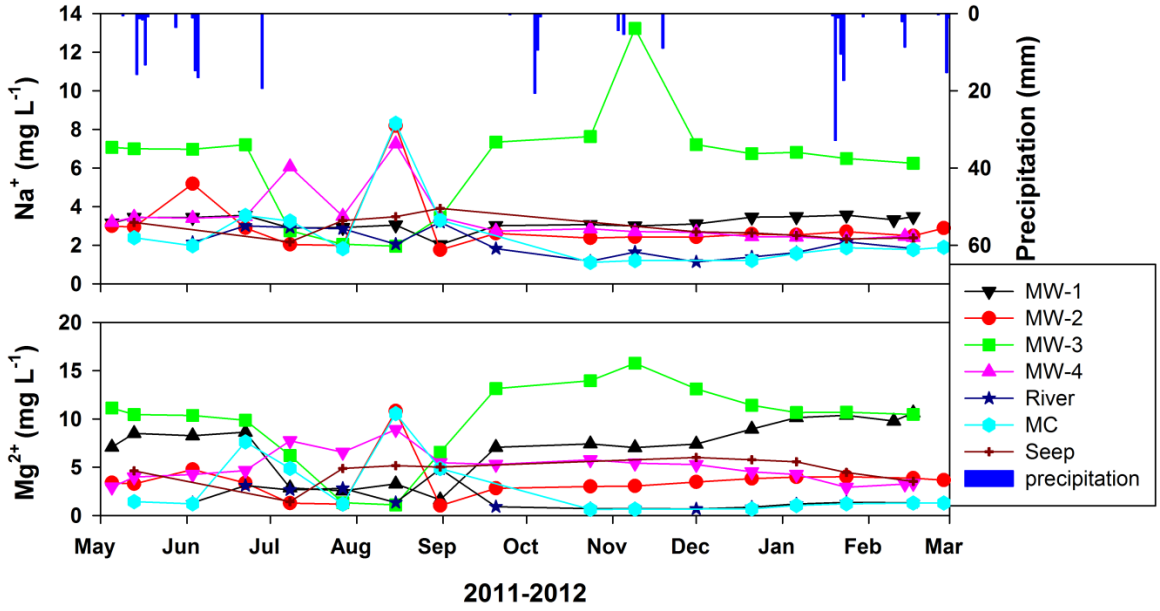

Figure 36 Trends in Na^+ and Mg^{2+} concentrations and precipitation for May 2011 through March 2012. Occasional high levels of Na^+ and Mg^{2+} occurred in MW-2 and 4, the seep, as well as the Main Canal (MC) during July and August. During this same period of time, MW-3 concentrations were at their lowest. MW-3 exhibited consistently high concentrations of Na^+ and Mg^{2+} and the concentrations were the greatest in November 2011. Precipitation was measured at Exchequer Dam for the duration of this study (May 2011 to March 2012) and is shown at the top of the graph. Lines are utilized for a visual reference.

Concentrations of dissolved sodium and magnesium ions showed similar trends during the period from May 2011 to March 2012. MW-3 presented the highest concentration through much of the year, except during July through September 2011. The Main Canal, MW-3, and MW-4 all disclosed elevated Mg^{2+} and Na^+ concentrations in July through September 2011. MW-4 is the exception, with Mg^{2+} trends similar to those of MW-3 (Figure 36).

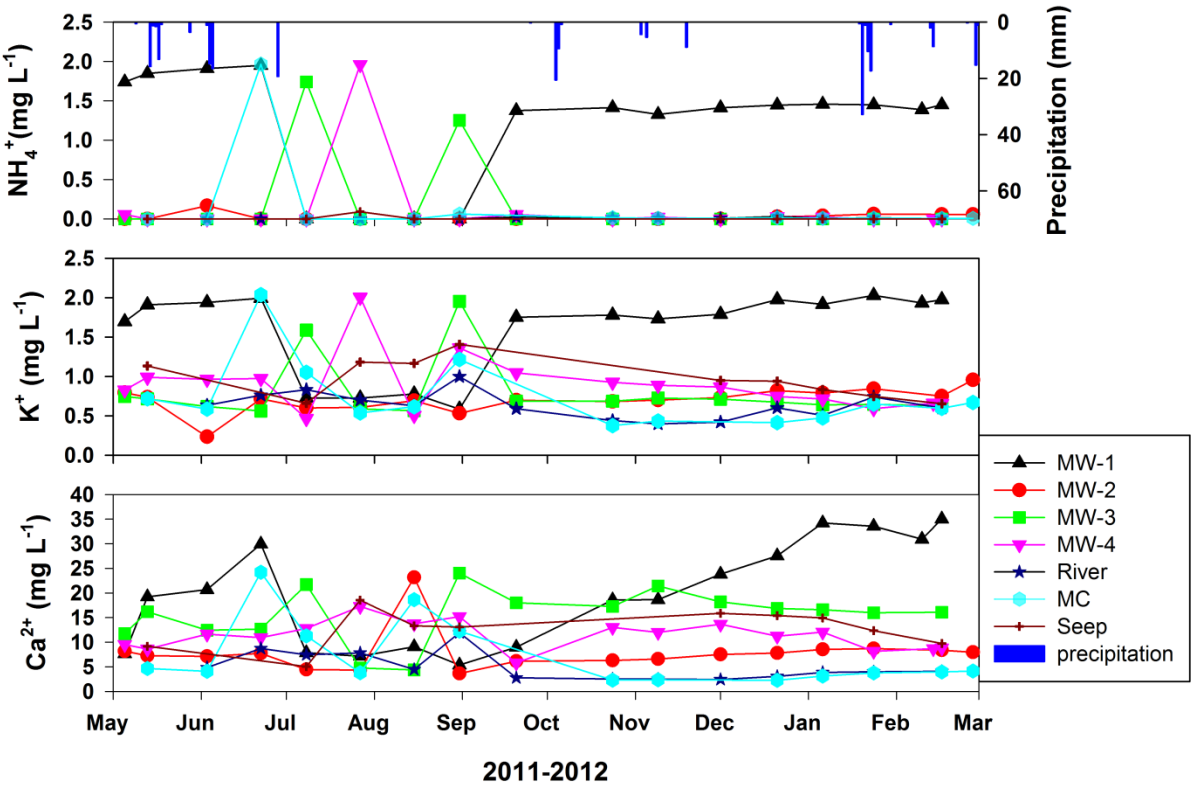

Figure 37 Trends in NH_4^+, K^+, and Ca^{2+} ionic concentration and precipitation for May 2011 through March 2012. There were consistently high concentrations of ammonium, potassium, and calcium ions in MW-1. The greatest fluctuation in ammonium, potassium, and calcium ions occurred in MW-3 and 4, as well as the Main Canal (MC) during the dry months (June through October), when MW-1 was at its lowest concentration. The seep concentration trends for K^+ and Ca^{2+} peaked in August through September and then again in December through late February. Precipitation was measured at Exchequer Dam for the duration of this study (May 2011 to March 2012) and is shown at the top of the graph. Lines are utilized for a visual reference.

NH_4^+, Ca^{2+}, and K^+ showed different trends, with MW-1 typically showing high concentrations (Figure 37). Both NH_4^+ and K^+ showed elevated concentrations in MW-1 except for July through September -- the lowest flow conditions in the Main Canal and Merced River. Ca^{2+} exhibited lowest concentrations during that same period, but also displayed a gradual increase in concentrations for September through January and a rapid decrease in July.

Elevated calcium levels could be found in MW-1, MW-3 and MW-4. In MW-3, it was apparent by an appearance of white water and was filterable, creating a solid precipitate. A dramatic increase in calcium concentration occurred between October 30, 2011 and February 20, 2012 (Figure 37).

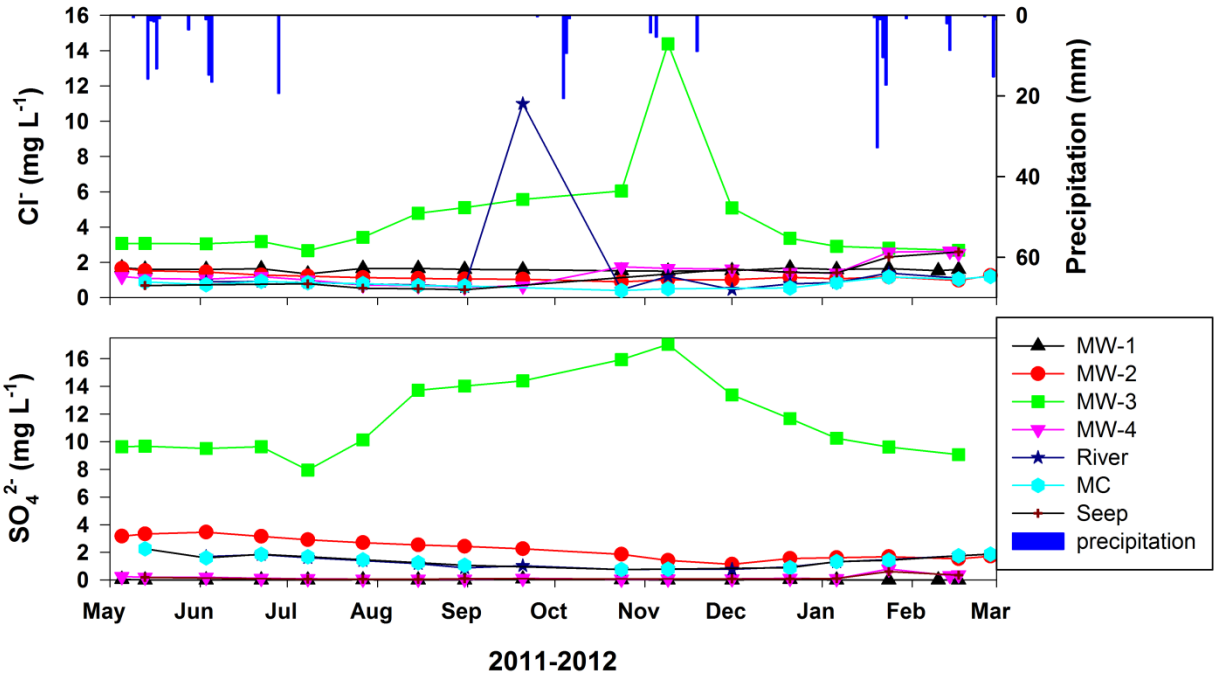

Figure 38 Trends in sulfate (SO_4^{2-}) and chloride (Cl^-). Note high levels of chloride in MW-3 consistent with the possibility that the source of this water is the precipitation. Increasing chloride levels during the course of the summer with a chloride spike on 11/9/11 after the irrigation season indicate that MW-3 is responsive to precipitation and evaporated during the summer months. Precipitation was measured at Exchequer Dam for the duration of this study (May 2011 to March 2012) and is shown at the top of the graph. Lines are utilized for a visual reference.

The anions concentrations of sulfate (SO_4^{2-}) and chloride (Cl^-) showed slightly different trends than the cation concentrations. MW-3 has the highest concentrations of both anions (except one sample from the Merced River in late September 2012); with spikes in November 2012, these are consistent with the high cation concentration observed in this well. There was little variance in the other monitoring wells, the Main Canal, seep, and the river for the duration of this study (Figure 38).

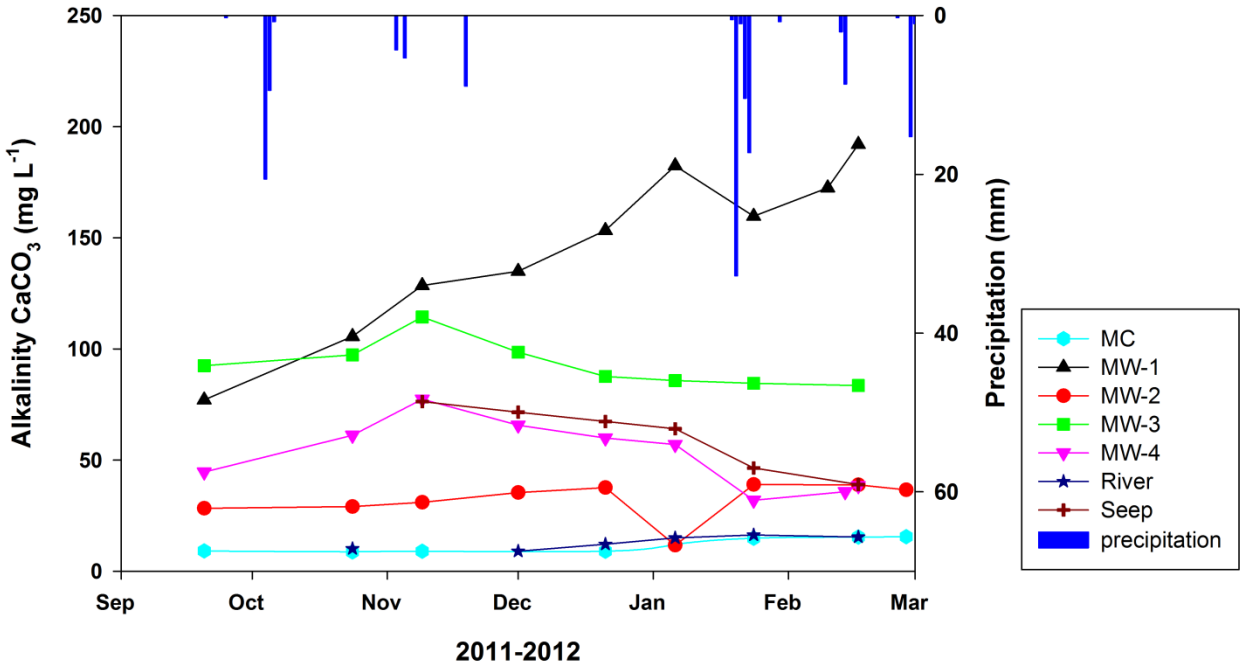

Figure 39 Alkalinity trends for 2011-2012. Note that alkalinity increased for MW-1 over this time period.

In Figure 39, alkalinity was the highest for MW-1 (reaching 200 mg $CaCO_3$/L); significantly lower for the other wells (40-110 mg $CaCO_3$/L); and much lower for both the Main Canal and the Merced River (5 mg $CaCO_3$/L). The alkalinity was slightly higher in the seep than in MW-4.

Figure 40 Purging MW-4 prior to testing water quality parameters for the second time. After purging and testing twice, water samples were obtained. This photograph is dated 06/03/2011.

Similar to Ca^{2+} trends (Figure 37), alkalinity showed a gradual increase from September to March for MW-1.The alkalinity levels in other wells and in the Merced River, Main Canal, and seep remained relatively stable throughout the monitoring period.

Trends in total Fe and dissolved Fe (Figures 41 and 42) mostly indicated increasing levels for the period of September through March. The obvious exceptions were constant Fe levels in MW-2 and 3. MW-1 showed a steady increase for this time period. MW-2 disclosed spikes; the spike in total Fe occurred after a rainstorm in November and was consistent with increases in other dissolved constituents (e.g., Cl^-,

Figure 38). The increase in MW-1 of dissolved Fe was consistent with temporal trends, reduced ORP and NO_3^-. One could observe rust-colored water frequently when purging MW-1 and MW-4 (Figure 40).

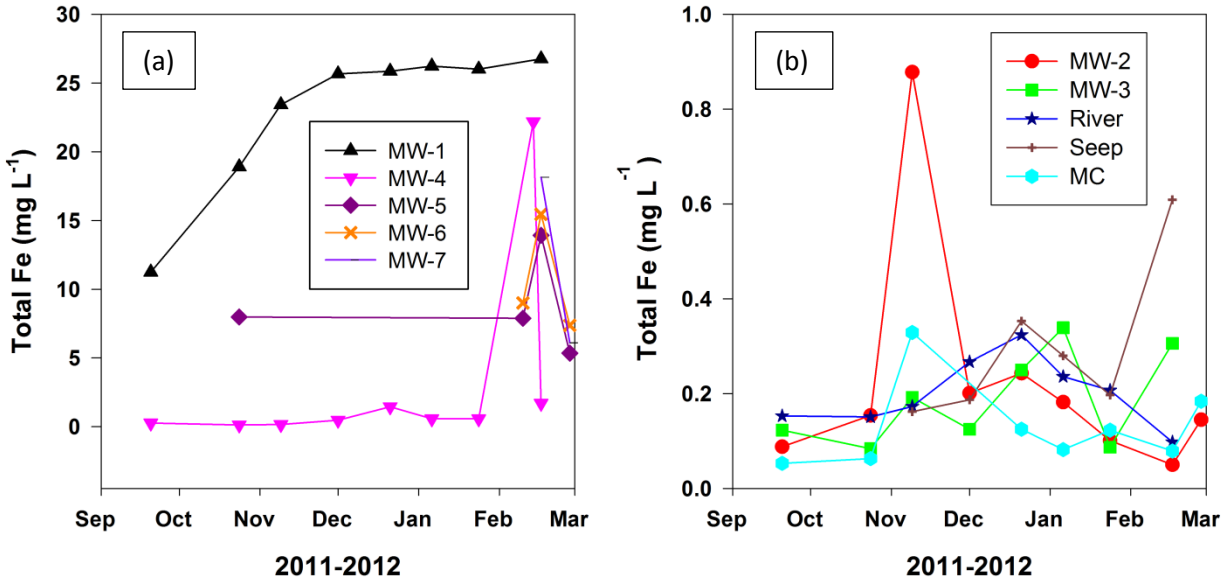

Figure 41 Trends in total Fe (a and b) MW-1, MW-4, and the Forest Monitoring Wells (MW-5-7). MW-1 revealed the greatest concentrations of total iron. Comparable increases in concentrations of various anions and cations can be observed in the figures to follow. Lines are utilized for a visual reference.

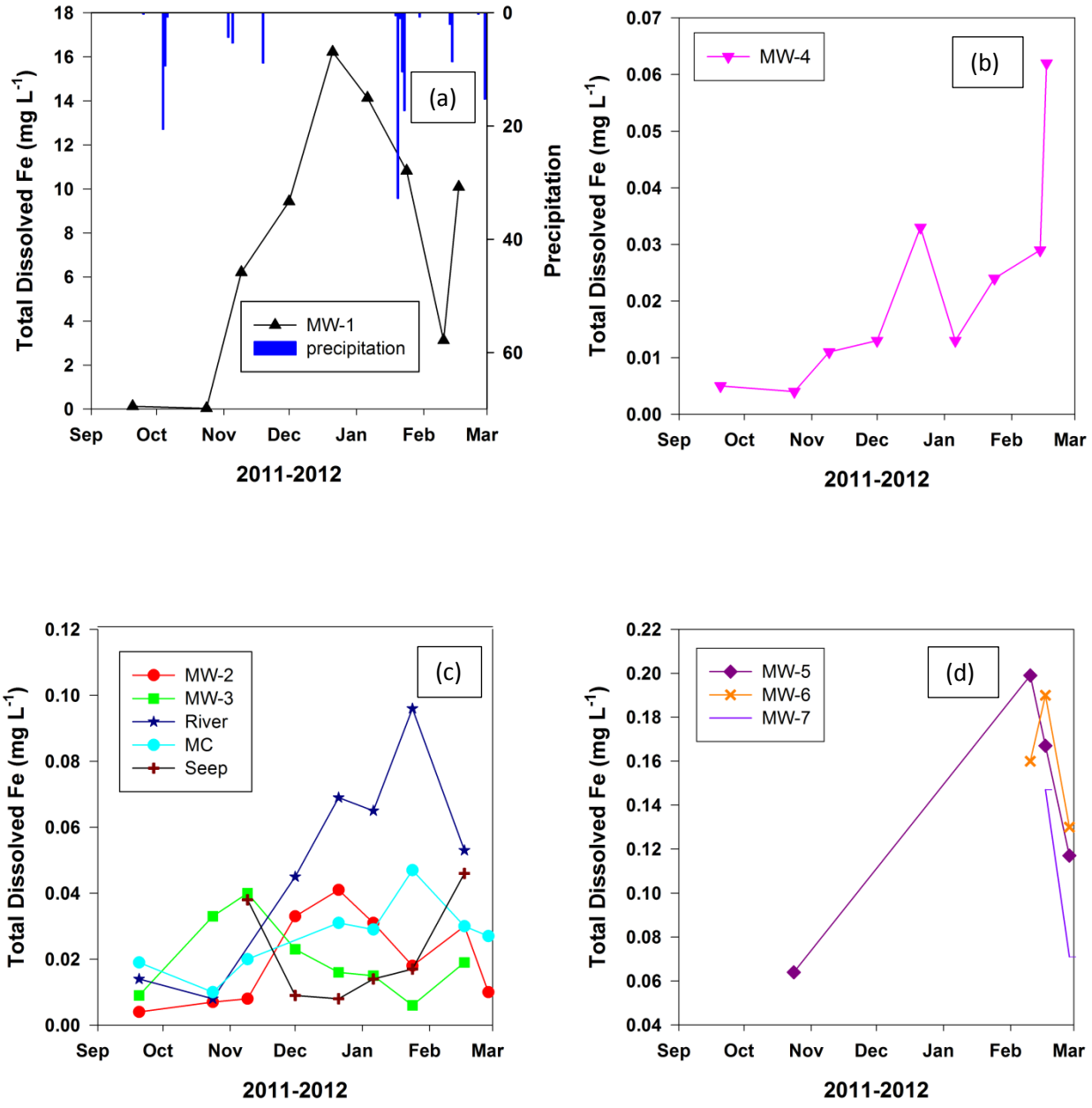

Figure 42 Trends for total dissolved Fe for all sample locations (a, b, c and d). Total dissolved Fe (mg L^{-1}) was obtained by filtering the samples initially and then acidifying the samples to a pH of 3.0. These levels increased during the year with the peaks of MW-1 and MW-4 occurring in late December. Note that the peak for total dissolved iron in the Merced River was delayed until late January. It should be emphasized that the entire period from September 2011 until March 2012 is the season for salmon spawning and rearing. The lines on these graphs are for visual aids. The errors are no bigger than the point sizes.

A piper diagram for all wells, Merced River, Main Canal, and seep samples provided a hydrochemistry evaluation (Appendix, Figure 51). A piper diagram was also created for the Forest Wells (Appendix, Figure 52). The charge balance error for all wells, Merced River, Main Canal, and seep samples was less than 12%, and for the Forest Wells, it was 13% (Appendix, Table 9). Some of the samples from these waters

had an excess negative charge in this analysis. The basic assumption in calculating the charge balance is that the alkalinity is being supplied by carbonate, although we may be missing another source of cations.

Table 1 Dissolved Organic Carbon and Total Nitrogen Analysis of Ground and Surface Waters Sampled from the Merced River Ranch for the Time Period September 2011-Jan 2012

Date	Sample Location	DOC Mg L^{-1}	DOC mmoles	TN Mg L^{-1}	TN mmoles
9/20/2011	MW-1	1.22	0.1	1.57	0.11
10/24/2011	MW-1	1.27	0.11	1.54	0.11
11/9/2011	MW-1	1.21	0.1	1.53	0.11
1/6/2012	MW-1	1.79	0.15	1.8	0.13
9/20/2011	MW-2	0.44	0.04	0.17	0.01
10/24/2011	MW-2	0.47	0.04	0.16	0.01
11/9/2011	MW-2	0.54	0.05	0.09	0.01
1/6/2012	MW-2	0.42	0.03	0.1	0.01
9/20/2011	MW-3	1.57	0.13	0.13	0.01
10/24/2011	MW-3	1.57	0.13	0.09	0.01
11/9/2011	MW-3	1.7	0.14	0.14	0.01
1/6/2012	MW-3	1.11	0.09	0.09	0.01
9/20/2011	MW-4	2.06	0.17	0.22	0.02
10/24/2011	MW-4	1.81	0.15	0.11	0.01
11/9/2011	MW-4	1.87	0.16	0.19	0.01
1/6/2012	MW-4	1.32	0.11	0.13	0.01
9/20/2011	river	2.15	0.18	0.2	0.01
10/24/2011	river	1.78	0.15	0.16	0.01

11/9/2011	river	1.77	0.15	0.24	0.02
1/6/2012	river	1.42	0.12	0.17	0.01
9/20/2011	canal	1.83	0.15	0.21	0.02
10/24/2011	canal	1.56	0.13	0.16	0.01
11/9/2011	canal	1.81	0.15	0.2	0.01
1/6/2012	canal	1.47	0.12	0.12	0.01
11/9/2011	seep	1.78	0.15	0.13	0.01
1/6/2012	seep	1.51	0.13	0.14	0.01

Selected samples characterized DOC and TN in all wells, Merced River, the Main Canal, and seep for the following timeframes: irrigation season, after irrigation season, and the salmon spawning/egg incubation season. Extremely high levels of TN levels were exhibited in MW-1. The TN levels were as much as 15 times the levels found in the other monitoring wells or the surface waters of the Merced River and Main Canal (Table 1). The concentration of DOC in the groundwater of MW-2 was one-fourth that of the other wells and surface waters. Trends of elevated DOC were seen in MW-4 and the Merced River on September 20, 2011.

Figure 43 Field observation of the future Forest Monitoring Well site. Note the ponded water that is typical of wet years (personal observation). Photo was taken on 4/20/11.

During the monitoring period, the conductivity of the groundwater tested at the Forest Monitoring Wells (FW) had higher levels than all the other wells and surface water samples (Figure 43). The conductivity was between 300 and 800$\mu S/cm$; double that found in MW-1, which itself had values that were three times greater than those found in MW-2 through 4. A relationship seems to be shared between MW-3 and the FWs (Appendix Table 5). The concentrations of Na^{2+}, Mg^{2+}, Ca^{2+} and Cl^{-} that were approximately double in the FWs were double that found in MW-3. The FWs do not share the same chemical relationship with MW-1, 2, and 4 (Appendix Tables 6 and 7).

Chapter 4 Discussion

4.1 Flow Paths

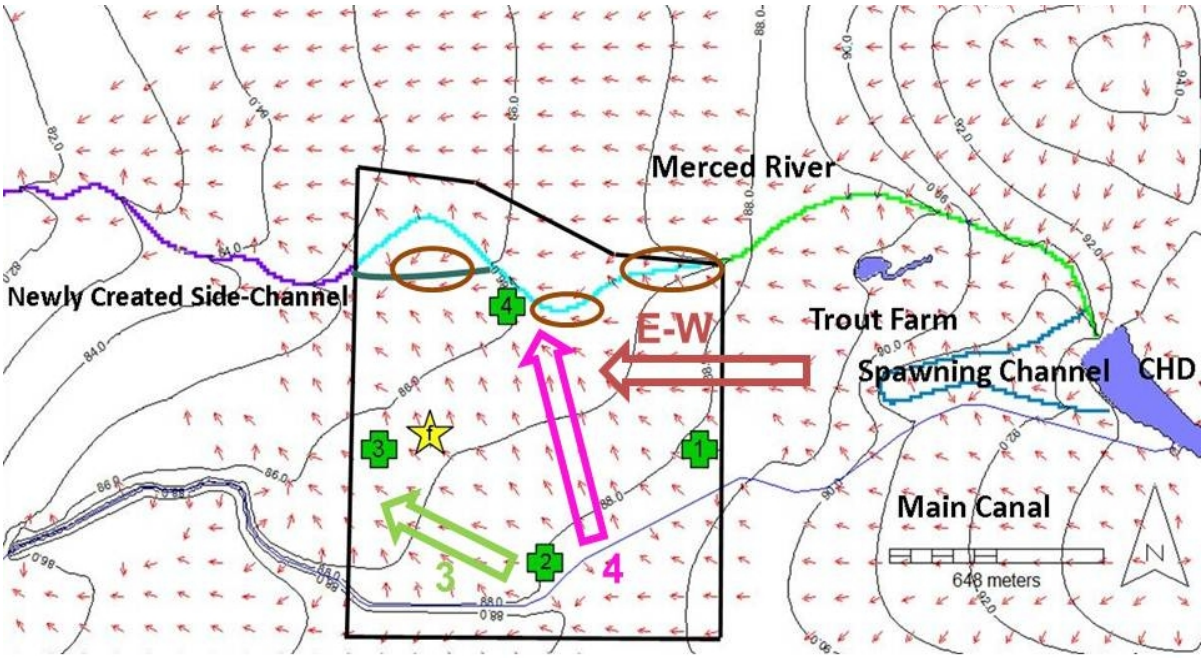

Figure 44 Three possible groundwater pathways of Merced River Ranch. Arrows are only guides for the eye, and relative lengths may be indicative of residence times. The dominant flow path is from the Main Canal (MC) to MW-2; then across the Merced River Ranch (MRR), the boundaries of which are outlined in black, to MW-4; the seasonal seeps, which are dark brown circles; and the Merced River, depicted as a pink arrow labeled as (4). Secondly is the groundwater flow path that flows down gradient from east to west, as depicted by the brown arrow labeled (E-W). This path originates from the impoundment of the Crocker Huffman Dam (CHD), travels either through the spawning channel or the Trout Farm (TF) to the Merced River, the seasonal seeps, and/or MW-4. Additionally, groundwater is able to leak from the Main Canal to MW-3, then ultimately travels to the Merced River, which is depicted as the green arrow labeled as (3). Small red vector arrows depict any directional flow of groundwater. Of considerable importance are the flow paths from the TF to the Merced River through MW-4. The presence of potential seepage sites can be noted at convergent vectors (depicted in the figure as dark brown circles) at the main channel of the Merced River, as well as its newly created side channel. The groundwater appears to flow across the Merced River Ranch beginning at the Main Canal, continuing through the swale ponds, and ultimately ending at the Merced River. Green crosses represent Monitoring Wells 1-4 and the yellow star, depicted as (f), represents Forest Monitoring Wells 5-7. The Merced River contains three MODFLOW river packages, depicted here in green, light blue, and purple. The spawning channel is incorporated as a river package drawn in dark blue, while the TF and Crocker Huffman Dam (CHD) were installed as lake packages. The Main Canal was analytically drawn into the figure. Direction of stream flow is from east to west. Groundwater levels of MW 1-4 were utilized as targets to validate the numeric model.

For over a century, the hydrological value of the Crocker Huffman Dam has been appreciated by agricultural customers of the Merced Irrigation District, which diverts high-quality water for crops. The hydrological gradient created by the Crocker Huffman Dam to divert the flow of the Merced River into the Main Canal controls the water quality

and the flow paths of the area (Figure 29). Further complicating the hydrological connection between the Merced River, the Main Canal, and the surrounding floodplain, the land mass has been extensively dredged. As a result, hydrological flow path possibilities are numerous and multifaceted.

Strategically, this diversion dam creates a critical hydrological area, as the impoundment affects the entire riverine/floodplain of this study reach of the Merced River. Environmental effects from the impoundment include possible seepage underneath the dam and a seasonal stratified reservoir. Water is diverted to one salmon hatchery and one trout farm, where the water quality of the river and the groundwater of the floodplain could be affected and possibly degraded (Figure 2). There is an artificial salmon spawning channel, where water is diverted from the river or becomes the river during low flows. This unlined shallow channel could potentially seep and provide an opportunity for the temperature of the stream water to rise.

If we follow the river from east to west, from the Merced Falls Reach of the Merced River to the Dredger Tailings Reach of the Merced River through the floodplain of the Merced River, and from the Main Canal through the Merced River floodplain to the Dredger Tailings Reach of the Merced River, we are considering three possible flow paths (Figure 44). Groundwater modeling and aquatic chemistry results indicate that each of the three possible flow paths that ultimately discharge into the Merced River is unique, both spatially and temporally. Particle-tracking groundwater modeling studies predict that residence times are between ten and 15 years (Figures 30 and 31). However, as mentioned above, this MODFLOW model does not consider preferential flow paths. There are seasonal variations in the chemistry of all wells. This seasonal response may be indicative of the flows of the subsurface system.

While numeric modeling results reveal the possibility of some seepage to the river upstream of MRR, this study concentrates on seepage sites within the MRR. Groundwater seeps into the Merced River in the northeastern half of the MRR, while groundwater seeps into the newly created side channel in the western half of the MRR.

The groundwater flow path driven by groundwater elevation, which creates a differential head between the Main Canal and the Merced River, is captured by MW-2 and MW-4, referred to as flow path 4, and depicted as the pink arrow in Figure 44. Secondly is the groundwater flow path that flows from east to west down gradient, which is referred to as the (E-W) flow path and depicted as the brown arrow (Figure 44). This groundwater flow path, which originates from the impoundment of Crocker Huffman Dam, travels either through the spawning channel or the trout farm to the Merced River, seasonal seeps, and MW-4. Additionally, groundwater is able to leak from the Main Canal to MW-2, and then from the MW-2 to the MW-3 at the bend near MW-2. This includes precipitation that falls in the clay lens of the Forest Well sites (Figure 43), ultimately traveling to the Merced River; this is referred to as flow path 3, which is

depicted as a green arrow (Figure 44). In studies conducted downstream of the MRR within the Dredger Tailings Reach, the low-lying areas between the rows of the tailings retained the precipitation, with little runoff to the Merced River (Santé Fe Aggregates, 2009). These bodies of perched aquifers were found in areas with low hydraulic conductivity. The higher concentration of salts was probably due to the process of evaporation and increased residence times.

An evaluation of the hydrochemistry and modeling results indicates that flow path 4 is the predominant pathway for groundwater to reach the Merced River. The conductivity and oxidation-reduction potential of MW-2 groundwater are slightly higher than those of the surface water of the Main Canal (Figures 32 and 34). The DO of MW-2 is the highest of all the wells and seasonal seeps (Figure 33). The Main Canal and MW-2 share similar trends in NH_4^+, Cl^-, and SO_4^{2-} concentrations, with the SO_4^{2-} concentration being slightly higher in MW-2 (Figures 37 and 38). Concentrations of Na^+ and Mg^{2+} are slightly greater in MW-2 when compared to the Main Canal (Figure 36). The alkalinity of the groundwater in MW-2 is slightly greater than that of the Main Canal (Figure 39). Furthermore, the groundwater elevation changes in MW-2 are most similar to those of the Main Canal (Figure 23). This suggests that the residence time of the water from the Main Canal to MW-2 is in the realm of days to months.

Further review indicates that the groundwater of MW-4 has higher conductivity than that of MW-2 (Figure 32). DO of MW-4 is lower than that of MW-2 (Figure 33). MW-2 and MW-4 contain similar concentrations of NH_4^+ and Cl^- (Figures 37 and 38). Concentrations of K^+, Ca^{2+}, and Mg^{2+} are slightly greater in MW-2 than in MW-4 (Figure 36 and 37). The alkalinity of the MW-4 is slightly greater than that of the Main Canal (Figure 39). These data indicate that MW-4 has slightly longer residence time than MW-2. Taking into consideration groundwater modeling and particle-tracking results, water movement occurs across the floodplain of MRR down a moderate gradient from Main Canal to MW-2 through the swale ponds to MW-4 and ultimately to the river (Figures 30, 31 and 32). Except for samples taken in June through late August, trends of Na^+ concentrations are slightly greater in MW-4 when compared to MW-2 (Figure 36).

Although the hydrochemistry of MW-4 and of the western seep, located to the west of MW-4, may be similar in their trends of Na^+, SO_4^{2-}, and Cl^- concentrations, water travelling along flow path 4 may divert west from MW-4 and seep into the bed of the newly created side channel. This is evident when comparing concentrations of Mg^{2+}, Ca^{2+} and K^+, as well as alkalinity, which are slightly greater in the western seep (Figure 36, 37 and 39).

MW-4 and the eastern seep, which is located slightly to the east of MW-4, share similar hydrochemistry results, although the Mg^{2+} concentration is slightly lower in the eastern seep (Figure 36).

From November through the end of February, when the Main Canal surface water is at its lowest elevation, Ca^{2+} concentrations increase as the groundwater flows across the MRR. Ca^{2+} concentrations are the lowest in the Main Canal (Figures 23 and 37). MW-2 concentrations are three to four times greater than the Ca^{2+} levels found in the Main Canal. MW-4 concentrations of Ca^{2+} are 1.5 times greater than those found in MW-2. The concentration of Ca^{2+} in the western seep is slightly greater than that of MW-4 (Figures 37).

The Crocker Huffman Dam creates an impoundment where surface water is diverted to the Main Canal. However, surface water also travels either through the spawning channel, to the TF and the salmon hatchery, or over the top of the structure of the dam, depending on flow. The possibility that seepage is occurring beneath the 6.7m high Crocker Huffman Dam is significant. The Merced River has a residence time of hours to days along its 5km impoundment (Vogel, 2007). Seepage flow beneath a dam is contingent upon reservoir surface elevation, which in our case fluctuated as much as 3m during the course of observation in this study (personal observation, 2011-2012). This river stage differential may affect the groundwater hydrology of the MRR.

While examining the E-W flow path down gradient from Crocker Huffman Dam, the spawning channel, and the TF, we discovered that the two wells closest to the TF, MW-1 and MW-4, exhibited the highest concentrations of total dissolved iron, total iron concentrations, and K^{+} (Figures 41, 42, and 37). MW-1, MW-4, and the seasonal seeps shared similar trends in Mg^{2+} and Na^{+} (Figure 36). Barring the months of July and August, MW-1 had consistently high concentrations of NH_4^{+} (Figure 37).

The water that transects the MRR by flow path 3 seeps from the Main Canal and possibly flows west to MW-3 and then north to the Merced River (Figures 44 and 29). Particle-tracking results from the groundwater numeric model indicate that the flow from the Merced River to the Merced River along this flow path 3 could take up to 15 years (Figures 30 and 31), without considering near-surface flows. Ca^{2+} concentrations increase as the flow path 3 proceeds. At its origin, the Main Canal had the lowest concentrations of Ca^{2+}, while MW-2 concentrations were greater. MW-3, however, were the greatest at almost five times the concentration of those observed in the Main Canal (Figure 37). A similar trend of increasing Mg^{2+}, K^{+}, and Na^{+} concentrations occurs, although the differences between the Main Canal, MW-2, and MW-3 are not as great (Figures 36 and 37).

When comparing the concentrations of SO_4^{2-}, the Main Canal exhibited the lowest concentrations, followed by almost doubled concentrations in MW-2. MW-3 displayed an increasing trend of concentrations of SO_4^{2-} during the summer months and peaking in November at concentrations eight times that of the Main Canal (Figure 38). A similar trend in concentrations of Cl^{-} occurred when compared to the Main Canal, MW-

2, and MW-3. The Main Canal had the lowest concentrations, MW-2 slightly higher, and MW-3 had an eight-fold summer peak concentration of Cl^- in November (Figure 38).

Various forms of fine sediments accumulate on a floodplain during a flood event. As the water recedes, as it did during this study between May and July, these fine sediments and silt deposits contain organic carbon and various forms of nitrogen. Respiration processes can cause low DO levels conducive to denitrification. The majority of fine silt and forms of nitrogen that accumulated could become suboxic and form a substantial habitat for denitrifying bacteria, which are able to convert NO_3^- to N_2. As a result, this floodplain acted as a significant sink of nitrate in this riverine system. If floodplains are not present, then sediments and nitrates are not trapped and are instead dumped into a receiving body of water such as the Merced River. This is most apparent in MW-2 (Figure 35)**.**

DO inhibits the process of reduction, whereby NO_3^- converts to N_2. Furthermore, denitrification only occurs in the absence of DO and the presence of electron donors. These electron donors are present in the various forms of carbon from DOC, Fe^{2+}, or Mn^{2+}. Ammonium (NH_4^+) competes for the same exchange sites on minerals, as do most other cations when a high concentration of sodium is present (Figure 35). The sorption of NH_4^+ on these exchanges sites would be lower and enter solution more (personal communication, Berhe).

Seasonal differences were apparent in MW-3, where reduction-oxidation processes released potential SO_4^{2-} retained in the soil below the cobbles (Figure 38). Sulfate reduction-oxidation occurs in seasonally anoxic areas such as wetlands with boggy water and bodies of stagnant water that undergo cyclical wetting and drying (Connell and Patrick, 1968, 1969; Berner, 1984; Kirchner et al., 1992). Given the low ORP measured in MW-3, there is the possibility that SO_4^{2-} is being released to S(II), but this cannot be addressed in this thesis. Low levels of H_2S are deadly to many organisms.

4.2 Carbon-to-Nitrogen Ratio Analysis

Nitrification is a key transformation in the aquatic nitrogen cycle because it is the only natural process in which ammonium (NH_4^+), an end product of protein metabolism, is converted to nitrate (NO_3^-) (Walsh and Wright, 1995). The process of nitrogen-cycling in aquatic ecosystems is becoming better understood (Duff and Triska, 2000).

The mineralization or ammonification of nitrogen is influenced by the C:N (the ratio of moles of DOC the moles of TN). The process of ammonification occurs when specific bacteria fix nitrogen and convert it into ammonium (NH_4^+). Furthermore, when the C:N in the system is high, nitrogen is largely captured in microbial organic matter. If the C:N is low, however, then a proliferation of ammonia and ammonium occurs and is

released into the surrounding system (Schlesinger, 1997), as seen in MW-1 (Figures 37 and 45). MW-1 has abnormally high levels of NH_4^+ that are frequently in the range of 1.3-1.9 mg N/L, well above acceptable levels of 0.025 mg N/L in aquaculture situations (Table 1, Figure 36). Ammonia is toxic to fish at concentrations above 1.5 mg N/L (Chen, 2006). In a hydrological system with stagnant water, total ammonium nitrogen frequently accumulates within a system because of insufficient nitrification activity (Grommen et al., 2002).

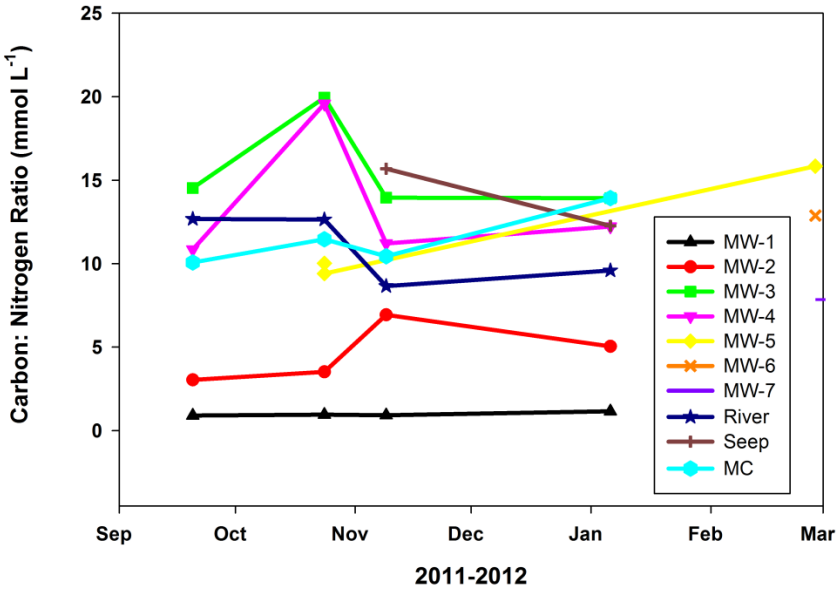

Figure 45 A C:N analysis of selected samples to characterize all wells, river, canal, and seep for the following timeframes: irrigation season, after irrigation season, and the salmon spawning/egg incubation season. MW-1 consistently represented a ratio of 1. Changes that occur may be a result of upstream management of the Merced River (River) and the Main Canal (MC). Lines have been added for visual aid.

Nitrification, which is characterized by the chemoautotrophic oxidation of ammonium (NH_4^+) to nitrate (NO_3^-), is also indirectly governed by the availability of organic carbon. The optimum rate of nitrification is reached when the ratio of carbon to nitrogen (C:N) is between 9.6 and 11.6. In many California streams, the process of nitrification is governed by the supply of NH_4^+ and O_2 (Triska, 1990) and can be linked with respiration and the mineralization of organic N to NH_4^+ (Jones et al., 1995). Other factors that influence this activity include pH, water temperature, O_2 concentration, competition for and availability of NH_4^+, and the presence of organic carbon (Jones et al., 1995; Triska et al., 1990; Strauss, 1995; Sarathchandra, 1978; Paul and Clark, 1989; Stenstrom and Poduska, 1980; Verhagen et al., 1995; Strauss and Dodds, 1997).

Bacteria require both nitrogen and carbon for integration into the chemical makeup of their cell structures. Various experiments have concluded that the metabolic rates of bacteria involved in methanogenesis can be optimized at a C:N of

approximately 8-20. The optimum range varies from case to case depending on the nature of the substrate.

Unfortunately, little is known about the factors that regulate C:N in aquatic ecosystems, except that the ratios generally increase over time and follow inputs of organic matter because nitrogen-containing amino acids and proteinaceous compounds are utilized more rapidly than carbohydrate-based compounds (Wetzel, 1983).

In the case of substrates that break down easily and are more labile, the optimum C:N is between 20 and 25. In materials that are resistant to microbial degradation, the C:N can be as high as 40 (Ghasimi, A. Idris, 2009).

C:N are useful in distinguishing between algal and land-plant origins of organic material, where the former have ratios from 4 to 10 and the latter have ratios of 20 or greater. In this case, an isotopic study may be useful for future research (Premuzic et al., 1982; Jasper and Gagosian, 1990; Prahl et al., 1994). This difference between the ratios is due to the presence of cellulose and the respective structures of the cell walls in algae and vascular plants (Ghasimi, 2009).

The analysis of the C:N was done on selected samples from the river, canal, seep, and all wells within the following timeframes: irrigation, post-irrigation, and salmon spawning and egg incubation seasons. Samples were analyzed for DOC and TN, and the carbon to nitrogen ratio (C:N) was plotted over time. MW-1 was consistently characterized by a ratio of 1. Processes in this environment were oxygen-limited and suboxic, and had ORPs in the range where methanogenesis can occur.

Examination of Figure 45 and Table 1 show higher C:N of MW-3 and MW-4 between Sept 2011 and October 2011 where an influx of carbon was observed. Within two weeks, a drastic decrease in carbon and nitrogen levels occurred in MW-3 and 4 following the cessation of Merced Irrigation District's irrigation season. Spikes in the C:N were also visible in both Main Canal and Merced River. They are delayed in relation to the spikes in MW-3 and MW-4, respectively, and occurred several months after the increases in MW-3 and MW-4. Merced Irrigation District ceased its water delivery in the Main Canal on October 31, allowing base flows to dominate the system.

Nitrification is possible when the C:N is less than 20, and the process operates ideally when the ratio is between 9.6 and 11.6 (Strauss, 2000). The average global C:N in rivers is approximately 11.1 (Schlesinger, 1997). The results from this study not only show that the ratios for Merced River, Main Canal, seep, and all wells never exceed 20, but also indicate that the average of Merced River is approximately 11, in the ideal range. In some California streams, the C:N ratio is regulated by the supply of ammonia and ammonium (NH_4^+) and oxygen, respectively (Triska, 1990), and can be connected to the respiration and mineralization of organic nitrogen (N) to ammonium (NH_4^+) (Jones et al., 1995). Other factors affecting this process include temperature, organic carbon

availability, and pH, with a pH level of 7.5 being optimum for nitrification (Strauss, 2000). In our system, MW-1 and MW-2 had considerably lower than ideal C:N ratios, indicating a limited supply of carbon and a possible abundance of nitrogen.

4.3 Ratio Chemistry to Support Flow Paths

In groundwater, only seven solutes make up nearly 95% of all water solutes (Runnells, 1993; Herczeg and Edmunds, 1999). These solutes are calcium (Ca^{2+}), magnesium (Mg^{2+}), sodium (Na^{+}), potassium (K^{+}), chloride (Cl^{-}), sulfate (SO_4^{2-}), and bicarbonate (HCO_3^{-}). Many possible sources and reactions influence the concentrations of these solutes. The hydrochemistry varies depending on several factors: the source of the water, its degree of evaporation, and the types of rocks and minerals present in the hydrological system.

The concentrations of anions and cations, as well as the alkalinity levels in the Main Canal and Merced River, were all quite similar (Figures 32 through 42, Appendix Tables 6-9). These dilute Sierra Nevada waters may be sensitive to the anthropogenic changes in the river, floodplain, and possible nutrient-loading from the TF that may have occurred in the MRR. An investigation of ratio-weathering products was performed to determine the possible reasons for significant variations in anion and cation ratios. These ratios may chemically define flow paths and mixing lines that imply that water of one composition is mixing with water of another composition. The chemical ratio results of similar compositions will be along one line.

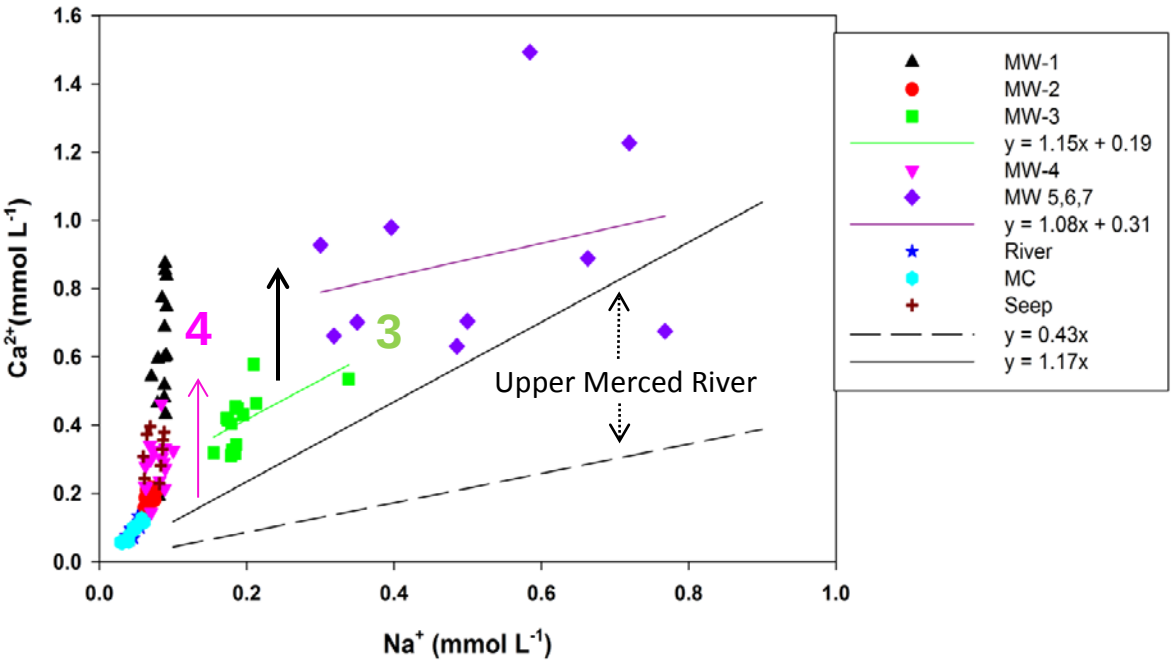

Figure 46 An investigation of Ca:Na of the Merced River Ranch surface- and groundwaters. There appears to be a linear relationship between the Merced River, the Main Canal (MC), MW-3, and the Forest Wells MW 5-7. This coincides with flow path 3 (Figure 44). Analysis of MW-3 resulted in a Ca:Na of 1.15 and R^2 of 0.37, while Ca:Na of 1.08,R^2 of 0.40. These results are similar to water samples retrieved from the upper Merced River Basin, which displayed Ca:Na between 0.43 and 1.17 (Clow et al., 1996). There seems to be a mixing line of water dependent on Ca^{2+} inputs that vary seasonally and spatially along flow path 4 (Figure 44). Seasonal changes are evident in MW-1 from September 2011 until February 2012, as depicted by the black arrow in the figure. These seasonal changes coincide with surface water elevation changes of the Main Canal.

Using our aquatic chemistry results to determine groundwater flow paths and possible mixing lines within the MRR, it appears there is a linear relationship between the Merced River, Main Canal, MW-3, and the forest wells Figures (46 and 47). Spatially this relationship is labeled as flow path 3 in Figure 44, which depicts groundwater traveling 700 m between the Main Canal and MW-3. Analysis of MW-3 resulted in a Ca:Na of 1.15 and R^2 of 0.37, while the FWs was in a Ca:Na of 1.08 and R^2 of 0.40. These results are similar to water samples retrieved from the upper Merced River basin, which displayed calcium to sodium ratios (Ca:Na) between 0.43 and 1.17 (Figure 46) (Clow et al., 1996). The Merced River is one of many watersheds that drain the Sierra Nevada Mountain Range; this parent material may supply the sediments for the Merced River Basin. Ca:Na in stream water can be portrayed by the weathering of silicate minerals, a process that also releases magnesium and potassium. The water samples gathered from lakes in the southern Sierra Nevada, an area of heavily granitic terrain, demonstrated ratios that were at the upper limit of 1.17 (Melack et al., 1985). Silicate weathering alone cannot account for the Ca:Na in the granitic lakes.

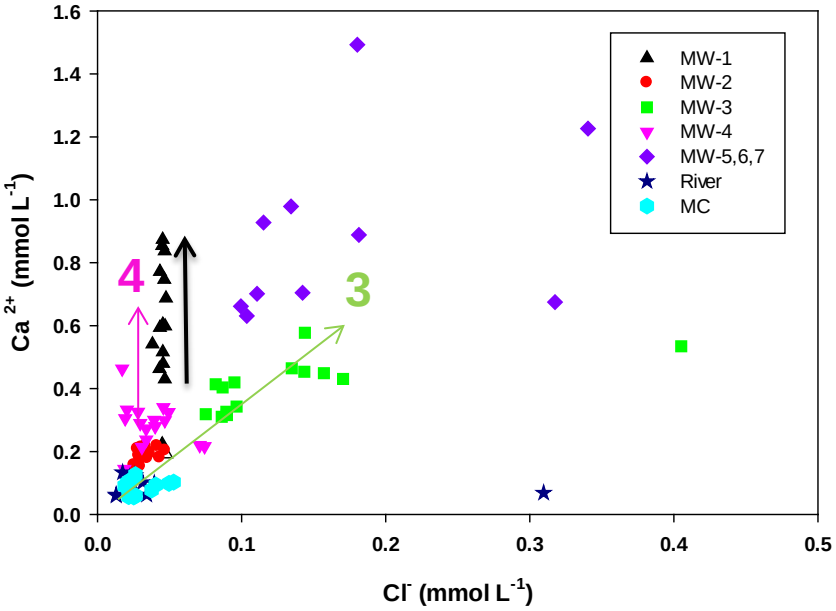

Figure 47 An investigation of Ca:Cl of the Merced River Ranch surface- and groundwaters. There appears to be a linear relationship between the Merced River (River), the Main Canal (MC), MW-3, and the Forest Wells MW 5-7. This coincides with flow path 3 (Figure 44). The Ca:Cl for the Merced River and the Main Canal are quite similar, indicating shared water sources; MW-2 receives its water from the Main Canal due to their proximity. There seems to be a mixing line of water dependent on Ca^{2+} inputs. Ca^{2+} inputs vary seasonally and spatially along flow path 4 (Figure 44). Seasonal changes are evident in MW-1 from September 2011 until February 2012, as depicted by the black arrow in the figure. These seasonal changes coincide with surface water elevation changes of the Main Canal.

When comparing the calcium-to-chloride ratios, Merced River, Main Canal, MW-2, MW-4, and seasonal seeps showed a gradual direct increase in ratios as mixing occurred from the E-W flow path from the TF (Figure 47). This process dominated during base flows, when the canal was not flowing.

MW-3 had the highest concentrations of chloride, reflecting its seasonality with evaporation. The broadest range in calcium-to-chloride ratios was found in the Forest Monitoring Wells; calcium is a function of chloride in these wells. One water sample taken during low stream flows in late September from the Merced River was unusually high in chloride (Figure 47).

The floodplain and channel deposits are made up of alluvium, which consists primarily of sands, gravels, and cobbles derived from the granites of the Sierra Nevada (Page and Balding, 1973). In the upper Merced River watershed, the Yosemite Valley, the source of chloride in spring water is probably due to the inclusion of water within the bedrock or the presence of connate water trapped in the interstices of porous rock during formation. The extreme age of the water prompts its other name: fossil water. Its hydrochemistry and composition can change over time due to weathering, contact with other rock formations, and biological processes. High chloride concentrations in the

main stem of the Merced River are most likely caused by the inflow of spring or fossil water (Clow et al., 1996). This is the essence of the source of Merced River water.

Streams dictated by precipitation have a high ratio of [Cl^-] to the sum of [Cl^-]+ [HCO_3^{2-}], with the concentration of Cl^- being the greatest during base flow (Schlesinger, 1997). In addition, the concentration of Cl^- is also greatest when the surrounding soil is in equilibrium with the processes of rock weathering and ion exchange (Schlesinger, 1997). During periods of high flow, studies have shown that concentrations of cations become greater as functions of increased discharge (Likens and Borman, 1995).

In the MRR groundwater system, another source of water appears to be creating a mixing line. This source of water is overwhelming the natural chemical signature or composition of parent materials. This mixing line appears to be dependent on inputs of Ca^{2+} and is neither a function of Na^+ nor Cl^- (Figures 46 and 47). Spatially this relationship is labeled as flow path 4 in Figure 44, depicting the groundwater traveling 850 m between the Main Canal and MW-4. There may be mixing of groundwater from the E-W flow path from the TF, located 950m up gradient from MW-4 and 700m up gradient from MW-1, resulting in a range in concentrations of Ca^{2+} (Figure 37 and 46).

There were also temporal variations in the calcium concentrations. During the timeframe that the canal was not flowing, there was a lower head of water pressure. Following the principle of Darcy's Law, discharge is proportional to the medium's permeability and to the magnitude of pressure drop between two points; in other words, the flow of groundwater between the Main Canal and the Merced River would be less. The E-W flow of groundwater from the TF could become dominant. The temporal variations in Ca^{2+} concentrations follow these trends. This is especially true with groundwater in MW-1, where Ca^{2+} became more concentrated from September 2011 through February 2012, depicted with the black arrow in Figure 46. Furthermore, MW-3 and the FWs do not appear to be involved in the flow path between the MW-2 to MW-4 since their ratios appear to be very different (Figure 46).

Nearly all the calcium, magnesium, and potassium present in stream water could be attributed to rock weathering, with the major source of calcium coming from the weathering of carbonates (Schlesinger, 1997). The weathering process of parent material is a slow process; one would not normally discover seasonal variations in calcium in a natural system. However, down gradient waters from a TF may contain effluent from undigested and digested high-protein food that consists of high levels of calcium phosphate (Hardy, 2000). Furthermore, adequate calcium levels are critical in a hatchery for the development of bone and tissue in the fish. Calcium is necessary for the hardening of eggs, increasing of embryo survival rates, and the shielding of alevin from high levels of ammonia and ammonium (Tucker, 1991).

4.4 Fe Redox Chemistry

In ground- and surface water systems, reduction-oxidation reactions are largely influenced by two primary factors: atmospheric oxygen dissolving in stream water to become what is referred to as DO, and the metabolic activity of bacteria, which are crucial in the Fe(II)/ Fe(III) redox chemistry. Ground- and surface water can be either oxidizing or reducing, with each process allowing certain chemical responses. Chemical forms of iron in our natural waters mainly exist as Fe(III) hydroxide and humic complexes (Kawakubo et al., 2002).

When DO is present in natural waters, it allows for the microbial respiration and decomposition of organic matter, the precipitation of iron, Fe(III), and manganese, Mn(III, IV), and the presence of chemical species with higher oxidation states, such as nitrate (NO_3^-) and sulfate (SO_4^{2-}). However, once the concentration of DO decreases drastically, thereby making the water suboxic, the conditions become reducing. Consequently, the system favors the cessation of the decomposition of organic matter, the reduction of oxyhydrates such as iron (Fe) and manganese (Mn), the subsequent release of reduced metals (Fe^{2+} and Mn^{2+}), and the presence of chemical species with lower oxidation states, such as ammonia (NH_3) and sulfide (S^{2-}).

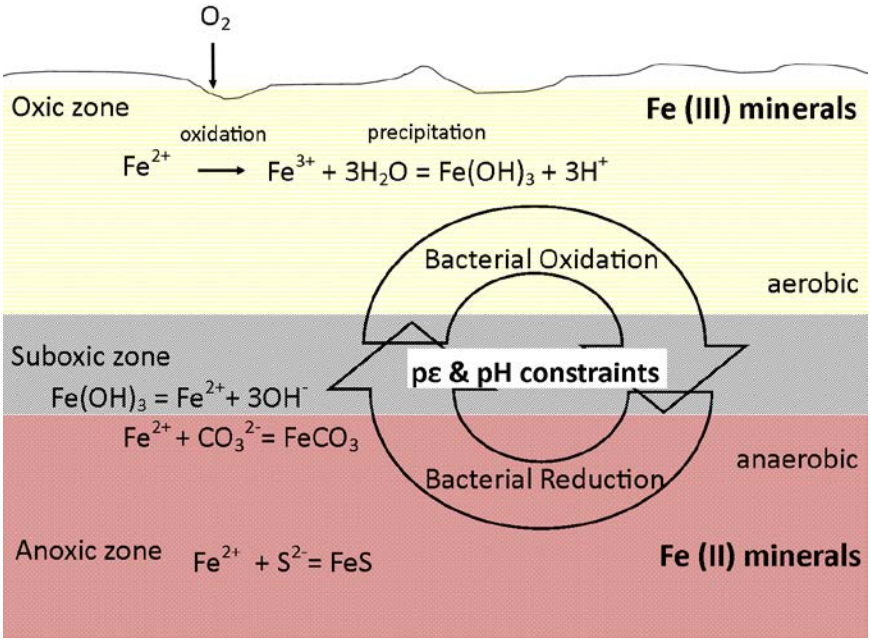

Figure 48 The iron cycle. The boundary between aerobic and anaerobic is defined by the species of interest. The iron cycle (i.e., presence of Fe (III) being aerobic) is dependent on pε and pH. Diagram modified from Fendorf (2000) and Houben and Treskatis (2007).

Terminal electron acceptors, which are crucial to understanding which ions oxidize organic matter, are typically in a set order from oxic and suboxic to anoxic sediment conditions (Meyers and Shaw, 1996). For many groundwater systems, this

sequence has the following steps: interstitial oxygen (DO), nitrate, Mn(IV) oxides, Fe(III) oxides, and sulfate (Froelich et al., 1979; Schulz et al., 1994). In other words, it begins with Fe(III) respiration, followed by the reduction of sulfate (SO_4^{2-}), and concluding in the process of methanogenesis. Microbial mineralization of organic matter under anaerobic conditions is thus regulated by both electron donors and acceptors (Sutton-Grier et al., 2011).

The relative concentrations, mobility, and bioavailability of dissolved chemical species such as ferric iron Fe(III), ferrous iron Fe(II), sulfate (SO_4^{2-}), and hydrogen sulfide (H_2S) can be traced under anoxic conditions (Lunvongsa, 2006; Jones and Mulholland, 2000). Furthermore, the iron cycle of hydrological systems is largely governed by the microbial reduction of ferric iron to ferrous iron (Figure 48). This reduction process also influences the nutrient exchange and presence of possible trace metals between sediments and surrounding water (Lovley, 1986). DO depletion and presence of Fe(II) are indicative of the respiration process (Jones and Mulholland, 2000).

To determine whether O_2 is controlling the chemical reactions, pε was calculated from our measured ORPs. The pε scale represents the availability of electrons. In other words, the "pε can be defined as the logarithm of electron concentration in a solution, which will be directly proportional to the redox potential" (Stumm and Morgan, 1981). The more negative the value of the pε, the more reducing the solution will be and the greater the fraction of each couple in its reduced form will be, with the lower ones being most affected. The pε of oxic soils is greater than 7, suboxic when pε is between 2 and 7, and anoxic when less than 2 (Fendorf, 2000). In natural waters, a high pε presents a high propensity for oxidation conditions (Stumm and Morgan, 1981).

Calculations were done in order to determine whether oxygen was the controlling factor in the redox chemistry of our stream system. In other words, does the MRR groundwater system correspond to oxic (oxygen present), suboxic (low concentrations of oxygen), or anoxic (oxygen depleted or lower than measurable levels) conditions? In order to determine this, p_{O2} must be computed. In this section, we will calculate p_{O2} for the measured ORP.

$$O_2(g) + 4\,H^+ + 4e^- = 2H_2O \qquad p\varepsilon^o = 20.8$$

because

$$p\varepsilon = p\varepsilon^o + \tfrac{1}{4} \log p_{O2} - pH$$

Given the measurements from MW-3 on 12/01/12

where $p\varepsilon = 3.71$ and $pH = 7.37$

Then

$$3.71 = 20.8 - 7.37 + \tfrac{1}{4} \log p_{O2}$$

The p_{O2} was calculated to be in the realm of 10^{-37}atm. This corresponds to ~ 10^{-40}M dissolved O_2, well within the limits of anoxic conditions (Stumm and Morgan, 1981). This is an extremely low value. A potential explanation is that the system is not in equilibrium, and the ORP was measuring a different redox couple. It is possible for the oxygen in wetland to be exhausted by heterotrophic respiration in wetland environments (Schlesinger, 1997). Generally redox processes are contingent on microorganisms that metabolize energy by electron transfer from the donor (frequently organic carbon) to the acceptor (often inorganic compounds) (Dimikic et al., 2011). In wetland soils, the oxidation state of iron is coupled with anaerobic microbial processes (Schlesinger, 1997). These iron bacteria exist very close to neutral pH and are frequently located where iron is proceeding from anoxic to oxic conditions, as seen in Figure 48 (Dimikic et al., 2011).

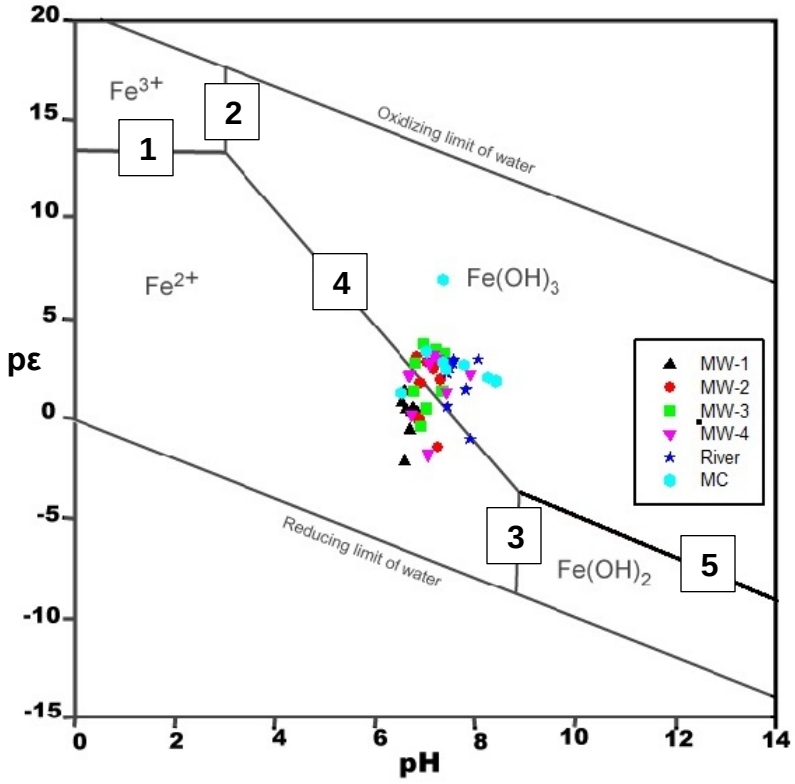

Figure 49 Diagram of pε verses pH diagram for the system Fe-H_2O. The solid phases are $Fe(OH)_3$. Lines are calculated for Fe(II) and Fe(III) = 10^{-5}M (25°C). Adapted from Stumm and Morgan (1981) and Froust (2004).

The pε-pH diagram for iron was constructed utilizing equilibrium constants for the Fe system found in Stumm and Morgan (Table 2). Field measurements of ORP were converted to pε and plotted with respective pH in order to interpret the redox patterns that occurred in the ground- and surface water of MRR (Figure 49).

Table 2 Equations Used for the Construction of Diagram pε Verses pH Diagram for the System Fe-H_2O (Figure 49)

Equation Used for the Construction of pε -pH	Functions pε	
$Fe^{3+} + e^- = Fe^{2+}$	$pε = 13.2 + \log[Fe^{3+}]/[Fe^{2+}]$	1*
$Fe(OH)_2 + 2H^+ = Fe^{2+} + 2H_2O$	$K= 8 \times 10^{12}$	2
$Fe(OH)_{3(amorph,s)} + 3H^+ = Fe^{3+} + 3\ H_2O$	$K= 9.1 \times 10^3$	3
$Fe(OH)_3 + e^- + 3H^+ = Fe^{2+} + 3\ H_2O$	$pε = 22.2 – 3\ pH$	4
$Fe(OH)_{3(s)} + e^- + H^+ = Fe(OH)_{2(s)} + H_2O$	$pε = 4.3 - pH$	5

*Numbers referred to equations placed in Figure 49. Chemical reactions given by Stumm and Morgan (1981) and Froust (2004).

As seen in Figure 49, much of the water plots near the range between the Fe(II) and Fe(III) equilibrium line. Looking at individual wells, MW-1 and MW-4 and occasionally MW-3 were in the reduced ion (Fe(II)) domain. When water containing dissolved Fe(II) is exposed to oxic conditions, Fe(III) precipitates. Rust-colored water, an indicator of reducing water being oxidized, was observed seeping into Merced River's newly created side channel, a project currently under construction by Cramer Fish Sciences (Figures 11 and 21). It appears the ORP values measured the Fe(II)/Fe(III) chemistry.

4.5 Merced River Ranch Swale Ponds

It is exceedingly rare for field soils to be homogeneous in makeup and composition. In fact, they are often quite heterogeneous and contain cracks, fissures, fractures, macropores (some of which are of biotic origin), and inter-aggregate pores (Gerke and van Genuchten, 1993a; Jarvis, 1998). These heterogeneities profoundly affect the movement of water and solutes in soils by creating non-uniform velocity fields with spatially variable flows. The resulting non-uniform flow process is often referred to as preferential flow. In this study reach, which is profoundly disturbed, there must be channels where water flows through areas of porous media at a relatively faster rate than other areas, thereby creating seasonal differences in water chemistry, as documented in Figures 32 through 42. In these avenues, there are swale ponds that may offer conduits for the preferential flow paths and a respite for nutrients.

The swale ponds in the MRR are located within the gullies between the rows of tailings or in flat areas where the dredgers turned around during the dredging process

Figure 50 Typical swale pond at Merced River Ranch.

many years ago (Figures 3, 9 and 50). The rain events that occurred during the winter months, when evaporation was low, raised the levels of the ponds (Figure 26). However, the porous cobble banks of the ponds appeared to effectively act as drainage connections to Merced River and the surrounding landscape, including ponds and gullies (Figures 2 and 50). The discharge rates of the ponds could be significantly influenced by the size of the pore spaces between the cobbles (personal observation). The ponds located between the piles of tailings are subject to year-round inundation, effectively making them perennial ponds. The groundwater dynamics are further complicated by unknown stratigraphy, i.e., the geological layers beneath the tailings have not yet been defined. This makes groundwater movement and patterns difficult to predict (Stillwater Sciences, 2007).

Intertwined throughout this area is a network of pools and canals that connect via the shallow groundwater aquifer. Similar studies on floodplains of dredged rivers have found that water within swale ponds is often redirected to the main stem of the stream (California Department of Water Resources, 1999). Seepage residence times may vary during the course of the year, as well as on a longer timescale in a wet versus a dry year.

This pond network is scattered between the Main Canal and Merced River and may link the hydrological system of ground- and surface water to the TF located upstream. They form a chain that extends to a downstream lateral canal, eventually discharging into the Merced River. Abandoned channels through this floodplain offer the possible E-W flow path (Figure 44). Subsurface waters that originate in the Main Canal could effectively flow via flow path 4 to the Merced River through the swale ponds, providing preferential flow paths, in addition to the flow paths identified through our groundwater numeric model (Figures 29 and 44).

These ponds may be effective in sequestering excess nutrients from the upstream TF until they fill with sediment or until the phosphorous sorption capacity is reached (Jackson and Pringle, 2010), i.e., thus serving as unintentional settling ponds. Typically ponds are important in aquatic nutrient cycling it is where extensive denitrification occurs (Fairchild and Velinsky, 2006) and where the rates of removal of excess nutrients increase as a function of residence times (Dendy, 1974). They enhance pollutant retention and cycle at a rate greater than a riparian buffer alone (Jackson and Pringle, 2010). Providing vegetative buffer strips within riparian zones could alleviate possible excess nutrients and chemically reduced waters before they are discharged into streams (Osborn, 2006).

4.6 Implications at the Seepage Sites

The season during which the canal is not flowing extends from November 1 through April 1. Seasonal trends can be witnessed within the hydrochemical results (Figures 32-42). Specifically, an increased trend in alkalinity was documented for the months of November through January in MW-1 and the western seep relative to MW-4 (Figure 39). Alkalinity can be used as an indicator of organic matter breakdown. Microbial communities acquire energy from organic carbon and thereby impact the carbonate alkalinity of surrounding waters (Dupraz et al., 2008). Aerobic respiration produces only slight changes in alkalinity, while anaerobic respiration produces greater alkalinity changes. These microbial metabolic activities could create increased alkalinity environments and encourage precipitation (Dupraz et al., 2008). The observed increase in alkalinity may be indicative of anaerobic respiration for the waters measured in MW-1 and the western seep and the presence of suboxic water. Within the intra-gravel environment, hydraulic gradients and hyporheic flows are influenced by stream discharge (Wroblicky et al., 1998). In our system, the seeps were present during this timeframe (November through February), and groundwater could dominate in the hyporheic zones during low flow or base flow, the same period of time when the salmon are spawning and the juveniles rearing. Consequently, low stream flows in winter, the same time when larval salmon are developing, and may be amplifying the effects of suboxic groundwater on the intra-gravel environment (McRae, 2012).

Seasonal groundwater seeps were sampled from two locations: one from the banks of the Merced River, eastern seep, and the other from just below the water level in the newly created side channel, the western seep (Figures 2, 11, and 14). Multiple lines of evidence indicate that these seasonal groundwater seeps contain chemically reduced Fe (Figures 32-42 and 49). Fe(II) was visually quite apparent when emanating groundwater showed rust color (Figure 11).

An examination of our Ca:Na and our Ca:Cl results indicated that the seasonal seeps had elevated Ca^{2+} inputs from the TF along flow path 4 (Figures 44, 46, and 47). Groundwater modeling results shown in Figure 44 indicate that water seeping into the Merced River could originate from the TF along the E-W path or along flow path 4. As a result of these paths, seasonal seeps occurred in the riverbed and along the banks below the water surface, and they can result in low DO environments. One of these seeps sampled was below the water level. Significant connections between sediment permeability and stream discharge are apparent, particularly in relation to the quality of water found in the hyporheic zone (Arntzen et al., 2006). Concentrations of DO have been linked to spawning site selection (Hansen, 1975; Geist et al., 2002; Quinn, 2005), and low concentrations of DO have been found to reduce the rates of survival and

growth of larval fish (Alderdice et al., 1958; Crisp, 2000). However, the correlation between hydrochemistry in the hyporheic zone and the selection of spawning sites by salmon remains unclear. It is therefore critical to ascertain the seepage sites and flow paths by which dissolved nutrients that are transported by water are discharged into the stream itself.

At spawning locations where suboxic groundwater upwelling is a prominent feature, the rates of embryo survival are reduced and are generally poor (Malcolm, 2003; Malcolm, 2004). In some locations where oxic surface water dominates the hyporheic zone, the rates of embryo survival are reported to be at or near 100% (Malcom, 2003). Seepage is a crucial component of stream morphology and the creation of vital microhabitats for fish (Bunn and Arthington, 2002). Phreatic groundwater, which originates deep in the subsurface, is anoxic due to long residence times, in addition to the fact that it contains a significant amount of dissolved solutes (Freeze and Cherry, 1979).

Chapter 5 Conclusions

Human intervention and manipulation of the Merced River floodplain, which is adjacent to what was once a prolific Chinnok salmon spawning and rearing habitat of the Sacramento-San Joaquin river systems, have adversely affected the ecosystem function of the area. Intervention by diversions, exploitation of mineral sources by dredging, and increased nutrients from aquaculture have created an environment not conducive to salmon spawning and incubation. Diversions have altered the temporal wetting and hydraulic gradients of the region, while the dredging process done during the 1930s, disrupted the natural ground- and surface water interactions and flow patterns of Merced River riparian habitat and floodplain habitats. The aquaculture upstream adds organic inputs to this floodplain system that it cannot remedy. The ecosystem function of this floodplain has been greatly impacted; it can no longer filter and purify water because it has no vegetative or soil trap for nutrients and therefore no longer provides a seasonal productive habitat for important fisheries, such as Chinook Salmon.

Chemical analyses from four groundwater wells, two seasonal seeps, the Merced River, and the Main Canal indicate that there are three sources of water for this floodplain: the Merced River and Main Canal (which are chemically very similar), the waters from the TF, and precipitation, resulting in three flow paths. Only one flow path (from the Main Canal to MW-4) has a mixing line dependent on Ca^{2+} inputs, which are most likely attributed to nutrient loading from the TF upgradient of the floodplain.

An attempt to clarify the possible nutrient contributions from the salmon hatchery and the TF were made by obtaining both DOC and TN levels. The C:N ratios were calculated, and nitrogen is in abundance for MW-1, which exhibited a ratio of 1 over the five-month monitoring period (Figure 45).

MODFLOW particle tracer experiments were performed in the middle of the top layer, and the results indicate that the travel time between the Main Canal and Merced River is approximately ten to 15 years. However the model was not designed to interpret near-surface groundwater flow through the undulating stacks of cobbles, ravines, and remnant ponds, which must provide preferred pathways. Based on the well levels and chemistry, this system responds on a much faster scale. Reconciling these results, there must be significant preferential flow paths. Candidate flow paths are the abandoned channels from the dredging era. The hydraulic gradient set up by the groundwater connection between the Main Canal and the Merced River ensures that any effluent released by the fish facilities will be transported to the Merced River in that timeframe. Of concern is the possibility that this effluent-like suboxic water is seeping in Merced River's natural salmon spawning grounds, thus creating suboxic environments.

Waters that seep from the Main Canal to the Merced River in this area *are* suboxic, which is not conducive to salmon spawning, and are detrimental to the developing salmon embryo.

Due to the causal connections between the hydrological system of the Merced River floodplain and the riverine system, habitat rehabilitation must target not only the surface water but also important subsurface hydrological components.

References

Alderdice, D. F., Wickett, W. P., Brent, R., 1958. Some effects of temporary exposure to low dissolved oxygen levels on Pacific salmon eggs. J. Fish. Res. Board Can. 15: 229-249.

American Geological Service Inc. and Wondijina Research Institute, 2007. Preliminary Aggregate and Gold Resource Study Wade Enterprises Property, Merced County, CA.

Arkley, J.R., 1962. Soil Survey Merced Area, California. California Agricultural Experiment Station United States Department of Agriculture Soil Conservation Service. Issued July 1962, Reissued March 1991.

Arntzen, E.V., Geist D.R., Dresel P.E., 2006. Effects of fluctuating river flow on groundwater/surface water mixing in the hyporheic zone of a regulated, large cobble bed river. River Res Appl. 22: 937-946.

Aryafar, A., 2007. Prediction of groundwater inflow and height of the seepage face in a deep open pit mine using numerical finite element model and analytical solutions IMWA Symposium, Water in Environments. Calgliari, Italy.

Bailey, S.W., Driscoll, C.T., and Hornbeck, J.W., 1995. Acid-base chemistry aluminum transport in an acidic watershed and pond in New Hampshire, Biogeochemistry. 28: 69-91.

Balding, GO, and Page, R.W., 1971. Data for wells in the Modesto-Merced Area San Joaquin Valley, California. US Geological Survey Open-File Report.

Balistrieri, L. S., Murray J. W. and Paul B., 1992. The biogeochemical cycling of trace metals in the water column of Lake Sammamish, Washington: Response to seasonally anoxic conditions. Limnol. Oceanogr. 37: 529-548.

Barr, C.B., 1991. The distribution, habitat, and status of the valley elderberry longhorn beetle Desmocerus californicus dimorphus. U.S. Fish and Wildlife Service. Sacramento, CA.

Bay Delta Conservation Plan, 2013. Biological goals and objectives. Sacramento, CA.

Baxter, J.S., McPhail, 1999. The influence of redd site selection, groundwater upwelling, and over-winter incubation temperature on survival of bull trout (*Salvelinus confluentus*) from egg to alevin. Can. J. Zool. 77: 1233-1239.

Bean, David, 2010. AMEC, Personal communication.

Berhe, Asmeret, 2012. Assistant Professor School of Natural Sciences, University of California, Merced, Personal communication.

Bjornn, T. and D. Reiser, 1991. Habitat requirements of salmonids in streams. In Meehan, W. ed., Influences of forest and rangeland management on Salmonids fishes and their habitat. American Fisheries Society Special Publication. 83-138.

Blakeman, Dennis, 2010. California Department of Fish and Game, Personal communication.

Boulton, A., Findlay S., 1998. The functional significance of the hyporheic zone in streams and rivers. Annu.Rev. Ecol.Syst. 29: 59-81.

Bouwer, H. and Rice, R.C., 1976. A Slug Test for determining hydraulic conductivity of unconfined aquifers with completely or partially penetrating wells. Water Resources Research.12: 3 424-428.

Bouwer, H., 1989. The Bouwer and Rice slug test—an update. Ground Water 27: 304–309.

Brett, J. R., 1962. Some considerations in the study of respiratory metabolism in fish, particularly salmon. J. Fish. Res. Bd. Can.19: 1025-1038.

Bricker, Owen P., Newell, Wayne L., Simon, Nancy S., Bog iron formation in the Nassawango Watershed, Maryland. U.S. Geological Survey Open-File Report 03-346 Online Only Version 1.0.

Brock, T. A., 1991. Effects of irrigation water quality, amendment and crop on salt leaching and sodium displacement. M. S. Thesis, Montana State University, Bozeman.

Brooks R.,H. and A. T. Cory, 1964. Hydraulic properties of porous media. Hydrology Paper no. 3, Civil Engineering Department, Colorado State University, Fort Collins, CO.

Brown, C. and D. Hallock, 2009. Washington State Dissolved Oxygen Standard: A Review and Discussion of Freshwater Intragravel Criteria Development. Publication No. 09-03-039. Environmental Assessment Program, Washington State Department of Ecology, Olympia, Washington 98504-7710.

Brunke, M., Gonser T., 1997. The ecological significance of the exchange process between rivers and groundwater. Freshwater Biology. 37:1-33.

Bunn, S.,E, Arthington A.H., 2002. Basic principles and ecological consequences of altered flow regimes for aquatic biodiversity. Environ Manag 30: 492-507.

Burleson, M. L. and Milsom, W. K., 1993. Sensory receptors in the first gill arch of rainbow trout. Respir. Physiol. 93: 97-110.

Burow, K.R., Shelton J.L., Hevesi, J.A. and Weissmann, G.S., 2004. Hydrologic Characterization of the Modesto Area, San Joaquin Valley California. 2004-5232, U.S. Geological Survey.

Burt, T.,P., Pinay G., 2005. Linking hydrology and biogeochemistry in complex landscapes. Prog. Phys. Geogr. 29, 297-316.

California Department of Fish and Game, 1998. Genetic concerns related to the use of out-of-basin fall-run Chinook Salmon for studies in the lower San Joaquin River. Presented to the State Water Resources Control Board Public Hearing; Phase 2 regarding “The responsibilities of the parties who are jointly proposing Joaquin River Agreement.” CDFG Exhibit 20. CDFG Region 4. June 1998.

California Department of Fish and Game Fisheries Branch, 2011. Anadromous Resources Assessment Grand Tab California Central Valley Sacramento and San Joaquin River Systems Chinook Salmon Escapement Hatcheries and Natural Areas.

California Department of Water Resources, 1980. Bulletin 118-80, Ground Water Subbasins in California.

California Department of Water Resources, 1999. Central District, Yuba Goldfields Fish Barrier Project, Yuba County, CA, November.

California Water Resource Control Board, 2005. San Joaquin River Agreement, Technical Report.

Camp, C., 1915. Field notes: Journal and catalog: Yosemite National Park, California. Volume 557, Section 3. Archives of the Museum of Vertebrate Zoology, University of California, Berkeley.

Carlson, Robert E., 1997. A trophic state index for lakes, Limnology and Oceanography.

Carpenter, S, Gunderson L, 2001. Coping with collapse: Ecological and social dynamics in ecosystem management. Bioscience. 51: 451-457.

Carrillo, Charlie, 2012. Personal communication.

Carson, B, Executive Director of the Natural Resource Council of Maine, www. Nrcm.org/news

CH2M Hill, 2001. Merced Water Supply Plan – Final Status. Prepared for City of Merced and Merced Irrigation District. September.

Chapelle, F., 1995. Deducing the distribution of terminal electron-accepting process in hydrologically diverse groundwater systems. Water Resources Research 31: 359-371.

Chapelle, F. E., McMahon PM, 1995. Deducing the distribution of terminal electron-accepting process in hydrologically diverse groundwater systems. Water Resources Research. 31:2 359-371.

Chen, S., Ling, J., Blancheton, J.P., 2006. Nitrification kinetics of biofilm as affected by water quality factors. Aquac. Eng. 34: 179–197.

CIMIS, 2012. California Irrigation Management Information System, Merced Station #148, www.cimis.water.ca.gov/cimis

Clow, David, M., Alisa Mast and Doonals H. Campbell, 1996. Controls on Surface Water Chemistry in the Upper Merced River Basin, Yosemite National Park Hydrological Processes.10: 727-746, US Geological Survey MS 415, Denver Federal Center Denver, CO 80225, USA.

Conard, S. G., R. L. MacDonald, and R .F. Holland, 1980. Riparian vegetation and flora of the Sacramento Valley, in riparian forests in California: their ecology and conservation. Institute of Ecology Publication No. 15, Agricultural Sciences Publications, University of California, Berkeley.

Crisp, D . T., 1993a. The environmental requirements of salmon and trout in fresh water. Freshwater Forum, 3: 176-202.

Crisp, T. D., 2000. Trout and salmon: ecology, conservation, and rehabilitation. Fishing New Books, Oxford.

Cramer Fish Sciences, 2010. Merced River Ranch Floodplain Restoration Project. 600 NW Fariss Rd., Gresham, OR 97030.

Davison, W., and E. Tipping, 1984. Treading in Mortimer's footsteps: The geochemical cycling of iron and manganese in Esthwaite Water. Fresh-water Biol. Assoc. Annu. Ren 52: 9 l-101.

Davis, J. C., 1975. Minimal dissolved oxygen requirements of aquatic life with emphasis on Canadian species: a review. Journal of the Fisheries Research Board of Canada. 32: 2295-2332.

DeVries, P., 1997. Riverine salmonid egg burial depths: review of published data and implications for scour. Canadian Journal of Fisheries and Aquatic Sciences 54: 1685-1698.

Dendy, F. E., 1974. Sediment trap efficiency of small reservoirs. Transactions of the American Society of Agricultural and Biological Engineers 17: 898–908.

Dimkic, Milan, Milenko Pusic, Brankica Majkic-Dursun, Vesna Obradovic, 2011. Certain Implications of Oxic Conditions in Alluvial Groundwater. Water Research and Management. 1:2 27-43.

Downs, Peter, Maia Singer, Bruce Orr, Zooey Diggory, Tamara Church, 2011. Restoring Ecological Integrity in Highly Regulated Rivers:The Role of Baseline Data and Analytical Environmental Management 48: 847–864.

Dosdat, A., Ruyet, J.P., CovÈs, D., Dutto, G., Gasset, E., Le Roux, A., LemariÉ, G., 2003. Effect of chronic exposure to ammonia on growth, food utilization and metabolism of the European sea bass (*Dicentrarchus labrax*). Aquatic Living Resources, Paris, 16: 509-520.

Duff, J.H., and F.J. Triska, 2000. Nitrogen biogeochemistry and surface-subsurface exchange in streams. 197-220, Streams and Ground Waters. Academic Press, San Diego, CA.

Dupraz, C., et al. 2008. Processes of carbonate precipitation in modern microbial mats, Earth-Science Reviews. doi:10.1016/j.earscirev.2008.10.005

Environmental Protection Agency (USEPA). 1986. Ambient Water Quality Criteria for Dissolved Oxygen. Office of Water. EPA 440/5-86-003. 35pp. Available online at <http://www.epa.gov/cgi-bin/claritgw?op-Display&document=clserv:OAR:0579; &rank=4&template=epa>. Website accessed February 17, 2013.

Fisher, L.H., and Healy, R.W., 2008. Water movement within the unsaturated zone in four agricultural areas of the United States. Journal of Environmental Quality, 37:3 1051-1063.

Fairchild, G.W., and Velinsky, D.J., 2006. Effects of small ponds on stream water chemistry. Lake and Reservoir Management 22:4 321-330.

Fendorf, Scott, 2000. Soil Chemistry Lecture Supplement 4 *Oxidation and Reduction (Redox) Reactions.* Stanford University.

Freeze, R. A., and J. A. Cherry, 1979. Groundwater. Prentice-Hall, Englewood Cliffs, New Jersey.

Froelich, P. N., Klinkhammer, G. P., Bender, M. L., Luedtke, N. A., Heath, G. R., Cullen, D., Dauphin, P., Hammond, D., Hartman, B., and Maynard, V., 1979. Early oxidation of organic matter in pelagic sediments of the eastern equatorial Atlantic: suboxic diagenesis. Geochim. Cosmochim.Acta, 43:1075-1090.

Froust, Richard, 2004. Environmental Chemistry Lecture 13 env440, Northern Arizona University.

Geist, David, 1998. Redd Site Selection and Spawning Habitat Use by Fall Chinook Salmon, Project No. 1994-06900, 125 electronic pages, (BPA Report DOE/BP-62611-14).

Geist, D. R., Hanrahan, T.P., Arntzen, E.V, McMichael, G.A., Murray, C.J., Chien, Y.J., 2002. Physiochemical characteristics of the hyporheic zone affect redd site selection by chum salmon and fall Chinook salmon in the Columbia River. N Am J Fish Manag 22: 1077-1085.

Geomatrix Consultants, Inc., 2007. Merced River Ranch Groundwater Study log of MW-1 Fresno, CA.

Gerke, H. H., and Kohne, J. M., 1999. Impact of clayey coatings on hydraulic properties of soil aggregates. Geophys. Res. Abstracts. 1:2 324.

Gerke, H. H., and van Genuchten, M. Th., 1993a. A dual-porosity model for simulating the preferential movement of water and solutes in structured porous media. Water Resour. Res. 29:2 305–319.

Gerke, H. H., and van Genuchten, M. Th., 1993b. Evaluation of a first-order water transfer term for variably saturated dual-porosity flow models. Water Resources Res., 29:4 1225-1238.

Ghasimi , A ., Idris , T., Chuah, and G B. T. Tey, 2009. The Effect of C:N:P ratio, volatile fatty acids and Na+ levels on the performance of an anaerobic treatment of fresh leachate from municipal solid waste transfer station S. M. D. Ghasimi , A. African Journal of Biotechnology. 8:18 4572-4581, 15 September.

Gilvear, D.J., Heal K.V., 2002.Hydrology and the ecological quality of Scottish river ecosystems. The Science of the Total Environment. 294:11,131-159.

Goldman, H. B., 1964. Sand and gravel in California: an inventory of deposits Part B - Central California. Bulletin No. 180-B. California Department of Mines and Geology Sacramento, CA.

Green, C.T., Fisher , L., Benkins, 2008. B. Nitrogen fluxes through unsaturated zones in five agriculture settings across the United States., J Environmental Quality. 37:1073-1085.

Grinnell, J., 1915. Field notes: mixed: Yosemite region, California, 1915 (summer). Archives of the Museum of Vertebrate Zoology. 484:2. University of California, Berkeley, CA.

Grinnell, J., 1921. Field notes: journal and catalog: Merced and Stanislaus counties, California, 1921. Archives of the Museum of Vertebrate Zoology. 1323:6 University of California, Berkeley, CA.

Grommen, R., Van Hauteghem, I., Van Wambeke, M., Verstraete, W., 2002. An improved nitrifying enrichment to remove ammonium and nitrite from freshwater aquaria systems. Aquaculture 211, 115–124.

Gronberg, J.M. and Kratzer, C.R., 2006. Environmental Setting of the Lower Merced River Basin, California. 2006-5152, U.S. Department of the Interior; U.S. Geological Survey.

Hancock, T., Sandstrom, M., 2008. Pesticide Fate and Transport through Unsaturated Zones in Five Agricultural Settings, USA. J Environmental Quality.37:1086-1100.

Hansen, E. A. 1975. Some effects of groundwater on brown trout redds. Trans Am Fish Soc 104: 100-110.

Hara, T. J., 1982. Structure activity relationships of Amino Acids as Olfactory Stimuli Chemoreception in Fishes, Elsevier Amsterdam 135-157.

Harbaugh, A.W. and McDonald, M.G., 1996, Programmer's documentation for MODFLOW-96, an update to the U.S. Geological Survey modular finite-difference ground-water flow model: U.S. Geological Survey Open-File Report 96-486, 220

Harden, J. W., 1987. Soils Developed in Granitic Alluvium near Merced, California. In Soil Chronosequences in the Western United States, J.W. Harden ed., U.S. Geological Survey Bulletin 1590-A.

Hardy, R. W., 2000. New developments in aquatic feed ingredients, and potential of enzyme supplements. In: Cruz -Suárez, L.E., Ricque- Marie, D., Tapia-Salazar, M., Olvera-Novoa, M.A. y Civera-Cerecedo, R., (Eds.). Avances en Nutrición Acuícola V.Memorias del V Simposium Internacional de Nutrición Acuícola. 19-22 Noviembre, 2000. Mérida, Yucatán, Mexico.

Hauer and Lamberti, 2006. Methods in Stream Ecology, 2nd ed., Elsevier.

Haycock, N. E., Muscutt, A.D., 1995. Landscape management strategies for the control of diffuse pollution. Landscape Urban Plan. 31:313-321.

Herczeg, A. L. and W. M. Edmunds. 1999. Inorganic ions as tracers. In Environmental Tracers in Subsurface Hydrology, ed. P.G. Cook and Herczeg, 31-77. Boston: Kluwer A.P.

Hill, A. R., Devito, K. J., Campagnolo, S. and Sammugadas, K., 2000. Subsurface denitrification in a forest riparian zone: interactions between hydrology and supplies of nitrate and organic carbon. Biogeochemistry, 51 193-223.

Holland, V. L. and D. J. Keil., 1995. California vegetation. Kendall/Hunt Publishing Company, Dubuque, Iowa.

Houben, G., and C. H. Treskatis, 2007. Water Well Rehabilitation and Reconstruction. McGraw Hill, New York. pp. 391. ISBN-13: 978-0-07- 148651-4.

Hvorslev, M. J., 1951. Time lag and soil permeability in ground-water observations. U.S. Corps of Engineers, Waterways Experiment Station, Bulletin 36, Vicksburg, Mississippi.

Jackson, Rhett C. and Catherine Pringle, 2010. Ecological Benefits of Reduced Hydrologic Connectivity in Intensively Developed Landscapes BioScience 60: 37–46.

Jarvis, N. J., 1998. Modeling the impact of preferential flow on non-point source pollution. In: Physical non-equilibrium in soils: modeling and application, (ed. H.H. Selim & L.Ma), Ann Arbor Press. 195-221.

Jasper, J. P., and Gagosian, R. B., 1990. The sources and deposition of organic matter in the Late Quaternary Pigmy Basin, Gulf of Mexico. Geochim. Cosmochim. Acta. 54:1117-1132.

Jones, J. B., S. G. Fisher, and N. B. Grimm. 1995. Nitrification in the hyporheic zone of a desert stream ecosystem. Journal of the North American Benthological Society.14: 249-258.

Jones, J. B., and P. J. Mulholland (Eds.), 2000. Streams and Ground Waters, 425 pp., Academic, San Diego, California.

Johnson, M.L., Pasternack G., 2002. North Coast River Loading Study: Road Crossing on Small Streams. Vol. I, status of salmonids in the watershed. CTSW-RT-02-040 (2002). Sacramento, CA Caltrans, California Department of Transportation.

Heming, T.A., 1982. Effects of temperature on utilization of yolk by Chinook salmon (*Oncorhynchus tshawytscha*) eggs and alevins. Can. J. Fish. Aquat. Sci. 39:184-190.

Kawakubo, S., Tachikawa, K. and Iwatsuki, M. 2002. Speciation of iron in river water using a specific catalytic determination and size fractionation. Journal Environmental Monitor. 4: 263-269.

Kondolf, G. M., A. J. Boulton, S. O'Daniel, G. C. Poole, F. J. Rahel, E. H. Stanley, E. Wohl, A. Bång, J. Carlstrom, C. Cristoni, H. Huber, S. Koljonen, P. Louhi, and K. Nakamura, 2006. Process-based ecological river restoration: visualizing three-dimensional connectivity and dynamic vectors to recover lost linkages. *Ecology and Society* 11:2 5.

Kondolf, G. M., 2000. Some Suggested Guidelines for Geomorphic Aspects of Anadromous Salmonid Habitat Restoration Proposals. Society for Ecological Restorations 8:1 48-56.

Kuhn, A. and Sigg L., 1993. Arsenic cycling in eutrophic Lake Greifen, Switzerland: Influence of seasonal redox processes. Limnol. Oceanogr. 38:5 1052–1059.

Lazzari, Rafael and Baldisserotto, Bernardo, 2008. Nitrogen and Phosphorous Waste in Fish Farming. B. Inst. Pesca, São Paulo. 34:4 591 - 600.

Levin, S. A., 1992. The Problem of Pattern and Scale in Ecology: The Robert H. MacArthur Award Lecture. Ecology. 73:6 1943-1967.

Likens, G .E., and F.H. Bormann. 1995. Biogeochemistry of a forested ecosystem. Springer-Verlag, N.Y. 162pp. 2nd ed. 2001.

Lovely, D.R. and Phillips E.J. 1986. Organic matter mineralization with reduction of ferric iron in anaerobic sediments. Appl. Environ. Microbiology. 51, 683-689.

Lunvongsa, S., M. Oshima, S. Motomizus, 2006. Determination of total and dissolved amount of iron in water samples using catalytic spectrophotometric flow injection analysis. Talanta 68: 969–973.

Malcolm, I. A., Soulsby C., 2002. Thermal Regime in the hyporheic zone of two contrasting salmonid spawning streams: ecological and hydrological implications. 9: 1-10.

Malcolm, I. A., Soulsby C., 2003. Heterogeneity in ground water-surface water interactions in the hyporheic zone of a salmonid spawning stream. Hydrological Processes. 17 601-617.

Malcolm, I. A., Soulsby C. 2005. Catchment-scale controls on groundwater-surface water interactions in the hyporheic zone: implications for salmon embryo survival. River Research and Applications 21: 977-989.

Malcom, I. A., Soulsby C., 2004. Hydrological influences on hyporheic water quality: implications for salmon egg survival. Hydrological Processes 18 1543-1560.

Mason, J . C ., 1969. Hypoxial stress prior to emergence and competition among coho salmon fry. J. Fish. Res. Bd Canada 26: 63-91 .

McRae, Kyla D. Warren, J. Mark Shrimpton, 2012. Spawning site selection in interior Fraser River coho salmon Oncorhynchus kisutch Endangered Species Research 16: 249–260.

McSwain, K. R., 1977. History of Merced Irrigation District, 1919-1977. Merced Irrigation District.

Melack, J. M., Stoddard, J. L. and Ochs, C. A. 1985. Major ion chemistry and sensitivity to acid precipitation of Sierra Nevada Lakes, Wat. Resour. Res. 21 27-32.

Mesick, Carl, 2009. The high risk of extinction for the natural Fall-Run Chinook Salmon population in the Lower Tuolumne River due to insufficient instream flow releases. Energy and Instream Flow Branch U.S. Fish and Wildlife Service, Sacramento, California.

Mesick, C. F., 2010a. The high risk of extinction for the natural Fall-Run Chinook Salmon population in the Lower Merced River due to insufficient instream flow releases. Report prepared for the California Sportfishing Protection Alliance.

Meyers, Phillip and Timothy J. Shaw Whitmarsh, R.B., Sawyer, D.S., Klaus, A., and Masson, D.G. 1996. Organic matter accumulation, sulfate reduction and methanogensis in Pliocene-Pleistocene Turbidites on the Iberia Abyssal Plain. Proceedings of the Ocean Drilling Program, Scientific Results, Vol. 149.

Montgomery, D. R., .2003. of Fish: The Thousand Year Run of Salmon. Boulder, CO: Westview Press.

Naiman, R. J., Bunn S.E., Nilsson C., Petts G.E., Pinay G., 2002. Legitimizing fluvial systems as users of water: an overview, Environ. Manag. 30: 455-467.

Naiman, R. J., Latterell J.J., Pettit N.E., Olden J.D., 2008. Flow variability and the biophysical vitality of river systems. Geoscience. 340: 9-10 553-700.

National Research Council, 1996. Upstream: Salmon and society in the Pacific Northwest. Washington, D.C.: National Academy Press.

Nielsen, J. L., Tupper, D., and Thomas, W.K. 1994. Mitochondrial DNA polymorphism in unique runs of Chinook salmon (Oncorhynchus tshawytscha) from the Sacramento – San Joaquin River basin. Conserv. Biol. 8: 882–884.

Nova´k, van Genuchten, 2000. Infiltration of Water into Soil with Cracks. Journal of Irrigation and Drainage Engineering J F.

Novacek, M., Cleland E., 2001.The current biodiversity extinction event: scenarios for mitigation and recovery. Proc. Natl. Acad. Sci. USA 98:10 5466-5470.

O'Day, Peggy, 2009. Professor, University of California, Merced, Lecture notes redox tutorial 10, Merced, CA.

Obeidat, Safwan et al., 2008A Multi-Source Portable Light Emitting Diode Spectrofluorometer, Applied Spectroscopy, 62: 3.

Osborn L., Kovacic D., 2006. Riparian vegetative buffer strips in water-quality restoration and stream management. Freshwater Biology. 29:2 243-258.

Page, R. W., Balding, G.O., 1973. Geology and Quality of Water in the Modesto-Merced Area, San Joaquin Valley, California, with a Brief Section of Hydrology. USGS Water Resources Investigations 6-73, 85.

Paul, E. A., and F.E. Clark, 1989. Soil microbiology and biochemistry. Academic Press, San Diego, CA. 275.

Peterson, N. P., Quinn, T.P., 1996. Spatial and temporal variation in dissolved oxygen in natural egg pockets of chum salmon, in Kennedy Creek, Washington. Journal of Fish Biology 48: 131-143.

Philip A. Meyers and Timothy J. Shaw Whitmarsh, R.B., Sawyer, D.S., Klaus, A., and Masson, D.G. (Eds.), 1996. Proceedings of the Ocean Drilling Program, Scientific Results, Vol. 149.

Piper, R. G., I.B. McElwain, L.E. Orme, J.P. McCraren, L.G. Fowler, and J.R. Leonard, 1982. Fish hatchery management. U.S. Department of Interior, Fish and Wildlife Service, Washington D.C. 517.

Pinay, G., O'Keefe, T., Edwards, R., Naiman, R. J., 2003. Potential denitrification activity in the landscape of a Western Alaska drainage basin. Ecosystems 6: 336–343.

Platts, W. S., Torquemada RJ, McHenry ML, Graham CK, 1989. Changes in spawning and rearing habitat from increased delivering of fine sediment to the South Fork Salmon River, Idaho. Fisheries Transactions of the American Fisheries Society. 118: 274-283.

Poff, N. L., Richter, B. D., 2009. The ecological limits of hydrological (ELOHA): a new framework for developing regional environmental flow standards. Freshwater Biology.

Poole, G., Berman C., 2001. An Ecological Perspective on In-Stream Temperature: Natural Heat Dynamics and Mechanisms of Human-Caused Thermal Degradation. Environmental Management. 27:6 787-802.

Prahl, F. G., Ertel, J. R., Goni, M. A., Sparrow, M. A., and Eversmeyer, B., 1994. Terrestrial organic carbon contributions to sediments on the Washington margin. Geochim. Cosmochim. Acta, 58:3035-3048.

Pringle, Catherine, 2001. Hydrologic Connectivity and the Management of Biological Reserves: A Global Perspective. Ecological Applications. 11:4 981-998.

Pringle, C. M., Triska, F. J., 2000. Emergent Biological patterns and Surface-subsurface interactions at landscape scales. In Streams and Ground Waters, Jones JA Mulholland P (eds.) Academic Press: Orlando, FL 167-196.

Premuzic, E.T., Benkovitz, C. M., Gaffney, J.S., and Walsh, J.J., 1982. The nature and distribution of organic matter in the surface sediments of world oceans and seas. Org. Geochem. 4: 63-77.

Puckett, L. J. et al., 2008. Transport and Fate of Nitrate at the Ground-Water/Surface-Water Interface. Journal of Environmental Quality, 37(3): 1034-1050. research. Rev. of Geophys., Supplement, 189–192.

Quinn, T. P., 2005. The behavior and ecology of Pacific salmon and trout. University of Washington Press, Seattle, WA

Roberts, W. G., J. G. Howe, and J. Major, 1980. A survey of riparian flora and fauna in California. Pages 3-19 in A. Sands, editor. Riparian forests in California: their ecology and conservation. Agricultural Sciences Publications, University of California, Berkeley.

Rombough, P. J., 1988. Growth, aerobic metabolism, and dissolved oxygen requirements of embryos and alevins of steelhead, Salmo gairdneri. Can J Zool 66: 651-660

Rumbaugh, James, 2011. A Guide to using Groundwater Vistas, Version 6.

San Joaquin River Restoration Program (SJRRP). 2010. Conceptual models of stressors and limiting factors for San Joaquin River Chinook Salmon Fisheries. Exhibit A. Management Plan: A Framework for Adaptive Management in the San Joaquin River Restoration Program.

Sante Fe Aggregates, 2009. Snelling Tailings Project Reclamation Plan, Merced County, California. Schaap, M, Feij, van Genuchten. 2001. Rosetta: a computer program for estimating soil hydraulic parameters with hierarchical pedotransfer functions. Journal of Hydrology 251 163-176.

Sarathchandra, S.U., 1978. Nitrification activities and the changes in the populations of nitrifying bacteria in soil perfused at two different H-ion concentrations. Plant and Soil 50: 99-111.

Schlesinger, William, 1997. Biogeochemistry An Anaysis of Global Change. Academic Press. New York.

Schulz, H.D., Dahmke, A., Schinzel, U., Wallmann, K., and Zabel, M., 1994.Early diagenetic processes, fluxes, and reaction rates in sediments of the South Atlantic. Geochim. Cosmochim. Acta, 58: 2041-2060.

Schultz, R.C., Collettil J.P., 2008. Design and placement of a multi-species riparian buffer strip system. Agriforestry Systems 29:3 201-226.

Silver, Stewart, Charles E. Warren & Peter Doudoroff, 1963. Dissolved Oxygen Requirements of Developing Steel head Trout and Chinook Salmon Embryos at Different Water Velocities, Transactions of the American Fisheries Society, 92:4, 327-343.

Skinner, J. E., 1962. A historical review of the fish and wildlife resources of the San Francisco Bay Area. Report No. 1. California Department of Fish and Game, Water Projects Branch.

Smart, R. P., Soulsby C., 2001. Riparian zone influence on stream water chemistry at different spatial scales: a GIS-based modeling approach, an example for the Dee, NE Scotland. The Science of the Total Environment. 280: 173-193.

Sommer, T. R., M. L. Nobriga, W. C. Harrell, W. Batham, W. J. Kimmerer, 2001. Floodplain rearing of juvenile chinook salmon: evidence of enhanced growth and survival Canadian Journal of Fisheries and Aquatic Sciences, 2001, 58:2.

Spence, B.C., and G.A. Lomnicky, R.M. Hughs, and R.P. Novitzki. 1996. An ecosystem approach to salmonid conversation. TR-4501-96-6057. ManTech Environmental Research Services Corp., Corvallis, Oregon. Available from the National Marine Fisheries Service, Portland, Oregon.

Stanford, J. A., M. S. Lorang and F. R. Hauer, 2005. The shifting habitat mosaic of river ecosystems. Plenary Lecture. Proceedings of the International Society of Limnology 29(1):123-136.

Stenstrom, M. K., and R.A. Poduska., 1980. The effect of dissolved oxygen concentration on nitrification. Water Research. 14: 643-649.

Stillwater Sciences, 2004. Channel and Floodplain Surveys of the Merced River Dredger Tailings Reach Technical memorandum #1, Prepared for CALFED ERP, Berkeley, CA.

Stillwater Sciences, 2004. Hydraulic Model of the Merced River Dredger Tailings Reach Technical memorandum #2, Prepared for CALFED ERP, Berkeley, CA.

Stillwater Sciences, 2004. Volume and Texture Analysis of the Merced River Dredger Tailings Technical memorandum #4, Prepared for CALFED ERP, Berkeley, CA.

Stillwater Sciences, 2007. Merced River Ranch Groundwater Study Technical memorandum #11, Prepared for CALFED ERP, Berkeley, CA.

Stillwater Sciences, and Inc. EDAW. 2001. Merced River corridor restoration plan baseline studies. Volume I: Identification of social, institutional, and infrastructural opportunities and constraints. Prepared by Stillwater Sciences, Berkeley, California and EDAW, Inc., San Francisco, California for CALFED Bay-Delta Program, Sacramento, California.

Strauss, E.A. 1995. Protozoa-bacteria interactions in subsurface sediments and the subsequent effects on nitrification. MS Thesis. Kansas State University.

Strauss, Eric, 2000. The Effects of Organic Carbon and Nitrogen availability on Nitrification rates in Stream Sediments, unpublished. Doctor of Philosophy dissertation.

Strauss, E. A., and W. K. Dodds. 1997. Influence of protozoa and nutrient availability on nitrification rates in subsurface sediments. Microbial Ecology. 34: 155-165.

Stroud Water Research Center, 2008. Contribution No. 2008006, StroudWater Quality Monitoring in the Source Water Areas for New York City: An Integrative Watershed Approach, A Final Report on Monitoring Activities, 2000-2005 October 2008.

Stumm, W. and Morgan, J. J., 1981. Aquatic Chemistry, 2nd Ed.; John Wiley & Sons, New York.

Sutton-Grier Electron donors and acceptors influence anaerobic soil organic matt mineralization in tidal marshes.

Sutton-Grier, Ariana. Jason K. Keller , Rachel Koch , Cynthia Gilmour, J. Patrick Megonigal, 2011 An imperiled population of anadromous salmon from a snow-dominated watershed. Soil Biology & Biochemistry.

Tetzlaff, D., Soulsby C., 2007. Connectivity between landscapes and riverscapes- a unifying theme in integrating hydrology and ecology in catchment science? Hydrological Processes 21: 1385-1389.

Teunissen, Karin., 2007. Iron removal at groundwater pumping station Harderbroek, Delft University of Technology, Netherlands.

Thiemann, Sabine and Kaufmann, Hermann, Determination of Chlorophyll Content and

Thompson, K., 1961. Riparian forests of the Sacramento Valley, California. Annals of the Association of American Geographers 51: 294-315.

Thompson, K., 1980. Riparian forests of the Sacramento Valley, California. In: Sands, editor. Riparian forests in California: their ecology and conservation, Priced publication 4101. Division of Agricultural Sciences, University of California.

Thomas, S.L., PiedrahitaI, R.H. 1998. Apparent ammonia-nitrogen production rates of white sturgeon (*Acipenser transmontanus*) in commercial aquaculture systems. Aquacultural Engineering, 17:45-55.

Tindall, J., Kunkel, J., 1999. Unsaturated Zone Hydrology for Scientists and Engineers, http://wwwbrr.cr.usgs.gov/projects/GW_Unsat/Unsat_Zone_Book/ Prentice Hall.

Triska, F. J., J. H. Duff, and R. J. Avanzino, 1990. Influence of exchange flow between the channel and hyporheic zone on nitrate production in a small mountain stream. Canadian Journal of Fisheries and Aquatic Sciences. 47: 2099-2111.

Triska, F. J., J. H. Duff, R. W. Sheibley, A.P. Jackman, and R.J. Avanzino, 2007. DIN Retention-Transport through Four Hydrologically Connected Zones in a Headwater Catchment of the Upper Mississippi River. Journal of the American Water Resources Association 43, DOI: 10.1111/j.1752-1688.

Tucker, Craig. 1991. Water Quantity and Quality Requirements for Channel Catfish Hatcheries Southern Regional Aquaculture Center Publication No, 461 November.

United States Geological Service, 1937. Historical photo of Merced River ABF-12-45 08/02/1937.

U.S. Environmental Protection Agency (USEPA). 1986b. Quality Criteria for Water. Office of Water. EPA 440/5-86-001. 477 http://epa.gov/waterscience/criteria/goldbook.pdf

van Genuchten, M. Th., 1980. A closed-form equation for predicting the hydraulic conductivity of unsaturated soils. Soil Sci. Soc. Am. J. 44: 892-898.

Van Hoorn, J. W., J. H. Boumans, G. P. Kruseman, and B. S. Tanwar, 1989. Reuse and disposal of brackish and saline drainage water. In Reuse of Low Quality Water for Irrigation in Mediterranean Countries. R. Bouchet (ed.). Proc. Cairo/Aswan Seminar, January 1989, 37-47.

Verhagen, F.J.M., H.J. Laanbroek, and J.W. Woldendorp. 1995. Competition for ammonium between plant roots and nitrifying and heterotrophic bacteria and the effects of protozoan grazing. Plant and Soil. 170: 241-250.

Vick, J. C., 1995. Habitat rehabilitation in the lower Merced River: a geomorphological perspective. Unpublished MS thesis, University of California, Berkeley, CA.

Visser, R. H., 2000. Using Remotely Sensed Imagery and GIS to Monitor and Research Salmon Spawning: A Case Study of the Hanford Reach Fall Chinook, U.S. Department of Energy Contract # DE-AC06=76RLO 1830.

Vogel, D., 2003. Anadromous Fish Restoration Program, Merced River Water Temperature Feasibility Investigation Reconnaissance Report, prepared for U.S. Fish and Wildlife Service Anadromous Fish Restoration Program.

Vogel, D., 2007. A feasibility Investigation of Reintroduction of the Anadromous Salmonids above Crocker-Huffman Dam on the Merced River, prepared for U.S. Fish and Wildlife Service Anadromous Fish Restoration Program.

Walsh, C. L., Kilsby C. G., 2007. Implications of climate change on flow regime affecting Atlantic Salmon. Hydrology & Earth System Sciences. 11:3 1127-1143.

Walsh, P.J., Wright, P.A., 1995. Nitrogen Metabolism and Excretion. CRC Press, Florida, USA. 352

Ward J. V., 1997. An expansive perspective of riverine landscapes: pattern and process across scales. River Ecosystems 6: 52-60.

Ward J. V., Stanford J. A., 1989. Riverine ecosystem: the influence of man on catchment dynamic and fish ecology. Fisheries and Aquatic Science. 106: 56-64.

Wetzel, R. G., 1983. Limnology. 2nd ed. Saunders College, Philidelphia, PA. 767

Williams, J. G., 2001a. Chinook salmon in the lower American River, California's largest urban stream. In: Brown, RL, editor. Contributions to the biology of Central Valley salmonids, Fish Bulletin 179: 2 1-38.

Winter, T. C., Harvey J. W., 1998. Groundwater and surface water: a single resource. Geological Survey Circular 1138.

Wood, C.M., 1993 Ammonia and urea metabolism and excretion. In: EVANS, D.H. (Ed.), The physiology of fishes, 1st, ed. CRC Press, Boca Raton, 379-425.

Wosten, J. H., Pachepsky, Rawls, 2001. Pedotransfer functions: bridging the gap between available basic soil data and missing hydraulic characteristics, Journal of Hydrology 251: 123-150.

Wroblicky, G. J., Campana, M. E., Valett, H. M., Dahm, C. N., 1998. Seasonal variation in surface-subsurface water exchange and lateral hyporheic area of two stream-aquifer systems. Water Resour Res 34: 317-328.

Yoshiyama, R. M., F. W. Fisher & P.B. Moyle, 1998. Historical abundance and decline of Chinook salmon in the Central Valley region in California. N. Amer. J. Fish. Mang. 18: 487–521.

Yoshiyama, R. M., E. R. Gerstung, F.W. Fisher & P.B. Moyle, 2000. Chinook salmon in the California Central Valley: an assessment. Fisheries 25:2 6–20.

Zhang, Ye, 2011. Groundwater Flow and Solute Transport Modeling Dept. of Geology & Geophysics University of Wyoming Draft.

Zhao, Liying, 2012. Director and Associate Project Scientist, Environmental Analytical Laboratory Sierra Nevada Research Institute, University of California, Merced. personal communication.

Appendix

Table 3 Well Installation Details

Well ID	Date Installed	Depth (m bgs)	Diameter (cm)	Screened Interval (m bgs)	Well Seal (m bgs)	Elevation Top of Well (ft NGD 29)	Elevation Top of Well (m)
MW-1	06/28/06	7.62	5.08/0.0508	3.22-6.11	0.61	298.53	90.99
MW-2	06/28/06	11.28	5.08/0.0508	5.10-7.99	0.61	304.51	92.81
MW-3	07/07/06	11.28	5.08/0.0508	2.01-4.90	0.61	301.00	91.74
MW-4	07/07/06	3.20	5.08/0.0508	1.79-4.68	0.61	288.74	88.01
MW-5	06/17/11	3.20	5.08/0.0508	0.61-3.20	0.25	286.78	87.41
MW-6	06/15/11	2.90	5.08/0.0508	0.61-2.90	0.25	286.71	87.39
MW-7	06/17/11	2.77	5.08/0.0508	0.61-2.77	0.25	286.65	87.37

Table 4 Surveyed Locations at Merced River Ranch

Description	Northing	Easting	Elevation (m)
MW-1	4154788.318	731127.209	90.99
Pond 1	4154808.024	731109.065	89.21
MW-2	4154452.871	730659.145	92.81
Bridge	4154411.582	730713.025	93.54
Pond 2	4154777.503	730710.622	88.30
Pond 3	4155008.887	730621.221	87.52
Pond 4	4155107.764	730491.844	87.36
MW-5	4154833.123	730302.436	86.86
MW-7	4154830.786±	730295.286±	
MW-6	4154831.190±	730297.929±	

Datum: UTM Zone 10

Table 5 Pumping Rates and Estimated Hydraulic Conductivity and Estimated Specific Yield

Well ID	Pumping Rate (m^3/sec)	Estimated Ks	Estimated Specific yield
MW-1	-1.46E-004	9.99943E-07	2.50E-02
MW-2	-1.46E-004	9.99943E-07	2.50E-02
MW-3	-1.46E-004	9.99943E-07	2.50E-02
MW-4	-1.46E-004	9.99943E-07	0.025
MW-5	-9.50E-006	9.99943E-07	2.50E-03
MW-6	-9.50E-006	9.99943E-07	2.50E-03
MW-7	-9.50E-006	9.99943E-07	2.50E-03

(Araujo, 2012)

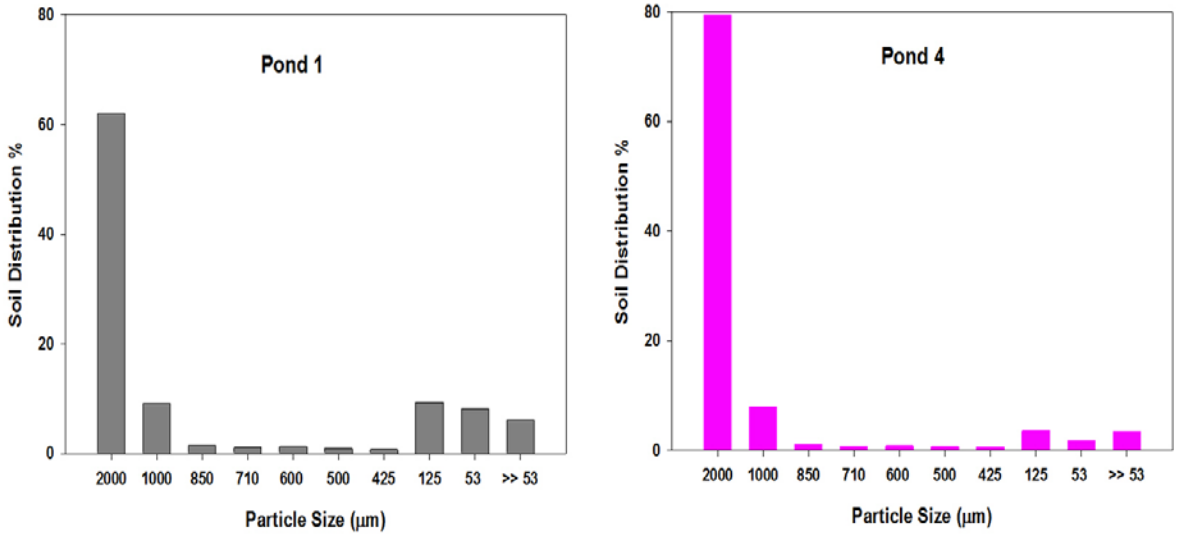

Figure 51 Soil distribution percentages of Pond 1 and Pond 4. The above diagrams show the percent particle distribution of dry soil samples (Araujo, 2012).

Table 6 Water Quality Field Measurements of the Forest Wells, MW 5-7, at Merced River Ranch July 2011-February 2012

Date	Location	Temp (Celsius)	DO (%saturation)	DO (mg L^{-1})	Conductivity (µS/cm)	pH	pH (mV)	ORP (mV)
7/8/2011	MW-5	17.5	7.2	0.69	811	7.08	-7.4	-120.9
9/13/2011	MW-5	18.2	3.1	0.27	567	7.05	-6.3	-186.2
9/20/2011	MW-5	18.5	4.6	0.38	569	7.12	-22	-287.9
10/24/2011	MW-5	17.9		2.22	579	7.16	-23.9	163
11/9/2011	MW-5	16.7	9.0	0.78	661	7.08	19.4	171.7
2/10/2012	MW-5	12.2	6.3	0.64	770	7.04	-18.2	-114
2/17/2012	MW-5	12.2	2.3	0.24	767	7.11	-21.9	-137
9/13/2011	MW-6	17.7	3.8	0.30	665	7.05	-5.2	-227
2/10/2012	MW-6	11.5	4.1	0.44	338	7.22	-27	-129
2/17/2012	MW-6	11.7	1.7	0.19	346.9	7.23	-28	-194
9/13/2011	MW-7	17.8	5.3	0.39	441	7.03	-4.3	-251
9/20/2012	MW-7	18.3	2.0	0.18	698	6.91	-10.4	-289.3
10/24/2011	MW-7	18.2	2.2	0.14	470	7.14	-22.1	-294
2/10/2012	MW-7	11.2	4.2	0.40	371.8	7.12	-21.8	-115
2/17/2017	MW-7	11.2	3.0	0.31	389	7.22	-28	-183

Table 7 Anion and Cation Analysis of Ground and Surface Waters Sampled from the Merced River Ranch with a Dionex ICS-2000 Ion Chromatograph System for the Time Period May 2011-August 2011

Date	Sample Location	Na^{+}	NH_4^{+}	K^{+}	Mg^{2+}	Ca^{+}	F	Cl^{-}	SO_4^{2-}	NO_3^{-}
		mg L^{-1}	mg L^{-1}	mg L^{-1}	mg L^{-1}	mg L^{-1}	mg L^{-1}	mg L^{-1}	mg L^{-1}	mg L^{-1}
5/5/2011	MW-1	3.15	1.74	1.70	7.08	7.68	0.13	1.69	0.05	n.a.
5/13/2011	MW-1	3.44	1.85	1.91	8.50	19.23	0.18	1.61	n.a.	n.a.
6/3/2011	MW-1	3.45	1.91	1.94	8.27	20.69	0.18	1.61	n.a.	n.a.
6/22/2011	MW-1	3.56	1.95	2.00	8.64	29.93	0.24	1.64	n.a.	n.a.
7/8/2011	MW-1	2.90	n.a.	0.73	2.85	7.85	0.21	1.35	n.a.	n.a.
7/27/2011	MW-1	2.93	n.a.	0.73	2.56	7.17	0.24	1.66	0.02	n.a.
8/15/2011	MW-1	3.05	n.a.	0.78	3.26	9.08	0.17	1.66	n.a.	n.a.
8/31/2011	MW-1	2.04	n.a.	0.59	1.62	5.36	0.22	1.61	n.a.	n.a.
5/5/2011	MW-2	3.00	n.a.	0.79	3.39	8.16	0.10	1.66	3.17	3.70
5/13/2011	MW-2	2.94	n.a.	0.74	3.28	7.25	0.04	1.53	3.34	3.39
6/3/2011	MW-2	5.19	0.17	0.23	4.76	7.12	0.04	1.46	3.46	2.17
6/22/2011	MW-2	2.90	n.a.	0.72	3.36	7.73	0.05	1.28	3.16	1.17
7/8/2011	MW-2	2.04	n.a.	0.60	1.28	4.44	0.04	1.22	2.91	0.74
7/27/2011	MW-2	1.99	n.a.	0.61	1.17	4.33	0.04	1.14	2.70	0.55
8/15/2011	MW-2	8.19	n.a.	0.69	10.83	23.14	0.05	1.10	2.54	0.50
8/31/2011	MW-2	1.77	n.a.	0.53	1.02	3.63	0.06	1.05	2.44	n.a.

5/5/2011	MW-3	7.07	n.a.	0.75	11.12	11.71	0.12	3.08	9.64	0.04
5/13/2011	MW-3	7.00	n.a.	0.72	10.46	16.19	0.15	3.08	9.68	n.a.
6/3/2011	MW-3	6.98	n.a.	0.62	10.36	12.44	0.11	3.06	9.51	n.a.
6/22/2011	MW-3	7.21	n.a.	0.56	9.86	12.67	0.13	3.19	9.64	0.02
7/8/2011	MW-3	2.76	1.74	1.59	6.21	21.70	0.17	2.66	7.95	0.03
7/27/2011	MW-3	2.06	n.a.	0.59	1.31	4.76	0.11	3.42	10.13	0.12
8/15/2011	MW-3	1.96	n.a.	0.57	1.09	4.38	0.14	4.78	13.73	0.04
8/31/2011	MW-3	3.44	1.25	1.95	6.55	24.00	0.11	5.11	14.03	0.02
5/5/2011	MW-4	3.20	0.06	0.83	2.93	9.53	0.06	1.20	0.25	0.12
5/13/2011	MW-4	3.46	n.a.	0.99	3.98	8.58	0.06	1.09	0.20	0.12
6/3/2011	MW-4	3.40	n.a.	0.96	4.25	11.63	0.07	1.05	0.21	0.17
6/22/2011	MW-4	3.49	n.a.	0.97	4.65	10.93	0.07	1.19	0.12	0.11
7/8/2011	MW-4	6.07	n.a.	0.47	7.74	12.77	0.08	1.00	0.09	0.10
7/27/2011	MW-4	3.51	1.96	2.01	6.55	17.26	0.08	0.72	0.07	0.04
8/15/2011	MW-4	7.26	n.a.	0.51	8.91	13.76	0.07	0.68	0.06	n.a.
8/31/2011	MW-4	3.44	n.a.	1.36	5.46	15.20	0.06	0.61	0.06	n.a.
6/3/2011	river	2.15	n.a.	0.64	1.32	4.85	0.08	0.90	1.70	0.22
6/22/2011	river	3.01	n.a.	0.76	3.10	8.71	0.01	0.92	1.83	0.28
7/8/2011	river	2.93	n.a.	0.83	2.64	7.43	0.01	0.86	1.61	0.30
7/27/2011	river	2.86	n.a.	0.70	2.81	7.82	0.03	0.79	1.40	0.17

8/15/2011	river	2.06	n.a.	0.63	1.34	4.46	0.02	0.73	1.19	0.18
8/31/2011	river	3.20	n.a.	1.00	4.82	11.91	0.04	0.62	0.88	0.14
5/13/2011	canal	2.39	n.a.	0.72	1.44	4.64	0.03	0.90	2.26	0.20
6/3/2011	canal	1.98	n.a.	0.59	1.21	4.08	0.03	0.74	1.61	0.20
6/22/2011	canal	3.54	1.97	2.04	7.63	24.21	0.06	0.93	1.86	0.29
7/8/2011	canal	3.26	n.a.	1.05	4.87	11.28	0.03	0.85	1.69	0.29
7/27/2011	canal	1.83	n.a.	0.54	1.18	3.79	0.03	0.80	1.47	0.15
8/15/2011	canal	8.32	n.a.	0.62	10.55	18.62	0.02	0.69	1.26	0.12
8/31/2011	canal	3.31	0.06	1.22	4.85	12.23	0.03	0.67	1.07	0.11
5/13/2011	seep	3.19	n.a.	1.13	4.61	9.16	0.05	0.69	0.19	0.12
7/8/2011	seep	2.18	n.a.	0.66	1.44	5.04	0.06	0.79	0.06	n.a.
7/27/2011	seep	3.28	0.09	1.18	4.87	18.55	0.08	0.54	0.06	0.03
8/15/2011	seep	3.49	n.a.	1.17	5.15	13.33	0.08	0.51	0.05	n.a.
8/31/2011	seep	3.92	n.a.	1.41	5.02	13.06	0.11	0.45	0.10	0.16
6/22/2011	MW-5	25.93	0.84	1.17	23.79	35.61	1.04	6.38	3.44	n.a.
7/27/2011	canal	1.83	n.a.	0.54	1.18	3.79	0.03	0.80	1.47	0.15
8/15/2011	canal	8.32	n.a.	0.62	10.55	18.62	0.02	0.69	1.26	0.12
8/31/2011	canal	3.31	0.06	1.22	4.85	12.23	0.03	0.67	1.07	0.11
5/13/2011	seep	3.19	n.a.	1.13	4.61	9.16	0.05	0.69	0.19	0.12
7/8/2011	seep	2.18	n.a.	0.66	1.44	5.04	0.06	0.79	0.06	n.a.

7/27/2011	seep	3.28	0.09	1.18	4.87	18.55	0.08	0.54	0.06	0.03
8/15/2011	seep	3.49	n.a.	1.17	5.15	13.33	0.08	0.51	0.05	n.a.
8/31/2011	seep	3.92	n.a.	1.41	5.02	13.06	0.11	0.45	0.10	0.16
6/22/2011	MW-5	25.93	0.84	1.17	23.79	35.61	1.04	6.38	3.44	n.a.

Table 8 Anion and Cation Analysis of Ground and Surface Water Sampled from the Merced River Ranch with a Dionex ICS-2000 Ion Chromatograph System for the Time Period September 2011-February 2012

Date	**Sample Location**	**Na^+**	**NH_4^+**	**K^+**	**Mg^{2+}**	**Ca^{2+}**	**Cl^-**	**SO_4^{2-}**	**NO_3^-**
		mg L^{-1}	**mg L^{-1}**	**mg L^{-1}**	**mg L^{-1}**	**mg L^{-1}**	**mg L^{-1}**	**mg L^{-1}**	**mg L^{-1}**
9/20/2011	MW-1	3.02	1.38	1.75	7.07	8.97	1.59	0.07	0.04
10/24/2011	MW-1	3.08	1.42	1.78	7.42	18.57	1.52	0.03	n.a.
11/9/2011	MW-1	3.00	1.33	1.73	7.03	18.65	1.50	n.a.	0.01
12/1/2011	MW-1	3.11	1.41	1.79	7.41	23.82	1.54	n.a.	n.a.
12/21/2011	MW-1	3.46	1.45	1.98	8.95	27.55	1.68	0.05	0.07
1/6/2012	MW-1	3.49	1.46	1.92	10.13	34.23	1.59	n.a.	n.a.
1/24/2012	MW-1	3.56	1.45	2.03	10.37	33.55	1.65	n.a.	n.a.
2/10/2012	MW-1	3.32	1.39	1.93	9.79	30.94	1.54	n.a.	n.a.
2/17/2012	MW-1	3.49	1.45	1.98	10.63	35.03	1.60	n.a.	0.02
9/20/2011	MW-2	2.62	n.a.	0.70	2.80	6.12	1.04	2.26	0.53
10/24/2011	MW-2	2.38	n.a.	0.68	3.00	6.29	0.90	1.86	0.41

11/9/2011	MW-2	2.43	n.a.	0.70	3.05	6.57	1.02	1.41	0.23
12/1/2011	MW-2	2.43	n.a.	0.73	3.47	7.51	1.02	1.13	0.44
12/21/2011	MW-2	2.58	0.03	0.82	3.81	7.78	1.16	1.55	0.22
1/6/2012	MW-2	2.54	0.04	0.79	3.98	8.54	1.07	1.62	0.14
1/24/2012	MW-2	2.71	0.06	0.84	4.01	8.69	1.18	1.68	0.15
2/17/2012	MW-2	2.49	0.06	0.75	3.86	8.37	0.99	1.54	0.11
2/28/2012	MW-2	2.89	0.06	0.96	3.65	7.94	1.25	1.72	0.40
9/20/2011	MW-3	7.35	n.a.	0.69	13.14	18.00	5.58	14.40	0.02
10/24/2011	MW-3	7.64	n.a.	0.69	13.96	17.28	6.05	15.95	n.a.
11/9/2011	MW-3	13.23	n.a.	0.73	15.77	21.43	14.38	17.04	n.a.
12/1/2011	MW-3	7.22	n.a.	0.71	13.11	18.19	5.09	13.38	n.a.
12/21/2011	MW-3	6.75	n.a.	0.68	11.41	16.84	3.37	11.67	n.a.
1/6/2012	MW-3	6.82	n.a.	0.64	10.67	16.59	2.91	10.25	n.a.
1/24/2012	MW-3	6.50	n.a.	0.65	10.70	15.99	2.80	9.62	n.a.
2/17/2012	MW-3	6.25	n.a.	0.63	10.47	16.07	2.69	9.07	n.a.
9/20/2011	MW-4	2.74	0.06	1.05	5.29	5.79	0.66	0.12	0.08
10/24/2011	MW-4	2.86	n.a.	0.93	5.77	13.01	1.75	0.06	n.a.
11/9/2011	MW-4	2.71	0.02	0.89	5.42	11.98	1.66	0.07	0.05
12/1/2011	MW-4	2.68	n.a.	0.87	5.28	13.64	1.62	0.09	0.04
12/21/2011	MW-4	2.45	0.03	0.75	4.51	11.22	1.42	0.12	0.11

1/6/2012	MW-4	2.44	0.03	0.72	4.25	12.04	1.39	0.10	0.03
1/24/2012	MW-4	2.31	n.a.	0.59	2.93	8.14	2.58	0.80	0.98
2/14/2012	MW-4	2.48	n.a.	0.66	3.25	8.68	2.63	0.32	0.15
2/17/2012	MW-4	2.42	n.a.	0.66	3.32	8.82	2.51	0.38	0.18
9/20/2011	river	1.82	0.03	0.59	0.90	2.76	10.99	1.03	0.17
10/24/2011	river	1.18	0.02	0.44	0.71	2.52	0.46	0.75	0.14
11/9/2011	river	1.65	0.01	0.40	0.72	2.51	1.21	0.79	0.29
12/1/2011	river	1.14	0.01	0.42	0.67	2.40	0.46	0.78	0.46
12/21/2011	river	1.40	0.03	0.60	0.86	3.07	0.78	0.95	0.42
1/6/2012	river	1.63	0.01	0.51	1.18	3.87	0.87	1.32	0.36
1/24/2012	river	2.18	0.01	0.74	1.36	3.98	1.40	1.48	0.42
2/17/2012	river	1.84	0.01	0.60	1.32	4.09	1.11	1.76	0.31
9/20/2011	canal	1.57	0.02	0.56	0.72	2.38	0.77	0.94	0.07
10/24/2011	canal	1.12	0.02	0.38	0.64	2.30	0.41	0.76	0.16
10/24/2011	canal	1.11	0.01	0.37	0.62	2.29			
11/9/2011	canal	1.21	0.01	0.43	0.65	2.35	0.50	0.78	0.10
12/21/2011	canal	1.22	0.01	0.42	0.68	2.24	0.55	0.89	0.08
1/6/2012	canal	1.58	0.01	0.47	1.04	3.13	0.86	1.33	0.04
1/24/2012	canal	1.87	0.01	0.65	1.21	3.77	1.18	1.43	0.14
2/17/2012	canal	1.78	0.01	0.60	1.29	3.97	1.06	1.76	0.10

2/28/2012	canal	1.90	0.01	0.67	1.30	4.13	1.20	1.87	0.15
11/9/2011	seep	3.34	0.01	1.11	6.46	13.19	1.82	0.15	0.09
12/1/2011	seep	2.70	n.a.	0.95	6.01	15.85	1.62	0.08	0.04
12/21/2011	seep	2.64	n.a.	0.94	5.77	15.40	1.44	0.09	0.05
1/6/2012	seep	2.52	n.a.	0.83	5.56	14.92	1.41	0.11	0.05
1/24/2012	seep	2.33	n.a.	0.75	4.46	12.32	2.31	0.61	1.94
2/17/2012	seep	2.39	n.a.	0.66	3.53	9.75	2.59	0.36	0.40
10/24/2011	MW-5	18.98	0.06	0.79	24.40	25.29	3.67	n.a.	n.a.
2/10/2012	MW-5	30.04	n.a.	1.00	51.46	27.06	11.27	1.11	n.a.
2/17/2012	MW-5	28.14	n.a.	0.96	46.66	49.16	12.09	1.67	1.08
2/28/2012	MW-5	22.86	n.a.	0.58	39.24	59.83	6.40	0.69	n.a.
2/10/2012	MW-6	12.45	0.10	0.86	20.66	26.52	3.53	2.82	n.a.
2/17/2012	MW-6	13.68	0.04	0.74	22.37	28.12	3.93	2.98	n.a.
2/28/2012	MW-6	19.53	n.a.	0.47	30.50	28.25	5.05	4.72	0.08
2/17/2012	MW-7	11.74	0.11	0.88	21.80	37.19	4.09	1.28	n.a.
2/28/2012	MW-7	15.49	0.02	0.65	26.71	39.24	4.77	1.46	n.a.

Table 9 Analysis of Total Iron and Total Dissolved Iron Utilizing Perkins-Elmer Optima 5300dv of Ground and Surface Waters from the Merced River Ranch for the Time Period September 2011-2012

Total Iron				Total Dissolved Iron			
Date	**Location**	**Fe (mg L^{-1})**	**RSD**	**Date**	**Location**	**Fe (mg L^{-1})**	**RSD**
9/20/2011	MW-1	11.2500	1.44	**9/20/2011**	MW-1	0.1270	1.21
10/24/2011	MW-1	18.9100	0.94	**10/24/2011**	MW-1	0.0350	1.06
11/9/2011	MW-1	23.4300	0.07	**11/9/2011**	MW-1	6.2130	1.74
12/1/2011	MW-1	25.6700	0.87	**12/1/2011**	MW-1	9.4280	1.88
12/21/2011	MW-1	25.8700	0.60	**12/21/2011**	MW-1	16.2200	0.88
1/6/2012	MW-1	26.2300	0.49	**1/6/2012**	MW-1	14.1300	0.89
1/24/2012	MW-1	26.0200	0.81	**1/24/2012**	MW-1	10.8200	1.03
2/10/2012	MW-1	0.0090	3.02	**2/10/2012**	MW-1	3.1250	1.26
2/17/2012	MW-1	26.7600	1.06	**2/17/2012**	MW-1	10.0900	1.10
9/20/2011	MW-2	0.0880	0.50	**9/20/2011**	MW-2	0.0040	8.16
10/24/2011	MW-2	0.1540	1.66	**10/24/2011**	MW-2	0.0070	1.17
11/9/2011	MW-2	0.8780	1.49	**11/9/2011**	MW-2	0.0080	1.00
12/1/2011	MW-2	0.2010	2.22	**12/1/2011**	MW-2	0.0330	0.79
12/21/2011	MW-2	0.2430	1.65	**12/21/2011**	MW-2	0.0410	1.88
1/6/2012	MW-2	0.1820	2.08	**1/6/2012**	MW-2	0.0310	1.10

1/24/2012	MW-2	0.1010	0.76	**1/24/2012**	MW-2	0.0180	3.49
2/17/2012	MW-2	0.0500	2.08	**2/17/2012**	MW-2	0.0300	0.34
2/28/2012	MW-2	0.1450	0.51	**2/28/2012**	MW-2	0.0100	2.97
9/20/2011	MW-3	0.1230	1.14	**9/20/2011**	MW-3	0.0090	3.20
10/24/2011	MW-3	0.0840	0.38	**10/24/2011**	MW-3	0.0330	1.48
11/9/2011	MW-3	0.1920	1.34	**11/9/2011**	MW-3	0.0400	0.45
12/1/2011	MW-3	0.1250	0.99	**12/1/2011**	MW-3	0.0230	3.13
12/21/2011	MW-3	0.2500	1.34	**12/21/2011**	MW-3	0.0160	3.27
1/6/2012	MW-3	0.3390	0.70	**1/6/2012**	MW-3	0.0150	3.01
1/24/2012	MW-3	0.0870	1.54	**1/24/2012**	MW-3	0.0060	4.95
2/17/2012	MW-3	0.3060	0.99	**2/17/2012**	MW-3	0.0190	2.04
9/20/2011	MW-4	0.2620	1.76	**9/20/2011**	MW-4	0.0050	5.31
10/24/2011	MW-4	0.1330	1.32	**10/24/2011**	MW-4	0.0040	4.77
11/9/2011	MW-4	0.1680	1.60	**11/9/2011**	MW-4	0.0110	2.39
12/1/2011	MW-4	0.4760	1.06	**12/1/2011**	MW-4	0.0130	0.70
12/21/2011	MW-4	1.4460	0.94	**12/21/2011**	MW-4	0.0330	2.15
1/6/2012	MW-4	0.5800	0.50	**1/6/2012**	MW-4	0.0130	4.46
1/24/2012	MW-4	0.5790	0.66	**1/24/2012**	MW-4	0.0240	1.56
2/14/2012	MW-4	22.1800	1.58	**2/14/2012**	MW-4	0.0290	0.99

2/17/2012	MW-4	1.7080	1.48	**2/17/2012**	MW-4	0.0620	0.95
10/24/2011	MW-5	7.9860	0.41	**10/24/2011**	MW-5	0.0640	0.92
2/10/2012	MW-5	7.8860	1.13	**2/10/2012**	MW-5	0.1990	0.61
2/17/2012	MW-5	13.9300	0.57	**2/17/2012**	MW-5	0.1670	1.15
2/28/2012	MW-5	5.3500	0.07	**2/28/2012**	MW-5	0.1170	1.33
2/17/2012	MW-6	15.4600	0.58	**2/17/2012**	MW-6	0.1900	1.76
2/10/2012	MW-6	9.0110	1.95	**2/10/2012**	MW-6	0.1600	0.55
2/28/2012	MW-6	7.3720	0.58	**2/28/2012**	MW-6	0.1300	0.76
2/17/2012	MW-7	18.1500	0.23	**2/17/2012**	MW-7	0.1470	0.49
2/28/2012	MW-7	6.0940	0.87	**2/28/2012**	MW-7	0.0710	1.50
9/20/2011	river	0.1530	1.46	**9/20/2011**	river	0.0140	3.19
10/24/2011	river	0.1510	0.10	**10/24/2011**	river	0.0080	3.13
11/9/2011	river	0.1730	2.17	**12/1/2011**	river	0.0450	0.94
12/1/2011	river	0.2670	1.91	**12/21/2011**	river	0.0690	1.31
12/21/2011	river	0.3240	1.41	**1/6/2012**	river	0.0650	1.57
1/6/2012	river	0.2360	1.54	**1/24/2012**	river	0.0960	0.37
1/24/2012	river	0.2070	0.83	**2/17/2012**	river	0.0530	0.81
2/17/2012	river	0.0980	0.63	**9/20/2011**	canal	0.0190	2.66
9/20/2011	canal	0.0530	1.32	**10/24/2011**	canal	0.0100	4.47

10/24/2011	canal	0.0630	0.45	**11/9/2011**	canal	0.0200	1.77
11/9/2011	canal	0.3290	2.31	**12/21/2011**	canal	0.0310	1.00
12/21/2011	canal	0.1250	0.63	**1/6/2012**	canal	0.0290	2.22
1/6/2012	canal	0.0820	1.15	**1/24/2012**	canal	0.0470	4.56
1/24/2012	canal	0.1230	1.39	**2/17/2012**	canal	0.0300	2.19
2/17/2012	canal	0.0790	1.05	**2/28/2012**	canal	0.0270	1.44
2/28/2012	canal	0.1840	1.79	**11/9/2011**	seep	0.0380	0.13
11/9/2011	seep	0.1620	0.51	**12/1/2011**	seep	0.0090	2.35
12/1/2011	seep	0.1870	0.34	**12/21/2011**	seep	0.0080	4.69
12/21/2011	seep	0.3530	0.87	**1/6/2012**	seep	0.0140	3.08
1/6/2012	seep	0.2800	0.88	**1/24/2012**	seep	0.0170	2.09
1/24/2012	seep	0.1970	0.06	**2/17/2012**	seep	0.0460	1.20
2/17/2012	seep	0.6090	1.13				

Table 10 Alkalinity as Measured by $CaCO_3$ and Charge Balance of MRR Ground and Surface Waters Sampled at the Merced River Ranch for the Time Period September 2011-February 2012

Date	Alkalinity Sample Location	$CaCO_3$ (mg L^{-1})	std	RSD	Charge Balance
9/20/2011	MW-1	77.07	1.67	2.17	-13.7
10/24/2011	MW-1	105.64	0.00	0.00	-11.3
11/9/2011	MW-1	128.56	0.44	0.34	2.4
12/1/2011	MW-1	134.95	2.57	1.91	-0.2
12/21/2011	MW-1	153.35	12.86	8.38	-10
1/6/2012	MW-1	182.42	0.00	0.00	-13.3
1/24/2012	MW-1	159.75	5.14	3.22	-31.6
2/10/2012	MW-1	172.47	1.75	1.01	-27.6
2/17/2012	MW-1	192.02	2.90	1.51	-25.4
9/20/2011	MW-2	28.27	0.24	0.84	2
10/24/2011	MW-2	29.07	0.61	2.10	2.7
11/9/2012	MW-2	30.94	0.61	1.97	12.9
12/1/2011	MW-2	35.34	0.24	0.67	7.6
12/21/2011	MW-2	37.60	1.20	3.19	3
1/6/2012	MW-2	11.62	1.12	9.62	47.3

1/24/2012	MW-2	38.94	0.24	0.61	-8.7
2/17/2012	MW-2	38.80	0.00	0.00	-2.7
2/28/2012	MW-2	36.61	0.29	0.79	2.3
9/20/2011	MW-3	92.40	0.69	0.75	0.3
10/24/2011	MW-3	97.34	0.61	0.63	-1.8
11/9/2011	MW-3	114.42	0.00	0.00	-12.3
12/1/2011	MW-3	98.55	1.00	1.02	-6.4
12/21/2011	MW-3	87.60	0.69	0.79	-1.6
1/6/2012	MW-3	85.74	0.84	0.98	8.9
1/24/2012	MW-3	84.54	0.46	0.54	4.7
2/17/2012	MW-3	83.47	0.61	0.73	2
9/20/2011	MW-4	44.55	0.22	0.49	-2.3
10/24/2011	MW-4	61.08	0.24	0.39	0
11/9/2011	MW-4	77.34	10.99	14.21	-19.3
12/1/2011	MW-4	65.62	0.69	1.06	-29.5
12/21/2011	MW-4	59.88	0.24	0.40	-21.5
1/6/2012	MW-4	56.95	1.89	3.32	-18.6
1/24/2012	MW-4	31.88	0.23	0.74	26.7
2/14/2012	MW-4	35.75	0.24	0.66	24.4

2/17/2012	MW-4	38.41	0.40	1.03	13.2
10/24/2011	river	10.15	0.24	2.33	3.2
11/9/1011	river	9.22	0.41	4.45	22.6
12/1/2011	river	8.95	0.24	2.65	26
12/21/2011	river	12.15	0.46	3.75	13.5
1/6/2012	river	14.95	0.24	1.58	-13.5
1/24/2012	river	16.28	0.24	1.45	-20.3
2/17/2012	river	15.35	0.23	1.50	-7.5
9/20/2011	MC	9.08	0.24	2.61	7.8
10/24/2011	MC	8.68	0.22	2.53	5.8
11/9/2011	MC	8.95	0.24	2.65	16.6
12/21/2011	MC	8.95	0.24	2.65	22.9
1/6/2012	MC	12.02	0.56	4.65	12.8
1/24/2012	MC	14.81	0.00	0.00	5.6
2/17/2012	MC	15.35	0.23	1.50	-18
2/28/2012	MC	15.48	0.46	2.95	-19.5
11/9/2011	seep	76.27	1.02	1.33	-8.1
12/1/2011	seep	71.47	6.89	9.64	-15.5
12/21/2011	seep	67.38	0.60	0.89	-22.8

1/6/2012	seep	64.01	0.69	1.08	1.1
1/24/2012	seep	46.41	1.20	2.59	18.8
2/17/2012	seep	38.94	0.24	0.61	25.5
10/24/2011	MW-5	257.47	12.86	5.00	-12.1
2/10/2012	MW-5	458.73	6.10	1.33	-15.8
2/17/2012	MW-5	500.00	6.93	1.39	-15.8
2/28/2012	MW-5	422.74	6.10	1.44	-9
2/10/2012	MW-6	211.27	10.51	4.97	-10
2/17/2012	MW-6	226.49	5.64	2.49	-9.9
2/28/2012	MW-6	294.44	2.23	0.76	-12.3
2/17/2012	MW-7	321.62	32.67	10.16	-22.2
2/28/2012	MW-7	286.97	0.95	0.33	-9.8

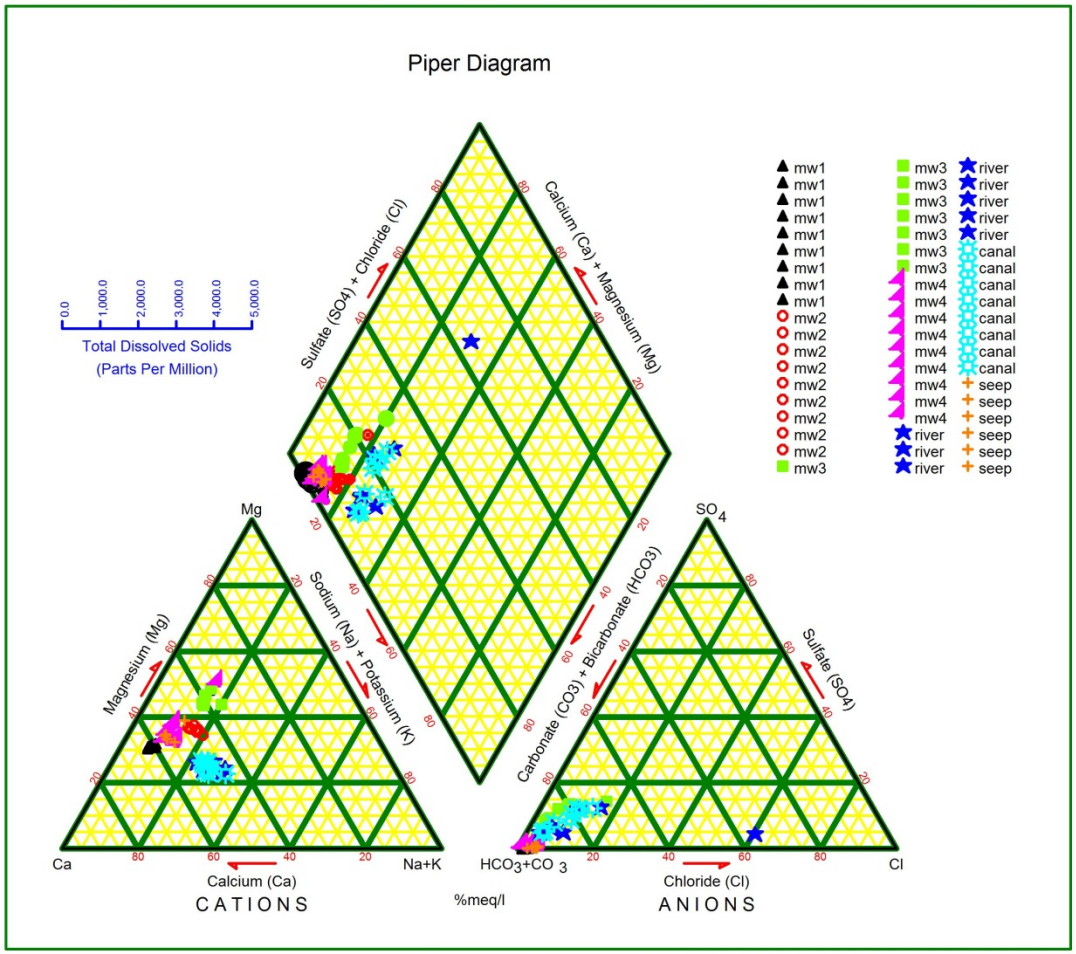

Figure 52 Piper diagram, a graphical representation of the chemistry of sampled ground and surface waters of the Merced River Ranch from September 2011-February 2012.

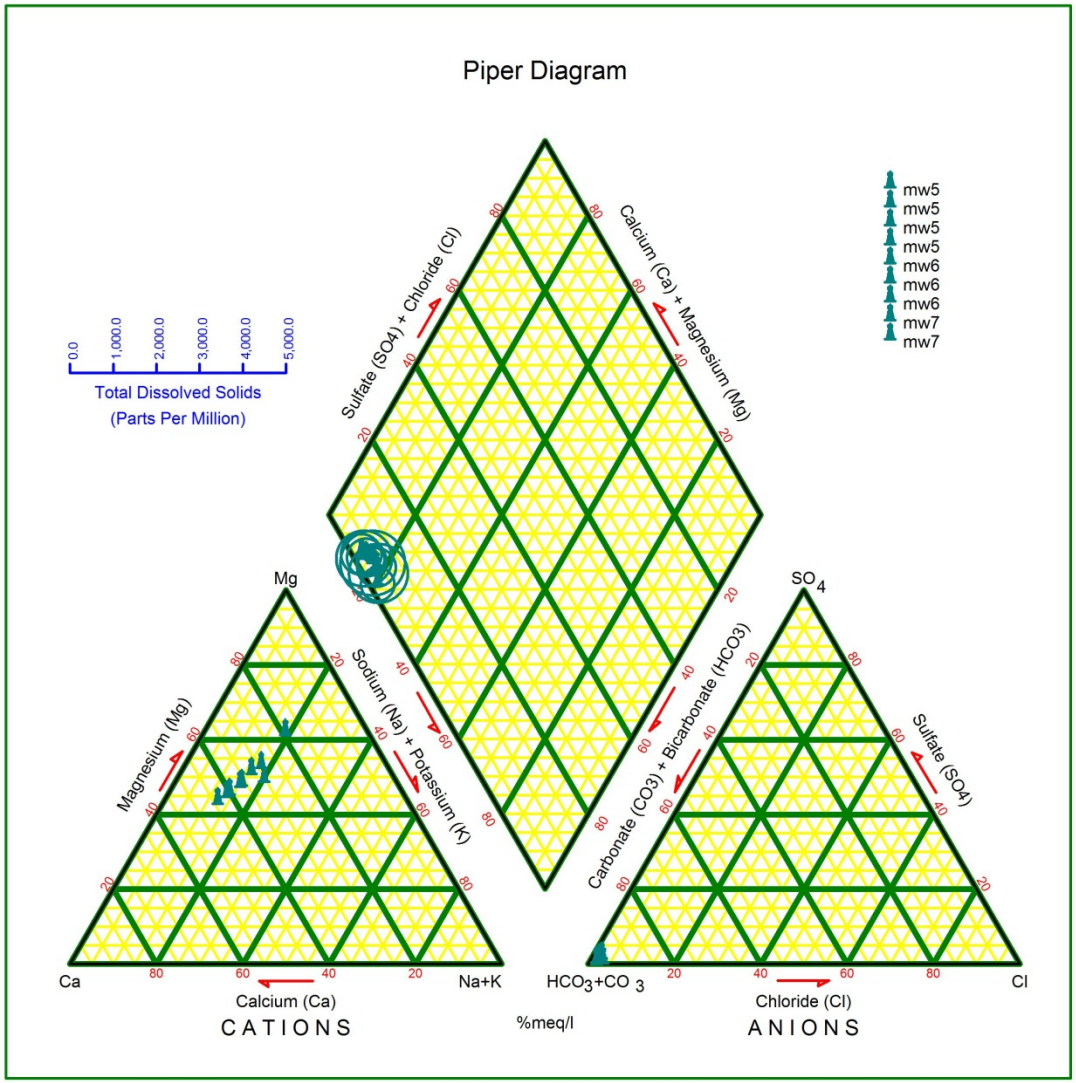

Figure 53 Piper diagram, a graphical representation of the chemistry of ground waters of the Forest Wells (MW 5-7) sampled at Merced River Ranch from September 2011-February 2012.